

A STUDY OF FLOW RATE EFFECTS IN DRILLING  
WITH EMBEDDED DIAMOND CORING BITS,  
AND THE COMMISSIONING OF A CERCHAR  
ROCK ABRASIVITY TESTER

REZA ALVARI







**A Study of Flow Rate Effects in Drilling with Embedded Diamond Coring Bits, and  
the Commissioning of a CERCHAR Rock Abrasivity Tester**

by

© Reza Alvani

A Thesis submitted to the

School of Graduate Studies in partial fulfillment of the requirements for the degree of

**Master of Engineering**

**Faculty of Engineering and applied Science**

**Memorial University of Newfoundland**

**August 2012**

St. John's

Newfoundland

## **ABSTRACT**

The research is composed of two separate efforts. First, a study of the effect of flow rate of drilling fluid on the drilling performance of two-inch coring bits; and second, the commissioning of equipment for the CERCHAR rock abrasiveness test. CERCHAR is a standard test to determine a measure of rock abrasiveness based on the wear flat that the rock produces on the tip of a scratching tool.

In the drilling tests the primary variables were the flow rate and weight on bit and also the drilling modes (vibration assisted and conventional). The bits were impregnated diamond coring bits and wear measurements were based on both microscopic photos of the bit surface and the diamonds and on the weight loss of the tool. The results show an overall increase of the rate of penetration for vibration assisted drilling compared to conventional drilling and also the boosting the effect of the flow rate on this increase in the rate of penetration.

A previously constructed CERCHAR testing facility was commissioned, including the determination of the appropriate heat treatment of the tool steel chosen for the styli. The effect on the CERCHAR Abrasiveness Index (CAI) of stylus hardness within the range of hardness of  $\pm 2\text{HRC}$  about the hardness stipulated in the standard is within the confidence limits for a CAI determination.

## 1 ACKNOWLEDGEMENTS

I would like to express my special thanks of gratitude to my graduate supervisors, Dr. Stephen Butt and Dr. John Molgaard who gave me the golden opportunity to work on a part of this advanced project for oil and gas drilling, which also helped me in doing this research and I came to know and discover new technologies and opportunities.

I would like to also thank to Steve Steele, Material Lab technical staff, and Hossein Khorshidian, graduate student, Alireza Noroozi for their support and encouragement.

I would like to also thank the Atlantic Canada Opportunity Agency (AIF Contract no.781-2636-1920044), Husky Energy, and Suncor Energy for funding this research over the past two and a half years. Additionally, the financial and academic support of the Faculty of Engineering and Applied Science is graciously acknowledged.

My special thanks to Moya Crocker and Dr. Leonard Lye for their help and supervision.

I will be always grateful to Babak Akbari, my close friend for his endless support and assistance.

Last but not least, I would like to give my special thanks to my mother Farangis, and my father Ahmad, without them I would have never made this accomplishment.

## Table of Contents

ABSTRACT .....	ii
ACKNOWLEDGEMENTS .....	iii
Table of Contents .....	iv
List of Tables .....	x
List of Figures .....	xii
List of Symbols, Nomenclature or Abbreviations .....	xix
List of Appendices .....	xxii
1 Introduction .....	23
1.1 Principles of Drilling .....	23
1.2 Background of the Research .....	25
1.3 Research Plan .....	27
2 Current State of Knowledge .....	28
2.1 Effect of Flow Rate on Drilling Performance .....	28
2.1.1 Fundamentals of Bit Hydraulics .....	28
2.1.2 The Concept of Rock Abrasiveness and its Measurement methods .....	37

2.1.3	CERCHAR Test for Measuring Rock Abrasiveness.....	40
2.1.4	Rock Abrasiveness and Drilling Performance (wear rate).....	44
3	Coring Drilling Experiments.....	49
3.1	Background and Previous Pertinent Work.....	49
3.2	Justification of the Work.....	52
3.3	Preparing Concrete Sample.....	53
3.4	Drilling Test Facilities.....	54
3.4.1	Experimental Setup.....	54
3.4.2	Bit Specifications.....	59
4	Design of the Experiments and Test Results.....	60
4.1	Design of Experiments.....	60
4.2	Results of Drilling Test.....	62
4.3	Analysis of Drilling Test.....	64
4.3.1	Effects of Flow Rate and WOB.....	64
4.4	Wear Rate Data Acquisition and Analysis.....	80

4.4.1	Acquisition of Data.....	80
4.4.2	A Summary of the Analysis of the Wear Data.....	83
5	CERCHAR Test Summary and Results.....	87
5.1	Heat Treatment and Preparation of Styli Required for a Standard CERCHAR Test.....	87
5.1.1	Conclusions of the Work.....	95
5.2	CERCHAR Tests Sensitivity to Stylus Hardness.....	96
5.2.1	Procedure of CERCHAR Tests Performed.....	97
5.2.2	The Results Obtained from the CERCHAR Tests.....	99
6	Conclusions.....	105
6.1	Coring Drilling Tests.....	105
6.2	CERCHAR Test Results and HRC.....	106
7	Recommendations for Future Work.....	107
7.1	Flow Rate of Drilling Fluid and its Effect on the Drilling Performance.....	107
7.2	CERCHAR Test and Hardness Effect.....	108
8	References.....	1099

Appendices.....	119
9 Appendix 1. Wear Study Data and Details.....	11919
9.1 Study on Leading Edge.....	120
9.1.1 One gpm Experiment.....	1200
9.1.2 Three gpm Experiment.....	1211
9.1.3 Five gpm Experiment.....	1222
9.2 Study on Trailing Edge.....	1244
9.2.1 One gpm Experiment.....	1244
9.2.2 Three gpm Experiment.....	1255
9.2.3 Five gpm Experiment.....	1266
9.3 Study on Diamonds.....	1277
9.3.1 One gpm Experiment.....	1277
9.3.2 Three gpm Experiment.....	1288
9.3.3 Five gpm Experiment.....	12929
9.4 Study on side view.....	1300

9.4.1	One gpm Experiment.....	1300
9.4.2	Three gpm Experiment.....	1311
9.4.3	Five gpm Experiment.....	1322
9.5	Study on Water Ways .....	1333
9.5.1	One gpm Experiment.....	1333
9.5.2	Three gpm Experiment.....	1344
9.5.3	Five gpm Experiment.....	135
9.6	Comparing Bit Profile Before and After Tests.....	1355
9.6.1	One GPM Experiment.....	136
9.6.2	Three GPM Experiment.....	1366
9.6.3	Five GPM Experiment.....	137
9.7	Comparing Conventional and Vibration Drilling .....	138
9.8	Study on Diamonds Before Starting the Runs and After Finishing all the runs.....	1388
9.9	Study on Weight Loss .....	1411

9.10 Study on Water Ways .....	1433
10 Appendix 2. Styli Heat Treating and Hardness Testing Details.....	1500
10.1 Sample (1).....	1500
10.2 Sample(2).....	1555

## List of Tables

Table 3-1. Concrete ingredients ratio.....	54
Table 4-1. Experiment results.....	63
Table 5-1. Diameter of the CERCHAR styluses' after standard CERCHAR test.....	100
Table 5-2.Pin HRC hardness and pin diameter data.....	103
Table9-1. Summary of wear types in vibratory and conventional drilling test.....	141
Table 10-1. Tip hardness test Results for sample(1).....	1511
Table 10-2. Base hardness test results for sample(1).....	1511
Table 10-3.knoop Tests on the base side of sample (1).....	1544
Table 10-4. knoop tests on the base side of sample (1).....	1544
Table 10-5. . Knoop tests on the tip side of sample (2).....	1555
Table 10-6. Knoop tests on the base side of sample (2).....	1566

Table 10-7. Knoop test for calibration.....	15959
Table 10-8. Standard with 60.91+-0.5HRC.....	15959
Table 10-9. Heat treatment of samples.....	1622
Table 10-10. Tempered at 275 Celsius for 45 min.....	1633
Table 10-11 Tempered stylus at 250 Celcius for 45 min.....	1644
Table 10-12 Tempered stylus at 225 Celcius for 45 min.....	1644
Table 10-13 Styli as received from Technical Services.....	1655
Table 10-14 Randomly Rockwell test on stylus.....	1666
Table 10-15 Stylus tempered at 225°C for 45 min.....	16767
Table 10-16 Stylus tempered at 225°C for 45 min.....	16767

## List of Figures

Figure 2-1. Schematic of a rig fluid circulating system (courtesy of Bourgoyne et al. [9]).....	29
Figure 2-2. Fluid jet exiting the nozzle.....	32
Figure 2-3. Schematic diagram of the circulating mud system used by Bizanti and Blick [17].....	33
Figure 2-4. Accumulation of cutting material around the bit in poor bit hydraulics condition (after Ledgerwood and Salisbury [18]).....	34
Figure 2-5. The CERCHAR test (after B. Nilson.[27]).....	41
Figure 2-6.Bit life of different rock types correlated with EQC (courtesy of Thuro[39]).	46
Figure 3-1. Schematic view of the drill setup.....	56
Figure 3-2. Drill setup.....	58
Figure 3-3. Drill bit used for the experiments (core barrel).....	59
Figure 4-1. Full general factorial set of experiments.....	61
Figure 4-2. Rate of penetration versus WOB for different flow rates and drilling modes.	65

Figure 4-3. Rate of penetration versus flow rate for different weights on bit and drilling modes.....	66
Figure 4-4. ROP versus WOB at each flow rate in conventional and vibratory drilling using the generated equations based on experimental results.....	69
Figure 4-5. Probable events during drilling with segmented embedded diamond coring bit.....	71
Figure 4-6. Spectrum of rock displacement at WOB of 60 kgf.....	74
Figure 4-7. Spectrum of rock displacement at WOB of 80 kgf.....	74
Figure 4-8. Spectrum of rock displacement at WOB of 100 kgf.....	75
Figure 4-9. Spectrum of rock displacement at WOB of 120 kgf.....	75
Figure 4-10. Stationary part of the signal at WOB of 60 Kgf.....	76
Figure 4-11. Stationary part of the signal at WOB of 80 Kgf.....	76
Figure 4-12. Stationary part of the signal at WOB of 100 Kgf.....	77
Figure 4-13. Stationary part of the signal at WOB of 120 Kgf.....	77
Figure 4-14. The Amplitude vs. WOB at 58 Hz.....	78

Figure 4-15. Bit state after drilling. (a): WOB:100 kgf - GPM:1 (CONV), (b): WOB:100 kgf - GPM:1 (VIB), (c): WOB: 100 kgf - GPM:1 (CONV), (d): WOB: 100 kgf - GPM:1 (VIB), (e): WOB: 120 kgf - GPM:2 (CONV) (f): WOB:120 kgf - GPM:2 (VIB).....	79
Figure 4-16. Optical Microscope.....	81
Figure 4-17. Weight measurement with digital balance.....	82
Figure 4-18, Replicas.....	82
Figure 4-19. Weight change per unit depth drilling versus flow rate for different drilling modes.....	85
Figure 5-1. Rockwell hardness test apparatus.....	89
Figure 5-2. Indentation by the Knoop testing machine on the sample.....	91
Figure 5-3. Knoop test apparatus used for the tests.....	91
Figure 5-4. Fixture developed to conduct the hardness tests on the tip of the styli.....	95
Figure 5-5. CERCHAR testing set-up in Memorial University of Newfoundland.....	97
Figure 5-6. Rock samples and styli used in the CERCHAR experiments.....	98
Figure 5-7. Plot of Correlation between HRC value of the styluses and tip diameter after test.....	101

Figure 5-8. Diameter in mm versus hardness.....	104
Figure 9-1 Before test.....	1200
Figure 9-2 After test.....	1200
Figure 9-3. Before test.....	1211
Figure 9-4. After test.....	1211
Figure 9-5. Before test.....	1222
Figure 9-6. After test.....	1222
Figure 9-7. Before test.....	1244
Figure 9-8. After test.....	1244

Figure 9-9. Before	
test.....	1255
Figure 9-10. After	
test.....	1255
Figure 9-11. Before	
test.....	1266
Figure 9-12. After	
test.....	1266
Figure 9-13. Before	
test.....	1277
Figure 9-14. After	
test.....	1277
Figure 9-15. Before	
test.....	1288
Figure 9-16. After	
test.....	1288
Figure 9-17. Before	
test.....	12929

Figure 9-18. After	
test.....	12929
Figure 9-19. Before	
test.....	13030
Figure 9-20. After	
test.....	1300
Figure 9-21. Before	
test.....	1311
Figure 9-22. After	
test.....	1311
Figure 9-23. Before	
test.....	1322
Figure 9-24. After	
test.....	1322
Figure 9-25. Before	
test.....	1333
Figure 9-26. After	
test.....	1333

Figure 9-27. Before test.....	1344
Figure 9-28. After test.....	1344
Figure 9-29. Before test.....	1355
Figure 9-30. After test.....	1355
Figure9-31. Superimposed photos of before and after test for conventional and vibratory drilling.....	136
6	
Figure9-32. Superimposed photos of before and after test for conventional and vibratory drilling.....	136
6	
Figure 9-33 Superimposed photos of before and after test for conventional and vibratory drilling.....	137
7	

Figure 9-34. Comparing vibrational and conventional drilling wear rates, superimposed photos.....138

8

Figure9-35. 'pull out' and 'unworn' diamonds identified.....13939

Figure9-36. Microfractured diamonds.....1400

Figure9-37. Weight loss of the bit for two drilling modes versus flow rate.....1422

Figure 9-38. Bit 4 segment 1; left: leading, right: trailing (Conventional).....1433

Figure 9-39. Bit 4 segment 2; left: leading, right: trailing (Conventional).....1444

Figure 9-40. Bit 4 segment 3; left: leading, right: trailing (conventional).....1444

Figure 9-41. Bit 4 segment 4; left: leading, right: trailing (Conventional).....1455

Figure 9-42. Bit 4 segment 5; left: leading, right: trailing  
(Conventional).....1455

Figure 9-43. Bit 1 segment 1; left: leading, right: trailing  
(Vibrational).....1466

Figure 9-44. Bit 1 segment 2; left: leading, right: trailing  
(Vibrational).....1477

Figure 9-45. Bit 1 segment 3; left: leading, right: trailing  
(Vibrational).....1477

Figure 9-46. Bit 1 segment 4; left: leading, right: trailing  
(Vibrational).....1488

Figure 9-47. Bit 1 segment 5; left: leading, right: trailing  
(Vibrational).....1488

Figure 10-1. five tests done on a stylus base and the proposed locations for conducting the  
Knoop  
test.....1533

Figure 10-2. Rockwell Hardness vs. temperature of heat  
treatment.....1622



## List of Symbols, Nomenclature or Abbreviations

ASTM	American Society for Testing and Materials
CAI	CERCHAR Abrasiveness Index
CONV	Conventional Drilling (as opposed to vibration assisted)
$C_{\text{set-up}}$	Drilling set-up operational cost
$C_{\text{vib-op}}$	Vibrational set-up operational cost
$C_{\text{wear}}$	Cost associated by the worn part of the cutting tool
DRI	Drilling Research Institute
EQC	Equivalent Quartz Content
GPM	Gallon Per Minute
HRC	Hardness Rockwell Conversion
ID	Internal Diameter
ISRM	International Society for Rock Mechanics

LPT	Linear Potentiometer Transducer
LVDT	Linear Variable Differential Transformer
OD	Outside Diameter
$P_b$	Pressure drop at bit
$P_d$	Pressure drop at the drill string and the annulus
$P_p$	Pressure provided by the pump
Q	Flow rate
ROP	Rate Of Penetration
TBM	Tunnel Boring Machine
TFA	Total Flow Area
UCS	Unconfined Compressive Strength
VFD	Variable Frequency Drive
VHN	Vickers's Hardness Number

VIB	Vibration assisted drilling
WOB	Weight on Bit
WR	Wear Rate
M	Flow exponent
$\Sigma$	Confining stress
P	Density
M	Viscosity

## **List of Appendices**

Appendix 1. Wear Study Data and Details

Appendix 2. Styli Heat Treating and Hardness Testing Details

# **1 Introduction**

## **1.1 Principles of Drilling**

Rotary drilling is the most accepted and practiced method of drilling ever since the exploitation of the underground fluids such as petroleum became a prolific business. In the rotary drilling a bit is used for the mechanical attack. The mechanical attack causes rock failure and generation of the fragment. Continuation of fragmentation by cleaning the previous generated chips creates a hole which is called wellbore, and the rock surface in front of the bit is called bottom hole. There are many parameters which influence the rock-bit interaction in a drilling operation, e.g., rock type, bit type, technology of mechanical attack and cleaning of bit. In order to generate a rock under a specific condition of penetration a certain amount of energy is required. The energy of rotary drilling is supported by a motor on the rig floor or downhole motor. The rate of penetration (ROP) is the length of penetration per unit of time which the bit drills the rock.

The basic parameters of rotary drilling such as the rotary speed, weight on bit and the flow rate have always been the subject of study either independently or interacting with each other. Setting the input parameters of a drilling system, results in a certain value of drilling response. The drilling responses which significantly impact the economic cost of drilling operation are the rate of penetration and rate of bit wear.

The cost of drilling operations is the function of time of operation. Reducing the time of operation decreases the total cost of drilling. Normally, the main part of a drilling operation is spent on rotary time, which the bit is generating rock fragments, and the tripping time, which is spent on taking the bit out of the well when it is worn off, and run it to the depth after installation of the new bit. The tripping time can be more significant in drilling operations at great depth and offshore drillings where the distance between water surface and ground is high.

Therefore, increase in ROP and decrease in bit wear can reduce the cost of drilling significantly.

The Advanced Drilling Group (ADG) at Memorial University of Newfoundland has undertaken a program of experimental and numerical investigations of vibration-assisted rotary drilling (VARD). The research examines fundamental rock penetration mechanisms for VARD and its application in reduction of the cost of the drilling, aimed at determining optimal bit operating conditions including optimum ranges of vibration frequency and amplitude, weight on bit (WOB), rotary speed, drilling fluid flow rate and bore hole pressure conditions. It is believed that the wear rate is affected by vibrations; therefore, this factor is also included in this work.

The present study is in an initial series of studies by the ADG of the relationship of ROP to WOB, and the effect of other pertinent variable on this relationship. In particular the additional effect of drilling fluid flow rate was studied, along with weight on bit (WOB)

and the rotary speed. Most of the other initial studies are conducted using an embedded diamond coring bits, as in this study.

## 1.2 Background of the research

Li [1] developed the vibration assisted drilling set-up used in this work, which was modified for subsequent studies. He also examined the effect of vibration on the rate of penetration using diamond impregnated coring bits and found that the rate of penetration can be increased by applying vibration on the rock specimen. Zhang [3] developed new techniques in tool wear measurement and discovered that the tool wear increases in vibration assisted drilling compared to conventional drilling when all the other operational conditions remaining the same. Abtahi [4] continued the wear study using 1” coring bit to increase the bit pressure with more detailed investigation of the wear rate including the bit profile and different modes of wear in the test. Only one flow rate 3 gallons per minute (GPM) is used. He found that changes in bit profile due to wear affected the performance of the bit. He also observed the same increasing trends in the rate of wear in vibration assisted drilling. Babatunde [4] then went into more detail of the input parameters of the vibration assisted drilling. He also used Polycrystalline Diamond Compact (PDC) bits to investigate the effect of vibration frequency combined with amplitude. Babatunde [4] suggested that the ROP can be also increased for PDC bit in VARD. Khorshidian [5] showed that increase in amount of energy of the mechanical attack can result in a higher rate of penetration.

The aforementioned body of knowledge is valuable and is essential in the development of the vibration assisted rotary drilling technology. Each one of the mentioned researchers added a piece of knowledge to the initially completely unknown puzzle, which bring a question of how the vibration enhances the ROP and increases the wear rate of the bit. The role of vibration is not clearly understood and needs much more detailed study and verification.

The previous studies, for the main part, contain lack of concentration on some of the drilling parameters, i.e., flow rate of the drilling fluid, which is water in these experiments. In the previous work, i.e., Abtahi [3] and Babatunde [4], water was provided by the available piping system in the laboratory, and the only means to control the rate was to use a valve to restrict the flow rate from the maximum possible at the supply pressure. There was no guarantee that the flow rate of the fluid in the system remains constant during the drilling due to change in the pressure of the water in the building and change in resistance to flow at the drill bit. There was also no means to measure the instantaneous flow rate of the fluid during the experiments.

Flow rate is undoubtedly one of the most influential factors in the drilling and the above mentioned weakness in the experiments should be of high priority to resolve. One of the main motivations of the current study was to modify the set-up which injects a constant and controllable rate of flow of fluid in the system.

### 1.3 Research Plan

This research adds to the current knowledge of the vibration assisted rotary drilling with impregnated coring drilling bit performance versus the hydraulic system properties (flow rate). The term 'bit performance' is a function of two parameters which are the rate of penetration and the wear rate, a combination of these two factors determine how good the bit performance is. The term performance means the two basic responses of the drilling system which are the rate of penetration and the rate of the wear of the cutting tool (impregnated diamond coring bit).

One of the widely accepted parameters, which are known to be very influential in the wear rate imposed on the tool, is called CERCHAR Abrasiveness Index (CAI) of the rock. This value can be used as one of the rock properties which impacts the bit wear. In order to obtain the CAI value, sacrificial pins, which are called styli, with a specific physical property, i.e., hardness can be used. A second task in this research was to modify and commission a recently constructed CERCHAR testing facility to be used later. Also some preliminary sets of tests were conducted that provide guidelines on the preparation of the material to be used for the styli.

## **2 Current State of Knowledge**

### **2.1 Effect of Flow Rate on Drilling Performance**

The flow of fluid in a drilling operation plays several roles which are vital for the performance of penetration. The main roles are the control of entry of unwanted formation fluids inside the wellbore, cooling the drill bit, transportation of the cuttings from the bottom of the well up in the annulus. Beyond the aforementioned applications, in this study the focus is on the cleaning of the borehole which directly affects the rate of penetration [6, 7]. The appropriate bit hydraulics, in addition to increasing the ROP, can increase the bit life. Tibbitts [8] reported the necessity of bit hydraulics in cooling the diamonds and consequently increase in the bit life.

#### **2.1.1 Fundamentals of Bit hydraulics**

The hydraulic system of drilling is a closed loop of circulation of fluids from mud tanks all the way to the surface piping systems and down the hole through drill string and finally back to the mud tanks [9]. Figure 2.1 shows a schematic of this system. As it can be seen, the mud is being pumped into the well and all the way back up into the annulus carrying the cuttings of the drilled formation. Then it is returned by the return line to the mud processing facilities, such as shale shaker, centrifuges and drill string, to remove the cuttings and prepare the mud again for pumping back in the circulation.

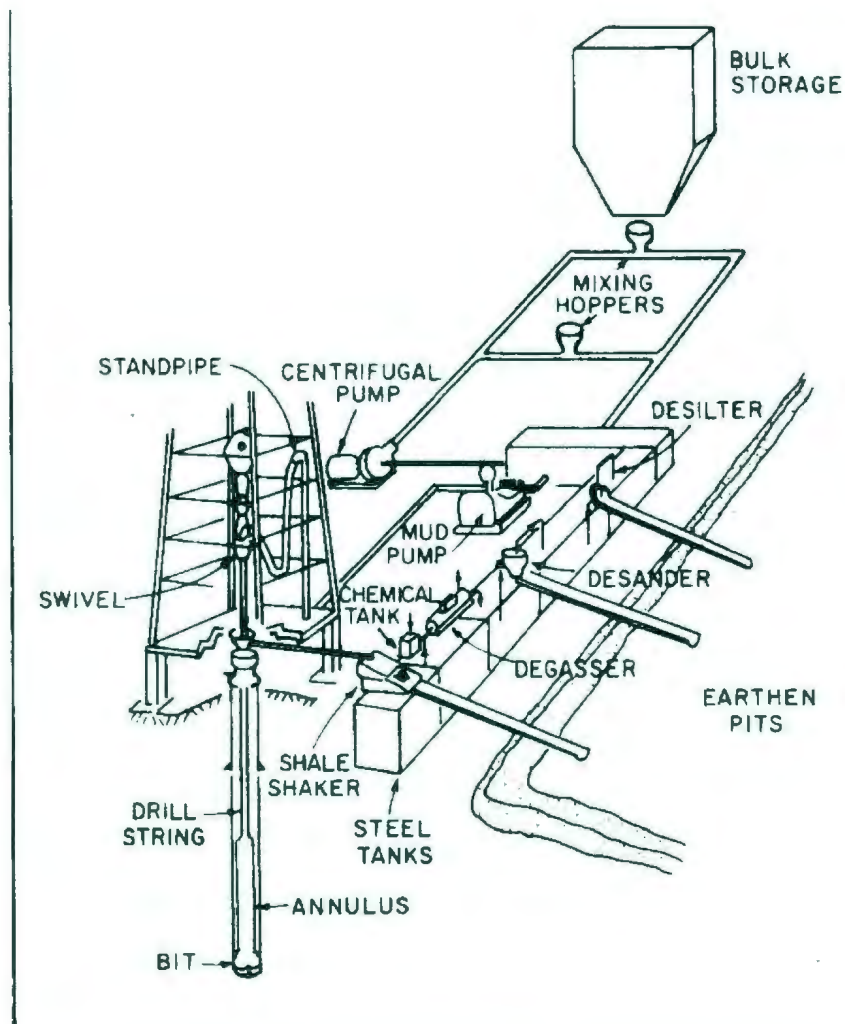


Figure 2-1. Schematic of a rig fluid circulating system (courtesy of Bourgoyne et al. [9])

Lim and Chukwu [10] made a series of experiments using an in house flow loop drilling simulator and aimed to investigate the effect of hydraulic horsepower of the fluid at the bit, and the impact force of the fluid at the bit on rate of penetration. These two parameters have always been the objective functions when it comes to maximizing the efficiency of a drilling system [11]. They concluded that the unbalanced jet force from the

bit nozzles can enhance cutting transportation and eases the process of removing the cuttings from the region right below the bit to the annular space.

A series of investigations conducted by Humble Oil and Refining Company were made to gain more insight into role of hydraulics and especially bottom-hole cleaning. Eckel and Nolley [12] made a mathematical analysis, which is based on the hydraulic parameters that they believed are influential on the rate of penetration. Then, they developed a series of charts which by utilizing them, choosing an optimum nozzle size and pump liner is made possible. Another report by Kendall and Goins [13] was concerned with the same objective but looking at different parameters which are bit hydraulic bit horsepower, impact force and nozzle velocity. They provided some sample charts showing optimum pump operating conditions based on each of those three parameters to be maximized.

Accompanying the same series of investigations, there is the work published by Bielstein and Cannon [14] who studied the factors affecting the rate of penetration for roller cone bits. Their approach was also experimental and they did not merely look into the hydraulic system effects. However, the hydraulic system studies took a significant portion of their work. They (like the majority of previous studies) stated that the fluid velocity at the nozzles highly affects the rate of penetration. They also proposed an optimized design of nozzles which maximizes the hydraulic horsepower transferred to the bottom hole and thereby the rate of penetration. They commented that the fluid distribution is an important factor in changing the drilling characteristics of the bit. They also indicated that the bit

durability can also be affected by the hydraulic factors. The same authors in another report [15] went through the details of nozzle design and how it affects the rate of penetration and also pump operating conditions. Their experiments were conducted in low and high pressure and among their results was the conclusion that drag bits, if the nozzles are placed close to the cutting edges, results in both increased bit life and rate of penetration.

Hellums [16] in the same series of investigations elaborated more on the effect of pump horsepower on the rate of penetration. This study also commented on the significance of hydraulics in the bit life or in the other words the bit wear rate. It was confirmed that the maximum achievable penetration rates can be reached for a certain drilling operation if the hydraulic horsepower of the pump is consumed mainly at the bit and the minimum horsepower required to lift the cuttings is consumed at the annular space.



**Figure 2-2. fluid jet exiting the nozzle**

In another research on effect of the bottom hole cleaning on penetration mechanism, Bizanti and Blick [17] studied the fluid dynamics of wellbore bottom hole cleaning. They ran a series of tests on a research rig investigating the variables affecting the rate of cutting removal. The distinctive point about these tests was that no rock cutting or penetration was done and the bit was set at a preselected height, above a packed column of cuttings. They then changed the hydraulic parameters of the system to see the

corresponding response in the bottom hole cleaning. Figure 2.3 shows a schematic diagram of their experimental set up.

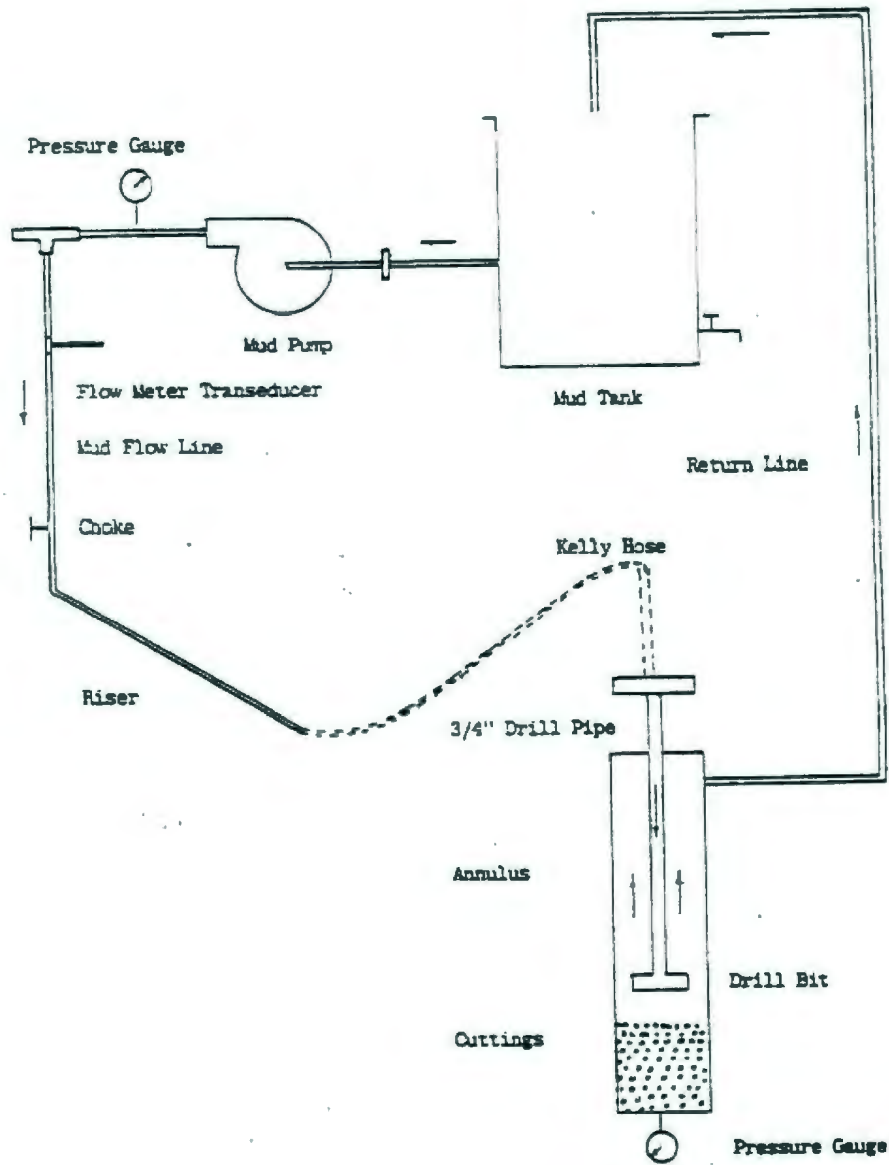


Figure 2-3. Schematic diagram of the circulating mud system used by Bizanti and Blick [17]

They defined a parameter which is a good indicator of the cleaning efficiency and is the ratio of cuttings mass flow rate to mud mass flow rate. This parameter was found to be a strong function of Reynolds number and nozzle height above the bottom of the hole and cutting density.

Ledgerwood and Salisbury [18] argued that poor bit hydraulics results in accumulation of cutting material around the bit. This condition of drilling, which is shown in Figure 2-4, is accompanied by a very low rate of penetration as the bit is not able to meet fresh surface of the rock for an efficient generation of the fragments.



**Figure 2-4. Accumulation of cutting material around the bit in poor bit hydraulics condition (after Ledgerwood and Salisbury [18])**

More recent studies, as mentioned in the beginning of this survey of literature, are more concerned with new techniques. Kuru et al[19] in 2005 made a similar study to those

mentioned previously [12, 13] with the difference that they studied foam as the drilling fluid. Foam is in nature a two-phase fluid consisting of liquid and gas phases plus surfactant, the hydrodynamics of the foam is more complicated than conventional drilling muds and this paper deals with introduction of a method to optimize liquid and gas injection rates to obtain the maximum penetration rate while drilling with foam.

Moving to more recent works, Qahtani and Amanulah[20] in 2010 presented a hole cleaning prediction tool which is claimed to be user-friendly and easy to use and at the same time provides a decent estimate of the borehole cleaning efficiency inputting the operational conditions such as hole geometry and mud properties and subsurface conditions and cuttings properties. They mainly used empirical correlations to estimate rheological properties of the mud in various temperature and pressures. Their cutting transport model mainly was based on the concepts of slip velocity of solid particles in the liquid and the slip velocity itself is calculated based on some more empirical correlations that they presented.

The work by Malekzadeh and Mohammadsalehi [21] presented a more accurate method to optimize the borehole cleaning efficiency in directional and mostly horizontal wells. Their study was an advanced combination of the works such as Qahtani and Amanulah [20] in the modeling of the cleaning efficiency and also the earlier works on drilling hydraulic optimization studies such as [12] and [11]. Their method gives the minimum flow rate required for the transport of cuttings for all ranges of inclination angles. They

also presented a plotting technique using which mud properties are given in a way that the calculated optimized flow rate becomes higher than the minimum flow rate required for cutting transport.

Ersoy [22] in laboratory study, made a brief discussion on the role of flow rate in the drilling performance. His drilling unit's hydraulic system had two components which are the power rack and hydraulic control. A flush tank was used to provide water supply for the drilling operation. He used three types of bits: pin, hybrid, and impregnated diamond. The drilled rocks were Sandstone, Siltstone, Diorite, Granite, and Limestone. He observed two main trends in their experiments; the first one was that there exists an optimum value for the weight on the bit in which the penetration rate and the drilling mechanical specific energy are almost maximum and minimum respectively. This trend has also been observed and confirmed in a lot of other experiments conducted later on by other researchers. With regards to the hydraulic system, his initial system has some flaws and leakages that prevented the proper operation of the system and that made them unable to have flow rates above 15 Liters/Minute in their system. After overcoming this problem, they reported that the rate of penetration increased with the flow rate for flow rates below 25 l/min and then it became independent of the flow rate above 30 l/min flow rates. His explanation for this observation is that for flow rates below a certain limit (which is different for various drilling operating conditions) the cleaning efficiency may be insufficient for the cutting process and, therefore, the higher the flow rate in this range, the better the cleaning efficiency and the better the rate of penetration. Above a certain

flow rate, the cleaning of the borehole is the maximum possible and there is no need to have higher flow rate as it will merely consume more energy and will not add to the efficiency of drilling.

In general, all the investigations on bit hydraulics stress on the impact of bottom hole cleaning on the ROP and bit performance, in which providing a better condition of cleaning of the generated fragments can significantly increase the ROP.

### **2.1.2 The concept of rock abrasiveness and its measurement methods**

Rocks have numerous measures of their physical properties, such as, compressive strength, modulus of elasticity, Poisson's ratio, grain sizes and the strength of the bond between grains. Thermal properties and a lot more are also associated with them. The abrasiveness of the rocks is a special measure that sometimes is confused with the rock hardness. The hardness of the rock is a measure of how strong the rock is when it comes to rock breakage and failure and it does not necessarily have anything to do with the abrasiveness which is a measure of how the rock affects another external body in contact with it. They might be correlated in some special cases but, in general, they are two independent properties of the rocks.

The term abrasivity describes the potential of a rock or soil to cause wear on a cutting tool [23]. As the potential to cause wear on a tool depends significantly on the specific circumstances of the observed system (e.g. involved tools, mechanisms of excavation,

temperature, applied loads, etc.) it should nevertheless be kept in mind that rock abrasivity can never be an intrinsic physical parameter as for example rock strength.

The abrasiveness of the rocks was long believed to be just a function of their quartz content and it was assumed that the main part of the abrasion comes from the quartz contained in the rock mineralogical composition. Over the time, by expansion of mineralogical knowledge, inclusion of other minerals into the measure of abrasiveness was considered. Moh's scale of hardness is a common measure to associate a hardness number to a mineral. When applied to a rock a Moh's hardness number is associated with each mineral in the rock and a weighted average determined, based on the weight percentage in the rock of each mineral present.

Other similar hardness measures include Rosiwal grinding hardness and Vicker's indentation hardness. These types of hardness measures are insensitive to rock grain size and shape and strength which might as well be influential. For example, according to these scales three sandstone samples with the same mineralogy but different degree of consolidation have the exact same value but they obviously may cause highly different amounts of wear on a cutting tool.

In order to develop a more descriptive measure of abrasiveness which also makes more sense in terms of wear rate too, Plinninger et al. [24] proposed a parameter called Rock Abrasivity Index (RAI) which takes into account both the mineralogy and strength properties of the rock. The RAI represents a modification to the Equivalent Quartz

Content (EQC) and is applicable not only to hard rock but also suitable for weak rock types (the EQC concept is discussed in 2.2.3). It is basically an average of the rock's individual mineral's UCS by their hardness and content. They claimed that this RAI parameter can be better correlated to the drill bit life time (or in the other words, wear rate).

Sometimes the term hardness is used for the concept of the abrasiveness which might cause some confusion. For example hardness is described as a concept related to the material behavior rather than a fundamental material property and depends on the type of the test being conducted [25]. There are three types of hardness tests: indentation tests and dynamic or rebound tests and scratch tests. The scratch test is one of those tests that merely measure the abrasiveness of the rock regardless of its hardness. A report [25], from the International Society for Rock Mechanics (ISRM), was an effort to standardize all the rock material properties tests and grouped rock hardness and abrasiveness into one single category without a clear distinction between them. These two concepts coincide if the Moh's point of view is accepted [26] (saying that material A is harder than B means that A can abrade B). On the other hand "penetration hardness" is more independent of the abrasiveness concept and the main reason is that the penetration hardness is a property of the rock that determines how the external contacting body penetrates inside the rock before any scratch is being made. This definition of hardness, in the author's opinion, is more clear and distinctive when it comes to comparing hardness and abrasiveness.

The wear on tunnel boring machine (TBM) tools can be estimated using abrasiveness measures such as Vicker's Hardness Number (VHN) and others; however, Moh's hardness again because of not considering some important parameters such as grain size, shape and the bond strength between the bonds has been reviewed by Nilsen [27]. However, evaluation of these properties is difficult. West [28] also reviewed and listed abrasiveness tests done on rocks categorizing them into petrological and mechanical tests; where the petrological tests are those which measure the abrasiveness using the mineral compositions, he also made interesting conclusions and evaluations, the main one being that there is no single test that could be totally descriptive of the rock abrasiveness and each test possesses its own advantages and disadvantages. A unique study done by Smorodinov [29] who estimated the value of abrasiveness based on radioactivity of a special standard "spot of grinding" which is the radioactive trace of grinding the rock using a specialized tool. The tool with which the rock was cut was radioactive and the Neutron flux was measured using a measurement device. No detailed description of the work is given in the paper.

In this research, equipment for CERCHAR tester which is one of the most accepted and applied abrasiveness tests was commissioned.

### **2.1.3 CERCHAR test for measuring rock abrasiveness**

CERCHAR scratch test was originally developed in 1970s by CERCHAR Institute in France and used in the French and British coal mining industries while gradually being

adopted for application in tunneling industry [30, 31]. Different setups are available for CERCHAR testing. In general, a CERCHAR test consists of a vice holding the sample while a hardened steel stylus with a 90 degree cone tip is scratched over the rock under constant load of 70N [32]. An illustration of the CERCHAR test is shown in figure 2-5 [27].

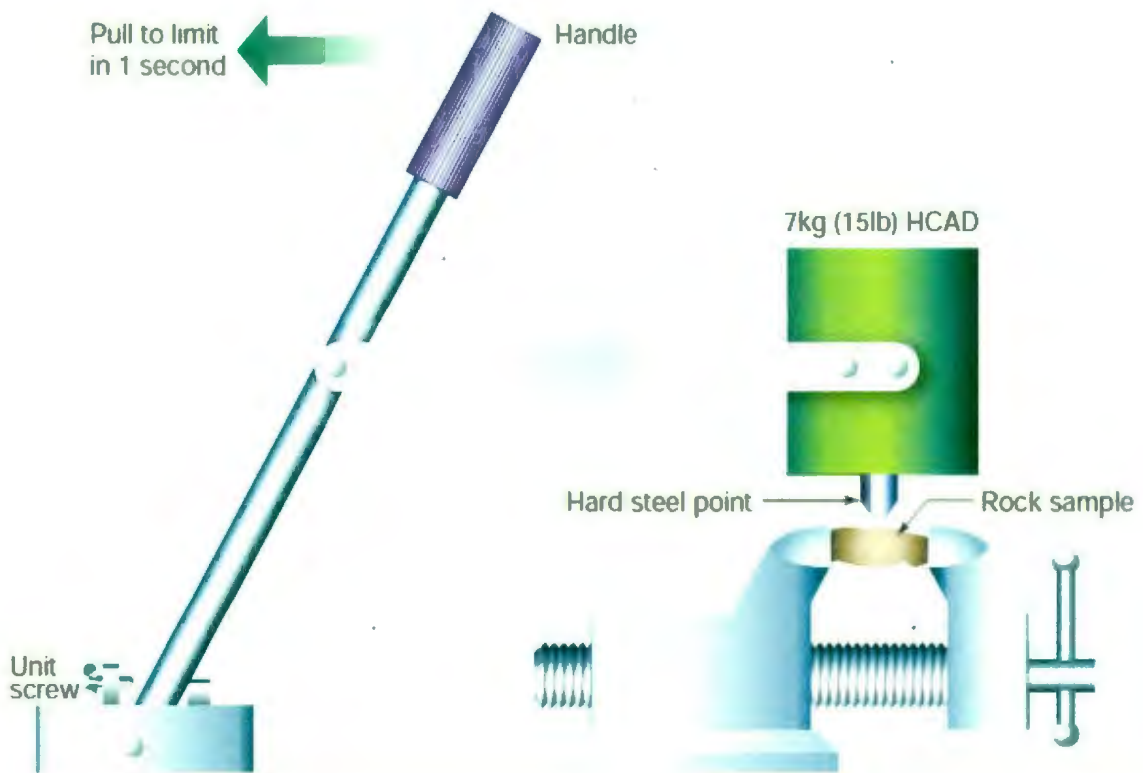


**Figure 2-5. The CERCHAR test (after B. Nilson.[27])**

As mentioned in the previous section, ISRM has published a series of standard tests for rock; however, in their hardness and abrasiveness category we cannot find a standard for CERCHAR test [25]. Recently in 2010, American Society for Testing and Materials

(ASTM) introduced a standard for the CERCHAR test [33]. Before that, the best description of the CERCHAR test that could be used as a standard reference was the French standard NF P 94-430-1 [34]. The result of a CERCHAR test measurement is a parameter called CERCHAR Abrasiveness Index (CAI) which is a valuable predictor of the wear induced on a rock excavating tool. However, the CAI value measured is highly sensitive to the hardness of steel styli and the method by which the experiment is done [35].

The value of CAI is calculated by measuring the wear flat diameter (d) of the stylus tip after performing the test in micrometers, [34].

$$\text{CAI} = 0.01 d \quad (2.3)$$

As mentioned above, the results of the test are very sensitive to the specifications of the steel styli. According to the French standard NF P 94-430-1 the tip of the steel stylus applied to the rock sample is formed as a sharp conical point of cone angle equal to 90 (with 3 degrees of tolerance) and 1mm length. The overall length of the steel stylus should be greater than 15 mm. This geometry is generally the same in various references; however, this is not the case for the hardness of styli [35].

Clearly the hardness of styli affects the outcome of the test [36]. Several authors proposed slightly different specifications for the steel stylus in some of them [28, 37, 38, 39, 40] in addition to some other specifications, the tensile strength of the styli was recommended to

be 2000 MPa , which is considered to be equivalent to HRC 57. The Rockwell hardness value for the styli in most of the references [34, 37, 39, 40, 41, and 42] is specified to be between 54 and 56. Some references have different specifications for the styli for example Al-Ameen and Waller [36] who have a recommendation of a steel styli of type EN3 and heat treated to approximately 19 HRC. Another example is West [28] who recommended an HRC value of 40. Based on all these observations, it seems that a standard steel stylus is better to have a Rockwell hardness value of 55 and a tensile strength of 2000 MPa. To be used as one reference, the ASTM standard for the CERCHAR test, D7625-10 [33], recommends the use of styli hardened to 55HRC and also lists criteria for the test, based on styli with a hardness of 40 HRC.

Gharahbagh et al. [32] reviewed other parameters that might also influence the results of a CERCHAR test. Among those parameters, we can find the number of tests done which is recommended to be more if the rock sample is coarse grained [28] (more than 1 mm : five or more tests). Even the confining stress around the sample (if any) can affect the results of test [30]. Another important test operational parameter is the method of measurement of the wear flat diameter and is not described in detail and the only specification is to use a microscope [36]; however, recently Rostami et al.[43] addressed the parameters that could affect the test results and described the test sensitivity with respect to them. They also suggested that in order to minimize the experimenter's error, it is better to take the measurement of the diameter of the wear flat on a view/picture of pins taken from side by a microscope.

The dependency of CAI on various parameters is investigated by some authors. For instance, Sascha and Michael [44] performed a series of experiments looking into the effect of the confining pressure on CAI value of the rocks and came up with a linear relation between CAI and confining pressure as shown below.

$$CAI_{\sigma} = m\sigma + CAI \quad 2.4$$

Where  $CAI_{\sigma}$  is the value of abrasiveness index of the specimen under  $\sigma$  confining pressure and CAI is the abrasiveness value for no confining pressure (atmospheric). The coefficient  $m$  depends on the rock type and is calculated to be equal to 0.1 for Coburg Sandstone.

#### 2.1.4 Rock abrasiveness and drilling performance (wear rate)

The aim of all the abrasiveness concept developments and testing methods to give quantitative measures of a rock abrasiveness is finally to apply the concept in order to optimize the performance of a certain system. In our studies, the system is a rock drilling system. This section is dedicated to a survey of available literature that has worked on the subject of drilling performance and the influence of abrasiveness of rock on the wear rate of a drill bit.

Thuro [45] looked at the relation between the drill bit wear and the abrasiveness of the rock which he mainly took to be the same as the parameter called Equivalent Quartz Content (EQC) of the rock. This parameter is defined as given in equation 2.5.

$$EQC = \sum_{i=1}^n A_i R_i$$

2.5

Where A is the percentage of the mineral amount in the rock, R is the percentage of Rosiwal abrasiveness and n is the number of minerals in the rock. It should be noted that R has a value of 100 for Quartz and has lower values for minerals less abrasive than Quartz and vice versa. Based on this concept they mapped the results of 42 case studies in 8 tunnel projects which is shown in figure 2-6.

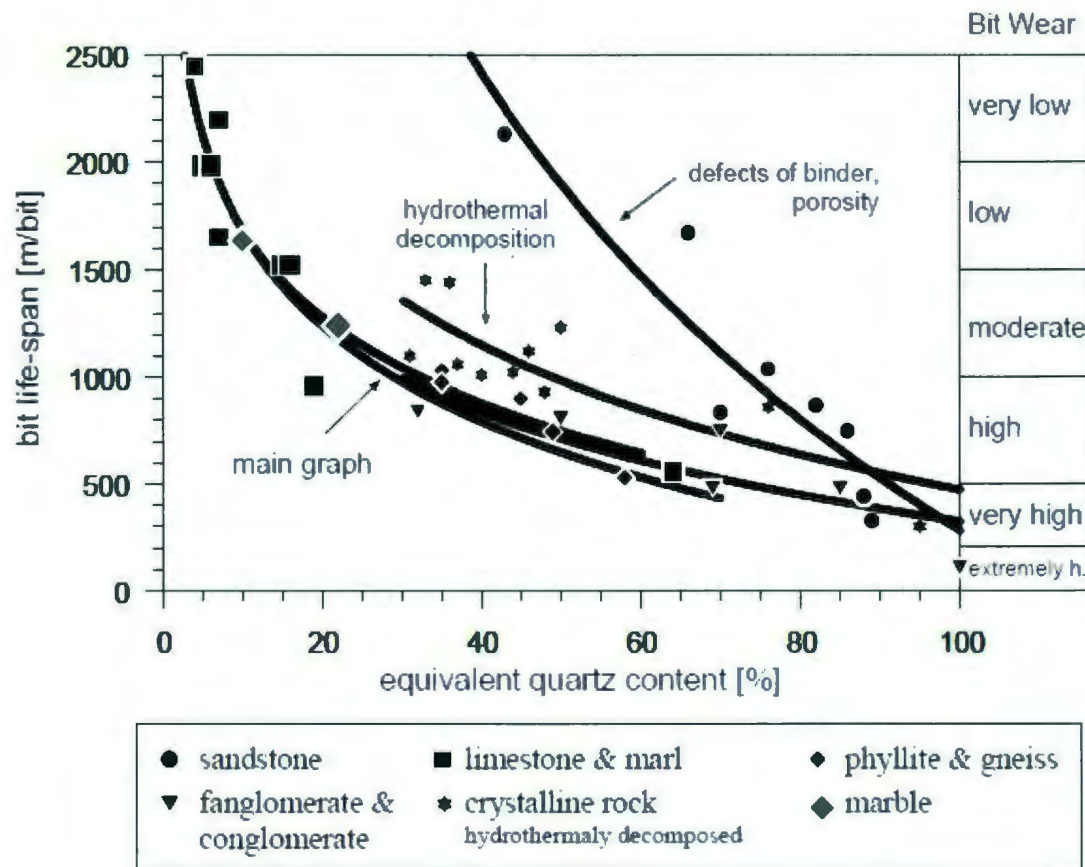


Figure 2-6.Bit life of different rock types correlated with EQC (courtesy of Thuro[39])

As it can be seen in the figure, there is a good correlation between this parameter and the bit life for the cases studied. Also, for each category of the rocks the trend is different; however, the general statement of decrease in the bit life by an increase in EQC stands for all the cases. They also developed some correlations relating the bit life to the logarithm of EQC. There is also another good indicative of drilling performance which is called Drilling Rate Index (DRI) [46].

Mensa-Wilmot and Fear in 2001 [47] investigated the effect of formation hardness and abrasiveness on Polycrystalline Diamond Compact (PDC) bits performance. They looked into the performance of these bits in harsh environment and they divided the harsh environments into two more categories of hard formations and abrasive formations. They considered carbonate bearing rocks such as limestone and dolomite as hard drilling environments and stated that these formations cause more wear on the inner part of the bit than the outer part (the inner part is being defined as the central two-thirds of the bit). This phenomenon reverses when drilling in abrasive formations which according to the authors are mainly sandstone and siltstone bearing formations. Based on these observations and other facts they brought some development methodology guidelines for drill bits in hard and abrasive formations. An important point in these guidelines is the fact that the durability of the bit is important in abrasive formations; however, for hard formations it is not influential. In formations composed of hard rocks, stabilization of the bit is the factor that needs to be enhanced in order to achieve the best bit performance. In other words, the harder the rock, the more focus should be on bit stabilization and the more abrasive the rock, it should be on bit durability (please refer to the Section 2.2.1 for a delineation between abrasiveness and hardness).

Dealing with abrasive formations, Besson et al. [48] presented their work on designing a specific bit that greatly improved the performance of a drilling system in an ultra-abrasive sandstone formation and reduced the number of bits needed to attack that formation. The features of the chosen roller cone bits were optimized in a way which reduces the sliding

or friction of the cutting structure on the formation. Some of the teeth were systematically selected to be enhanced with diamonds. The results of this new design reduced the number of bits required to drill this formation from 11 bits in the first well to 6 bits in the fifth well which means a significant cost saving and enhancements in oilfield development feasibilities.

### 3 Coring Drilling Experiments

#### 3.1 Background and Previous Pertinent Work

In order to study the phenomena affecting penetration mechanism of impregnated diamond coring bit a drill setup was fabricated. Li [1] set up a drilling apparatus which was basically composed of a drilling head which was attached to a coring drilling bit. He attached a vibratory table at the base of the device, where the rock sample is placed, and made arrangements so that the device vibrates the core to be drilled while conducting the coring experiments.

Zhang [3], made a study of bit wear and reported on the techniques developed and used it to investigate bit wear in particular the very small amount of wear in short laboratory tests. He drilled two types of material with impregnated diamond coring bits using the laboratory drilling rig that was developed by Li at one rotational speed and over a range of weights on bit under conventional and also vibrational rotary drilling condition. He made replicas of cutting segments on impregnated coring bits to record the status of the bits after drilling. He measured the wear (weight loss and height loss) of each bit after a series of holes were drilled in concrete specimens. Also, the wear of diamonds and the matrix on each bit used in hard rock drilling was measured on replicas with optical microscopes. He observed that the wear amount after each drilling increased with an increase in weight on bit. According to the results, the vibration assisted drilling produced more cutting tool wear than the conventional rotary drilling under the same weight on bit.

This study, in the sense of drilling response, compliments the one that was done by Li[1] and provides insight into the rate of wear rather than the rate of penetration of the cutting tool. Both studies used the same type of bit (coring bit), which was also used for this study, and also in both studies, the flow rate of the drilling fluid (water) was not considered in the analysis.

Following the initial investigations mentioned above, Abtahi [4] made a more detailed study on the wear of this drilling set-up. He discussed an interesting set of wear measurement techniques both for coring and full faced bits. This is the first study in this sequence of studies in which full-faced bits are actually discussed. He described simple techniques such as weight measurement, height measurement and also more rigorous methods such as microscopy as well as more advanced techniques such as replica and indentation tests. Regarding the replication methods for the measurement of coring bit wear, he mentioned that, according to his experience, the microscope photos taken from the coring bit itself is more descriptive of the wear state than those of replicas. In the experiments that he conducted, he confirmed that the bit profile changes as the bit wears and that profile shape affects ROP significantly. In all his experiments, three main profile shapes appeared after some drilling in the sequence of: V-grooved, flat end, and rounded edge. The highest ROP results were obtained with V-grooved, decreasing in the order: unused, flat end, and rounded edge. Nevertheless, he found that vibration has more effect on bit wear than profile shape. The change in ROP/wear rate with respect to profile is a factor that was not considered in the research work brought in this thesis; since, the aim of this research is

different and there was no practical way available to conduct the experiments keeping the bit profile perfectly constant. However, arguably, the change in the input factors of the current study (WOB and flow rate) has an order of magnitude higher effect than the small profile changes resulting from one experiment to the other. Abtahi acknowledged the issue of the drilling fluid source and the deficiencies it caused and suggested a modification to the set-up.

Babatunde [4] had an emphasis on the rate of penetration as a function of frequency and amplitude and WOB for full-faced bit (impregnated diamond and PDC) and his experiments were also carried out accordingly. For his particular drilling conditions he found that there is an optimum vibration frequency (55 Hz) in which the ROP maximizes. He also made wear study on the bit he used using microscopy methods and found that there was negligible wear of the bit used in his experiments, which therefor had little effect on the drilling performance in the consecutive tests that were run. According to his study, the effect of the so-called 'bit hydraulics' is negligible compared to the vibration effect. This claim was made on the basis of the differences in specific energy calculations for the conventional and vibration assisted drilling cases and also hydraulic contributions to the specific energy. He put more emphasis on the vibration characteristics of the system when he switched to PDC drilling experiments, mainly due to the observation that the vibration amplitude could not be kept at a determined value by changing the WOB and it tends to decrease as the WOB increased. In a similar bit hydraulics analysis he made the same claim that the hydraulics contribution to the drilling energy is much less compared to the vibrations for PDC bit as well. These results, again, makes it demanding

to take a closer look at the hydraulics of the drilling system and observe the effect of hydraulic in action, i.e. by systematically changing the flow rate and observing the performance. This will give a more tangible conclusion than those made in Babatunde's [4] study in which the flow rate was, supposedly, kept constant.

### **3.2 Justification of the Work**

This work adds to the previously done investigations in the Advanced Drilling Group by Zhang [2], Abtahi [3] and Babatunde [4]. In all of these the flow rates essentially could not be controlled throughout the process. As reported by Abtahi [3], the flow rate decreases as the drilling head penetrates more into the rock sample. The reason for this is that, as the drilling head penetrates more into the sample, there is more pressure needed to be overcome and the tap water pressure is not sufficient and therefore the flow rate decreases. In this work, it was tried to account for this and therefore a constant flow rate was maintained during the experiments. Maintaining a constant flow rate is the common drilling practice.

In order to have flow rates as high as 5 gallon per minute established throughout a complete experiment with a core drill we can compute the minimum pump power requirements for the pump to be used. We can use the frictional pressure loss relationships that were discussed in the literature review of this thesis in the related section [8].

In order to provide the drill setup with an accurate hydraulic system, a pump, a fluid reservoir, control valve and flow meter are added to the previous drill setup. A ball valve and a flow meter are located in between the pump and the swivel of the drill head. By adjusting the opening of the ball valve the amount of flow rate can be adjusted at desired value. Additionally, a pressure transducer measures the injection pressure of the flow behind the swivel. The flow rate control will give more insight into the performance of drilling; especially, when the efficiency of the bottom hole cleaning is the point of view. Also the combined effect of the flow rate, other vibration-assisted rotary drilling parameters and other conventional common drilling parameters, e.g., weight on bit, will add one more piece to the currently semi-complete puzzle of vibration assisted rotary drilling. The output parameters to study in conjunction with adding the flow rate control capability were the rate of penetration and wear rate.

Section 3.4 describes the conceptual drilling system and a simple descriptive model and the associated pump power calculations.

### **3.3 Preparing Concrete sample**

One type of concrete sample was used, as analog for rock, in all of the experiments. That is made from aggregate and type 10 Portland cement. According to CSA A3001-03 the previous designation Portland cement type 10, is now GU (General use) Portland cement. [The ASTM designations are type I (ASTM C150) corresponding and type GU (ASTM C 1157)]. The aggregate was sieved to include only sizes less than 1mm. The samples were

cured in 100% relative humidity for a month to achieve the highest possible strength value. To ensure 100% relative humidity, all of the samples were submerged in water, after initially setting for 24 hours, according to the ASTM standard ASTM C873. UCS values at the standard time test of 7 and 28 days were 38.7 MPa and 45.08 MPa respectively. Table 3-1 shows concrete ingredients ratio and UCS values. UCS is an acronym for ‘Unconfined Compressive Strength’ which is a widely used parameter to determine the hardness of the rock; this parameter is a measure of the maximum compressive stress that a rock sample can withstand before failure in unconfined conditions.

**Table 3-1. Concrete ingredients ratio**

Aggregate Mass	Cement Mass	Water mass	Cement/Agg	Water/Cement	UCS 7 days	UCS 28 days
78 kg	40 kg	24 liter	0.5	0.6	38.7	45.08

### 3.4 Drilling Test Facilities

#### 3.4.1 Experimental setup

The experimental drill setup in a laboratory size was used for the experiments. Experimental drilling facility of the VARD project is built up from a Milwaukee 4079 electrical powered coring drill rig which is able to deliver maximum power of 4 kW to the

bit. The rig has two rotary speeds: 300 and 600 RPM of which the RPM of 300 is selected for performing entire tests. The drill and motor assembly can move vertically on a carriage along a guide rail. Figure 3-1 shows the drill setup schematically.

The source of WOB is a suspended weight on a wheel which is connected to rack and pinion with a gear ratio of 10. In this way the bit is provided by the load of the drill head assembly (25 kgf) plus a force which is 10 times greater than the weight of the suspended mass.

For the work in this thesis the following was added:

A tank reservoir with capacity of 40 liter, a submersible centrifugal pump (EI00ELT, Flotec), a globe valve and an in line flow meter (FL46300, Omega) and a digital pressure transducer. The globe valve can be used to adjust the rate of water injection at levels selected for the tests. The flow meter shows the flow and the pressure transducer measures the injection pressure behind the swivel of the drill setup.

A magnetic force vibrator is attached to a plate below the rock specimen. The rock specimen is also fixed on the surface of this plate. Compliant elements are located in between this plate and the frame of the drill setup through which the plate can be oscillated when the vibrator is active in the VARD tests. Those compliant elements also keep the plate in its place and cause the plate to vibrate in specific displacement amplitudes.

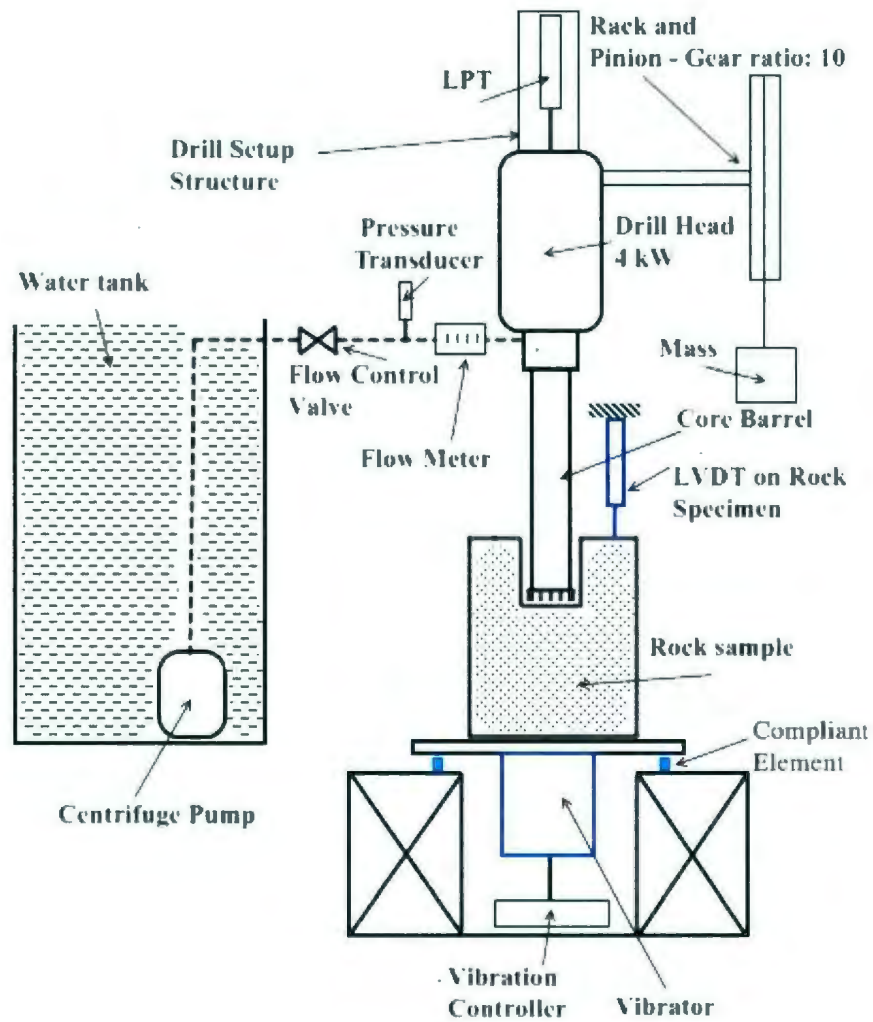


**Figure 3-1. Schematic view of the drill setup**

A Linear variable differential transformer (LVDT) is attached to the rock to measure the vibration displacement of the rock, when the vibration table creates a relative displacement between the bit and rock while drilling operation. A linear potentiometer

transducer (LPT) is also attached to the drill head to measure the position of the drill head vs. time. This data can be used to evaluate ROP of the bit.

All the output data of the electronic instruments are recorded on a data acquisition computer system with frequency of 128 Hz for an accurate data analysis. Figure 3-2 shows the fabricated drill set up.

The characteristics of the vibrator can be adjusted by two controlling systems. The first system is a variable frequency drive (VFD) which adjusts the dominant frequency of the vibrator, and secondly is a potentiometer which adjusts the input power of the vibrator. These two parameters of vibration were adjusted to achieve the best characteristics of displacement of amplitudes. The characteristics of the vibration are presented in chapter 4.

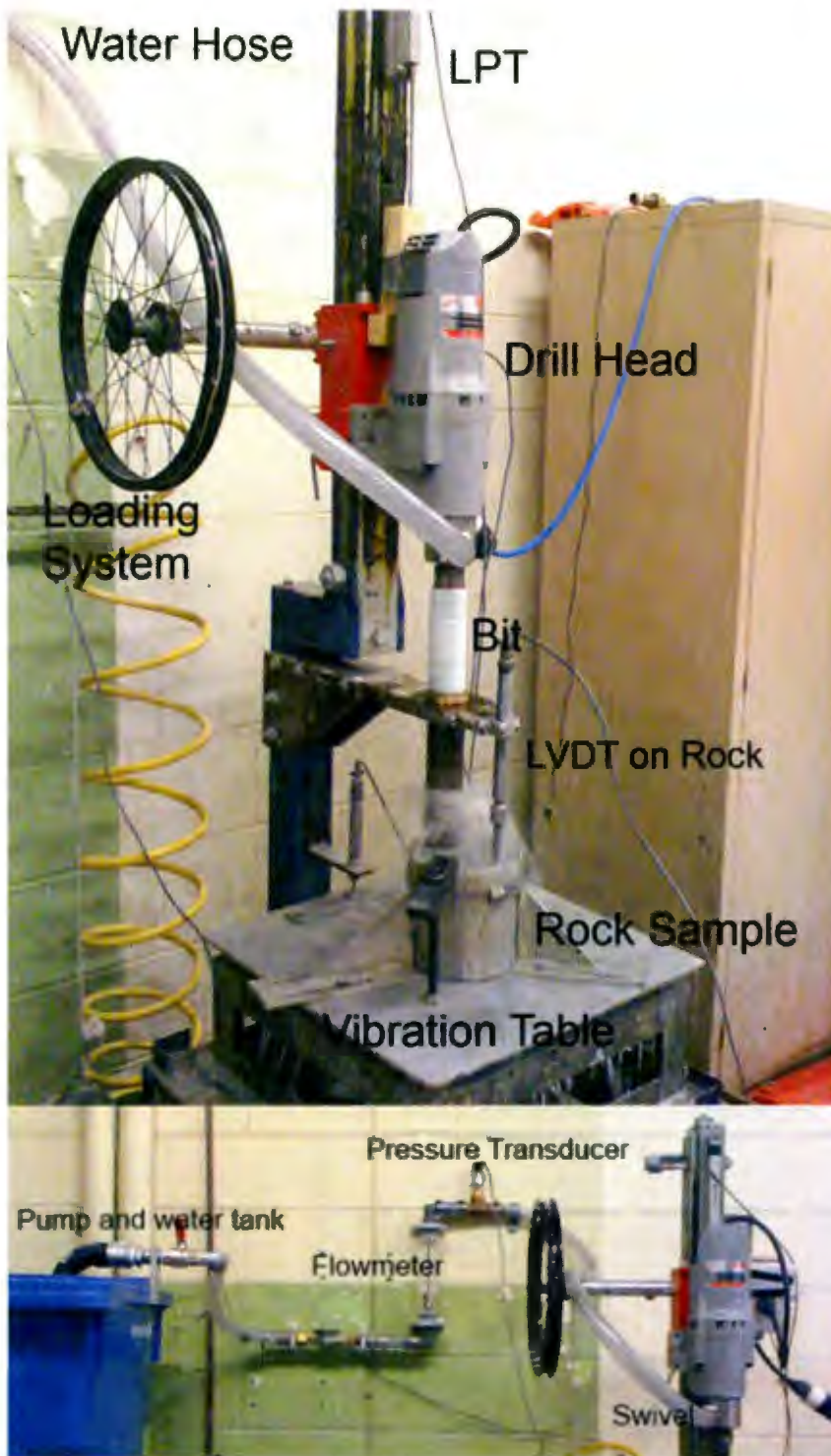


Figure 3-2. Drill setup

### 3.4.2 Bit specifications

The two bits used in this experiment were 2 inch coring formula 400 bits from Diamond Systems Inc. with approximate length of 41 cm and approximate weight of 1.3 kg. One bit was dedicated to tests without vibration and one for the tests with vibration. The cutting end (left in Figure 3-3) consists of five segments with diamonds impregnated in a metal matrix. The segments are separated by water ways through which most of the drilling fluid, i.e. water, flows. The outer diameter of the bit is 2.1", inner diameter is 1.5" and distance between water ways is 0.2".

Each bit was drilled for 30 cm with 120 WOB and flow rate of 4 gpm to ensure that both bits started in the same condition.



**Figure 3-3. Drill bit used for the experiments (core barrel)**

## 4 Design of the Experiments and Test Results

### 4.1 Design of Experiments

The purpose of the set of drilling experiments carried out was to explore the effect of water flow rate, vibration and WOB on drilling response of selected impregnated coring bit.

From the viewpoint of design of experiments, this experimental design is called general full factorial design with two numerical factors (weight on bit and flow rate) and one categorical factor (drilling mode, vibration assisted/conventional) [49]. This kind of a design will give one correlating equation for each element in the categorical factor (in this case two equations). Figure 4-1 shows the experimental matrix; the big advantage of factorial designed experiments is that they can provide invaluable information regarding the interaction of the factors.

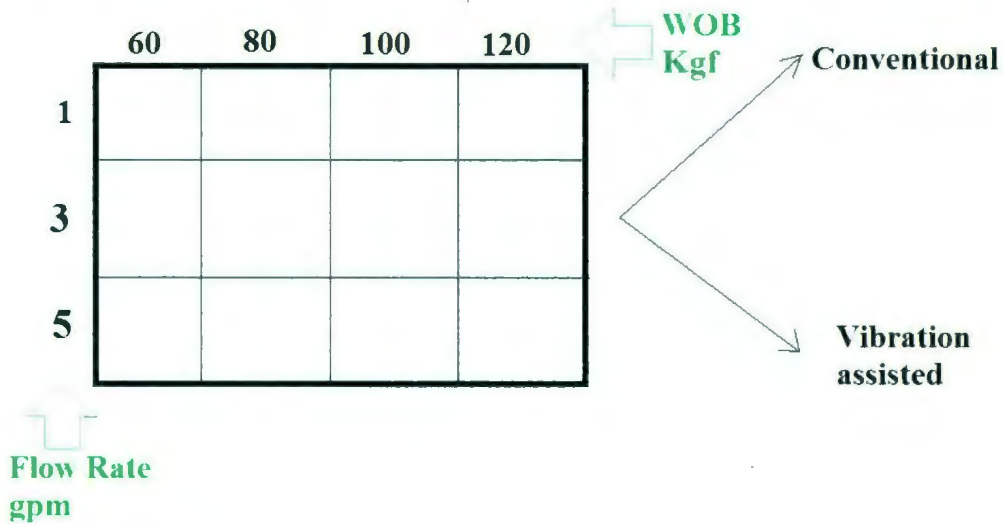


**Figure 4-1. Full general factorial set of experiments**

It can be seen that the WOB is varied over four levels of 60, 80, 100, 120 kgf, and the water flow rate is varied over three levels of 1, 3, 5 gpm. Therefore 12 runs is conducted for each level of the categorical factor which are called conventional drilling test and vibrational drilling test.

In this design set; the data can reveal information on whether the two factors of weight on bit and flow rate have an influence on each other. For example, whether or not higher flow rates start to diminish the boosting effect of the WOB.

In section 4.3, a statistical analysis is conducted using Design Expert [49] to generate equations predicting the ROP based on the experimental data.

## 4.2 Results of drilling Test

Table 4-1 shows the result of the drilling experiment at specific levels of the selected factors with respect to the designed test matrix. The Rate of Penetration (ROP) for conventional drilling and vibratory drilling tests are reported in table 4-1. Additional information such as length of drilled section and the water pressure are also represented.

The test was conducted in three stages in which four levels of WOB examined at the three levels of the flow rate. The first runs are related to the flow rate of 1 gpm and the last runs are for high level of flow rate which is 5 gpm. The aforementioned sequence of the test performed similarly for both conventional and vibratory drilling.

**Table 4-1. Experiment results**

---

<b>FLOW</b> <b>(GPM)</b>	<b>WOB</b> <b>(Kgf)</b>	<b>VIB. ROP</b> <b>(mm/sec)</b>	<b>CONV. ROP</b> <b>(mm/sec)</b>	<b>Water</b> <b>pressure (psi)</b>	<b>Drilling</b> <b>Depth(VIB)</b> <b>(mm)</b>	<b>Drilling</b> <b>Depth(CONV)</b> <b>(mm)</b>
<b>1</b>	<b>60</b>	<b>1.19</b>	<b>0.69</b>	<b>0.15</b>	<b>58</b>	<b>53</b>
<b>1</b>	<b>80</b>	<b>1.28</b>	<b>0.78</b>	<b>0.15</b>	<b>59</b>	<b>52</b>
<b>1</b>	<b>100</b>	<b>1.42</b>	<b>0.84</b>	<b>0.15</b>	<b>60</b>	<b>55</b>
<b>1</b>	<b>120</b>	<b>1.46</b>	<b>0.78</b>	<b>0.15</b>	<b>56</b>	<b>55</b>
<b>3</b>	<b>60</b>	<b>1.52</b>	<b>0.95</b>	<b>1.4</b>	<b>51</b>	<b>53</b>
<b>3</b>	<b>80</b>	<b>1.93</b>	<b>1.18</b>	<b>1.4</b>	<b>53</b>	<b>51</b>
<b>3</b>	<b>100</b>	<b>2.47</b>	<b>1.32</b>	<b>1.4</b>	<b>49</b>	<b>56</b>
<b>3</b>	<b>120</b>	<b>2.55</b>	<b>1.31</b>	<b>1.4</b>	<b>49</b>	<b>48</b>
<b>5</b>	<b>60</b>	<b>2.24</b>	<b>1.64</b>	<b>3.5</b>	<b>53</b>	<b>56</b>
<b>5</b>	<b>80</b>	<b>2.7</b>	<b>1.44</b>	<b>3.5</b>	<b>71</b>	<b>54</b>
<b>5</b>	<b>100</b>	<b>2.67</b>	<b>1.59</b>	<b>3.5</b>	<b>58</b>	<b>57</b>
<b>5</b>	<b>120</b>	<b>2.94</b>	<b>1.87</b>	<b>3.5</b>	<b>54</b>	<b>56</b>

---

The pressure transducer was located 1 m above the rock. The reported pressure in Table 4-1 was measured at a point before the water reaches to the swivel of the drill head. The maximum pressure was observed for the maximum flow rate of 5 gpm. In an individual pressure test at a flow rate of 5 gpm, the drill bit was raised from the surface of the rock and the pressure reading at the gage did not show any significant changes. Therefore, it is concluded that the main part of pressure drop in the drill setup occurred at the swivel of the drill head. Therefore, a backward force which Li [1] considered, applied to the swivel in opposite direction of applied load is negligible. However, due to the 1 m vertical distance between the location of the pressure transducer and zone of drilling (at the bit tip) the hydrostatic component of the fluid pressure at the bit can be in the order of 1.5 psi. Considering the small value of pressure drop on the coring bit with the diameter of 2 inches, the maximum backward force can be only 2kgf, which only existed for the maximum level of the flow rate of 5gpm. This low value of backward force in comparison to the amount of applied WOB is negligible.

### **4.3 Analysis of Drilling Test**

#### **4.3.1 Effects of Flow Rate and WOB**

Results of the experiment are depicted in figure 4-2 and figure 4-3 which are ROP vs. WOB and ROP vs. flow rate respectively.

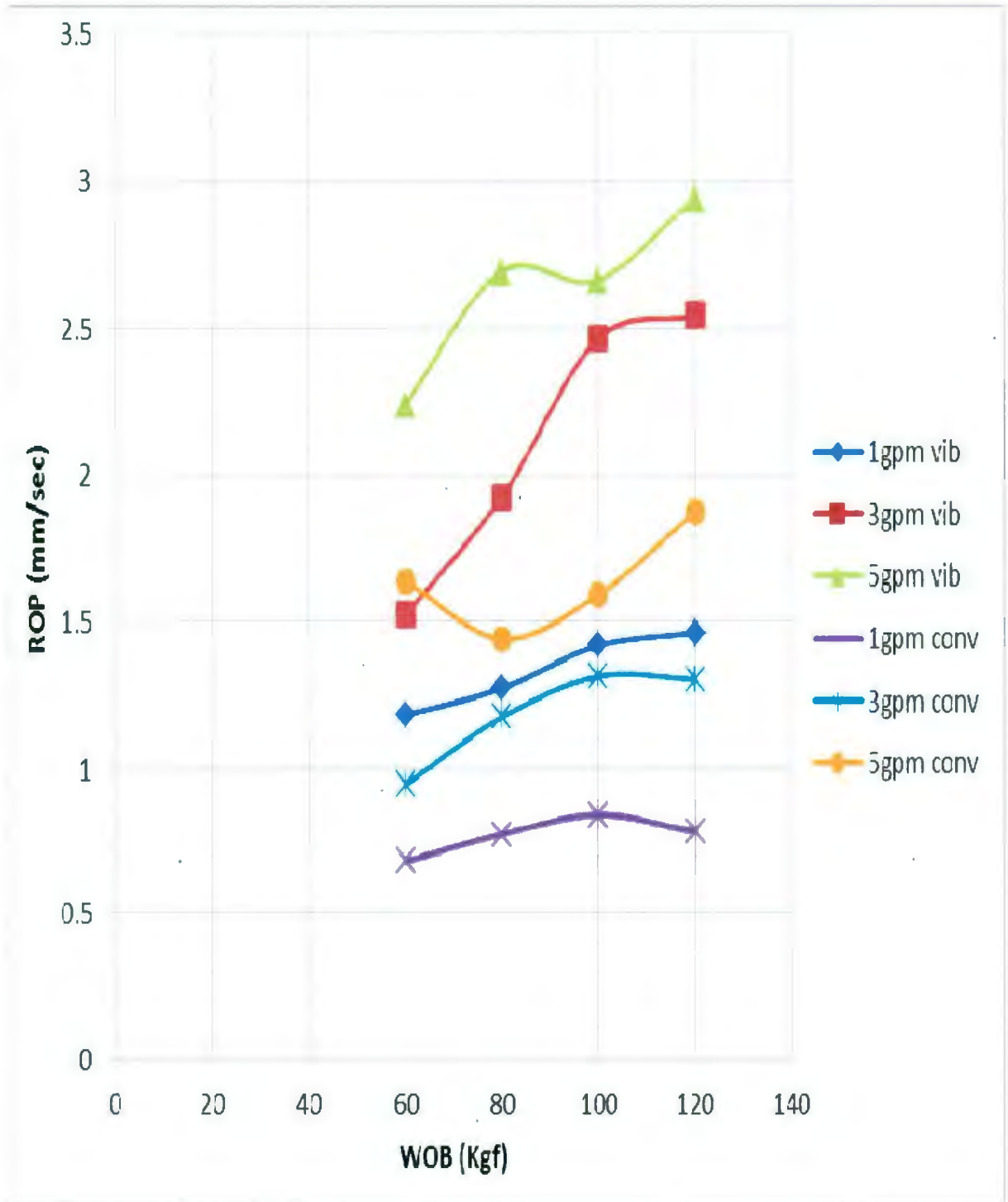


Figure 4-2. Rate of penetration versus WOB for different flow rates and drilling modes

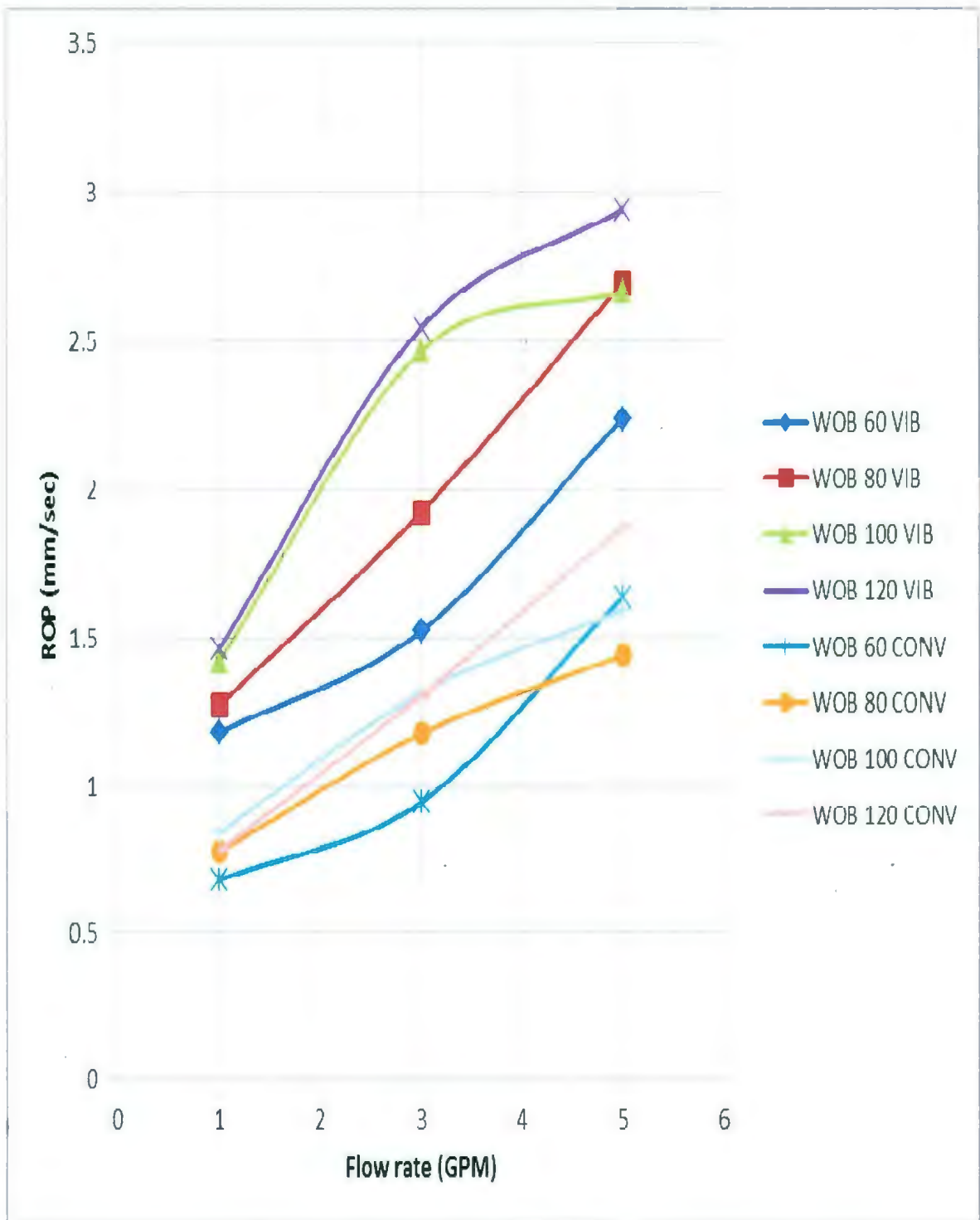


Figure 4-3. Rate of penetration versus flow rate for different weights on bit and drilling modes

There is a consistent pattern in the research except for three of the tests of which are the test with WOB of 60 kgf, flow rate of 5 gpm in the conventional drilling and the test with WOB of 100 kgf, flow rates of 3 and 5 gpm in the vibratory drilling.

In the conventional drilling at flow rate of 1 and 3 gpm the ROP was increased by increasing the WOB from 60 to 100 kgf, but increase the WOB to 120 kgf yeild decrease in ROP which indicates the founder point. In addition, at flow rate of 5 gpm no bit floundering was observed. The existence of founder point implies that the efficient cleaning of the generated rock fragments plays an important role for applying a higher power of mechanical attack to the rock by increase in WOB. This objective can be achieved by applying appropriate bit hydraulic power.

In the vibrational drilling tests, due to contribution between the flow rate and vibration no bit founder will be observed. Also, vibration causes enhancement in ROP.

The result of the experiment was analyzed [50] to achieve following empirical correlations, which equation (4-1) shows the the correlation of ROP vs. WOB and flow rate in the vibrational drilling and the equation (4-2) shows the correlation of ROP vs. WOB and flow rate in the conventional drilling.

$$\begin{aligned}
 ROP(vib) = & -0.644 + 0.395 \times Flowrate + 0.027 \times WOB + 1.361 \\
 & \times 10^{-3} Flowrate \times WOB - 0.032 \times Flowrate^2 - 1.135 \\
 & \times 10^{-4} \times WOB^2
 \end{aligned}
 \tag{4-1}$$

$$\begin{aligned}
 ROP(Conv) = & 0.564 + 0.148 \times Flowrate - 2.571 \times 10^{-3} \times WOB \\
 & + 4.001 \times 10^{-4} \times Flowrate \times WOB + 5.878 \\
 & \times 10^{-3} Flowrate^2 + 2.873 \times 10^{-5} WOB^2
 \end{aligned}
 \tag{4-2}$$

In Figure 4-4 plots of equation 4-1 and 4-2 are shown with extension to 7 gpm. The original experimental points are also shown.

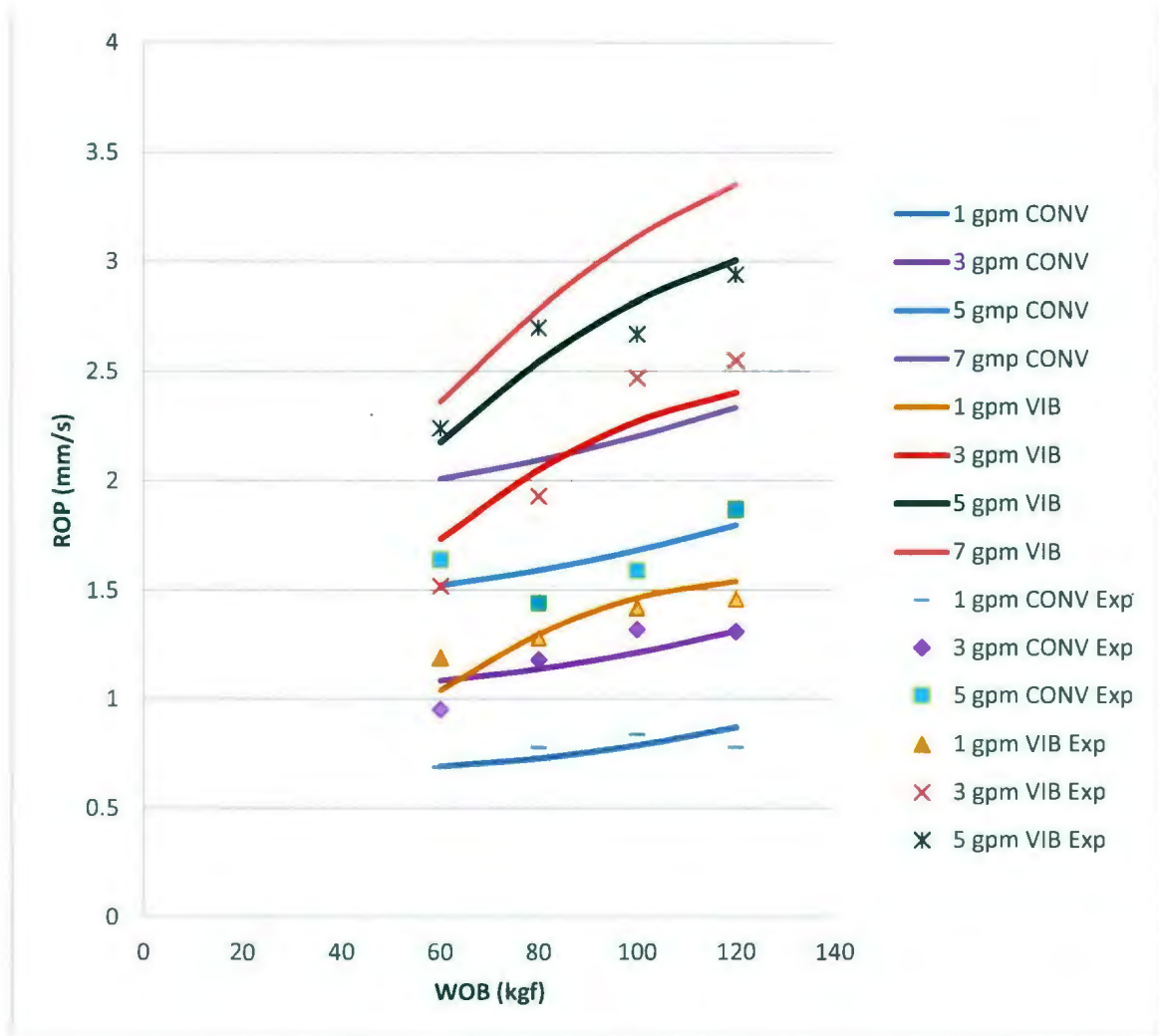


**Figure 4-4. ROP versus WOB at each flow rate in conventional and vibratory drilling using the generated equations based on experimental results**

Figure 4-4 shows that vibratory forces increase the ROP at each WOB and flow rate. Subtracting equation 4-1 from equation 4-2 we get the following relationship. Vibration increase ROP at all WOB and flow rates. Also, when drilling with vibration, increasing the WOB has a bigger effect on ROP than is the case in conventional drilling.

$$\begin{aligned}
ROP_{vib} - ROP_{conv} &= -1.208 + 0.247 \times Flowrate + 0.029571 \times WOB \\
&+ 9.61 \times 10^{-4} Flowrate \times WOB \\
&- 3.78810^{-2} Flowrate^2 - 1.422 \times 10^{-4} WOB^2
\end{aligned} \tag{4-3}$$

Equation 4-3 indicates that the improvement of the ROP depended on WOB and flow rate. To recap, both WOB and vibratory forces increase the ROP.

Figure 4-4 shows that within the range of parameters used in experiments. Flow rate has an almost identical effect on ROP at all flow rates. With vibration flow rate also increase ROP but with decreasing effect as ROP goes up. However with vibration, WOB has more effect on ROP at a given flow rate. Relative to the effect of WOB.

Figure 4-5 indicates the drilling process in more detail.

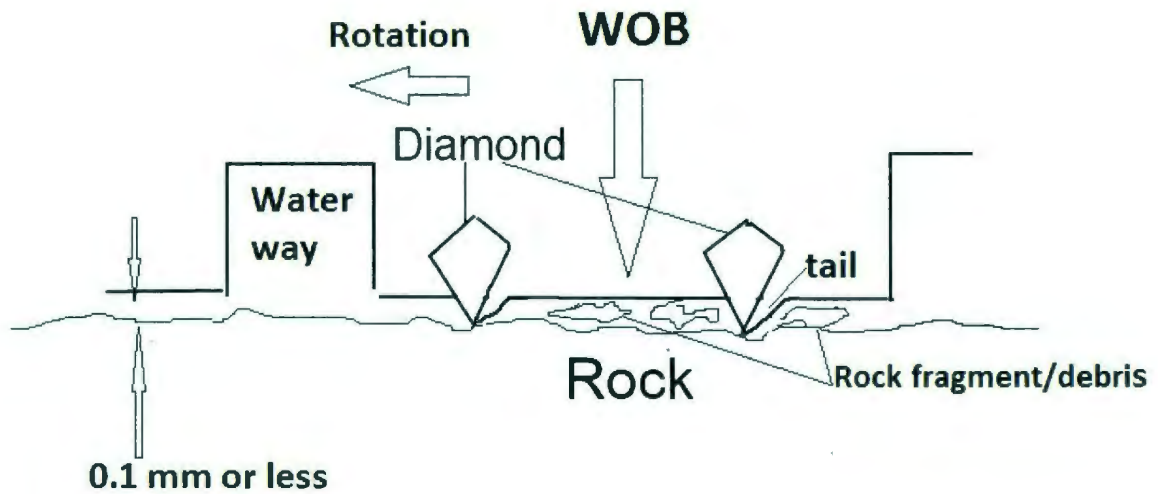


**Figure 4-5. Probable events during drilling with segmented embedded diamond coring bit**

In conventional drilling, the gap between bit segments and rock face at bottom of hole is less than 0.1mm; therefore most of the water flows through waterways. The “tails” seen on the bit matrix surface behind each protruding diamond, show that the flow of water and debris is circumferential, not radial, in the space between segment and rock. Flushing action of the water occurs primarily in the water ways as they move along the rock surface. Only a small part of the WOB is carried by the diamonds which are cutting the rock. The major part of the WOB is transmitted through matrix-rock contact, as at the “tails” and through rock debris between the matrix and the rock. Therefore ROP is somewhat, but not very sensitive to increases in WOB. Increasing the WOB will increase diamond penetration somewhat, but will also increase crushing of the rock debris and third-body abrasion of the rock by its own debris.

By increasing the flow rate of water, flushing action in the water ways is improved, i.e flushing of debris that exits from the trailing edge of each segment before it is trapped under next segment under its leading edge, is increased. Therefore increasing flow rate (within the range used in this work) has a relatively big effect on ROP, by more effectively removing rock debris that “interferes” with diamond-rock contact and penetration.

However in the case of vibratory drilling, the vibration generated provides loss of contact between the bit and the rock surface and hence widening the gap between them. This allows some radial flushing of rock debris from that space. Therefore a smaller portion of WOB acts through the rock debris and the WOB has stronger effect on the ROP. Increasing the flow rate does increase overall flushing and therefore has an effect on ROP. Also, with vibration and more radial flow between cutting surfaces and rock, there is less likelihood of tail development on the matrix behind diamonds. This can be observed for instance in Figure 9-18, in which the tails are evident from the conventional drilling while they can hardly be found at the vibratory drilling.

To validate the vibratory analysis in these experiments, a spectral analysis is performed on the dynamic position of the rock when it is vibrated during drilling operation. The dynamic vertical displacement of the rock has been recorded by the LVDT with sampling frequency of 128 Hz on data acquisition system. These analyses are conducted for all four levels of WOB when the rock was being drilled with flow rate of 3 gpm. Figure 4-6, 4-7,

4-8 and 4-9 show the spectrum of displacement of the rock under WOB of 60, 80, 100 and 120 kgf respectively, in which the peaks of the displacement amplitude can be seen vs. frequency of the vibration. It should be noted that the stationary part of each signal was picked up and plotted in Figure 4-10, 4-11, 4-12 and 4-13. The amplitude vs. WOB at 58 Hz is shown in Figure 4-14 which is verifying a decreasing amplitude vs. WOB after certain value of WOB (100 kgf) the significant change is in transition between WOB of 100 kgf to WOB of 120 kgf.

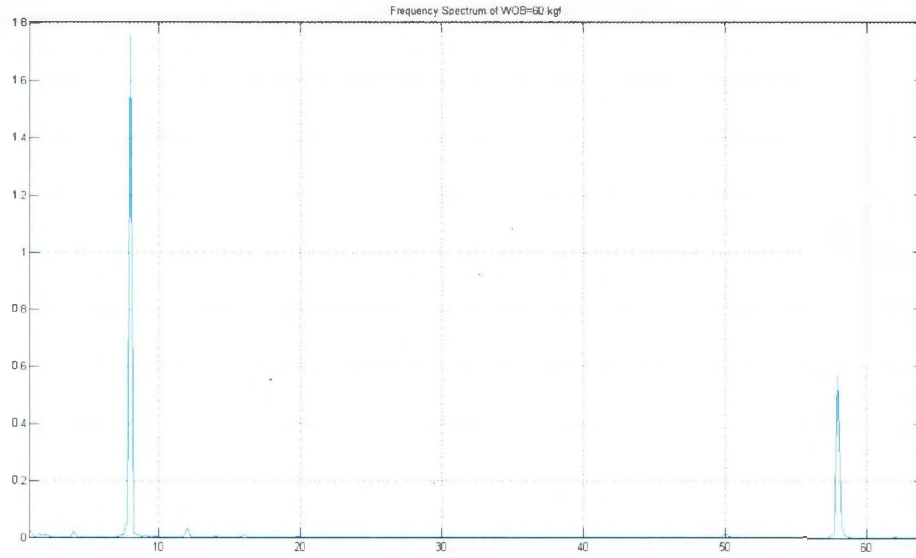


**Figure 4-6. Spectrum of rock displacement at WOB of 60 kgf, the frequency unit is Hz.**

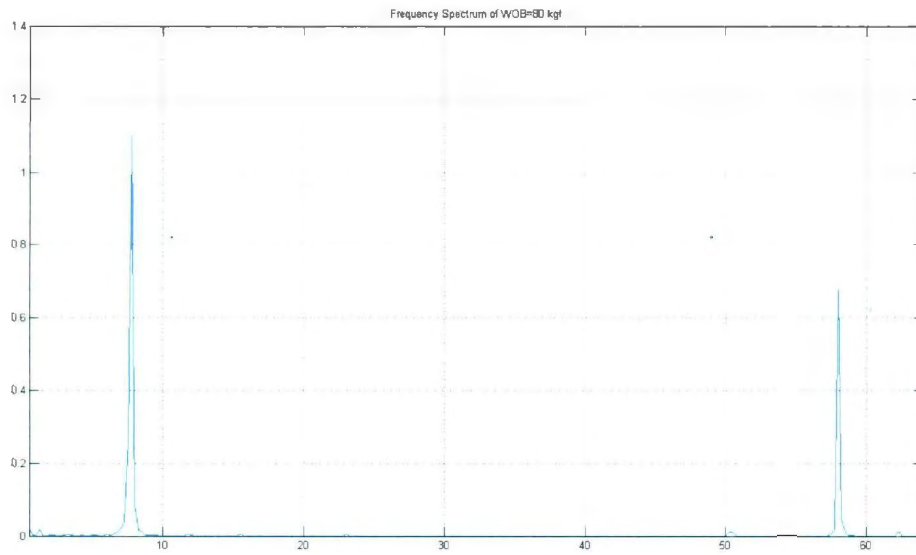


**Figure 4-7. Spectrum of rock displacement at WOB of 80 kgf, the frequency unit is Hertz.**

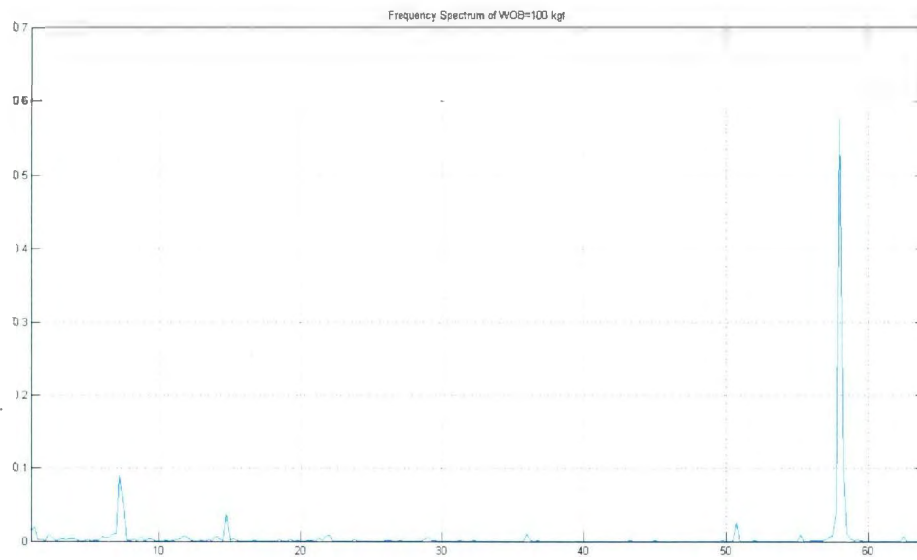


**Figure 4-8. Spectrum of rock displacement at WOB of 100 kgf, the frequency unit is Hz.**

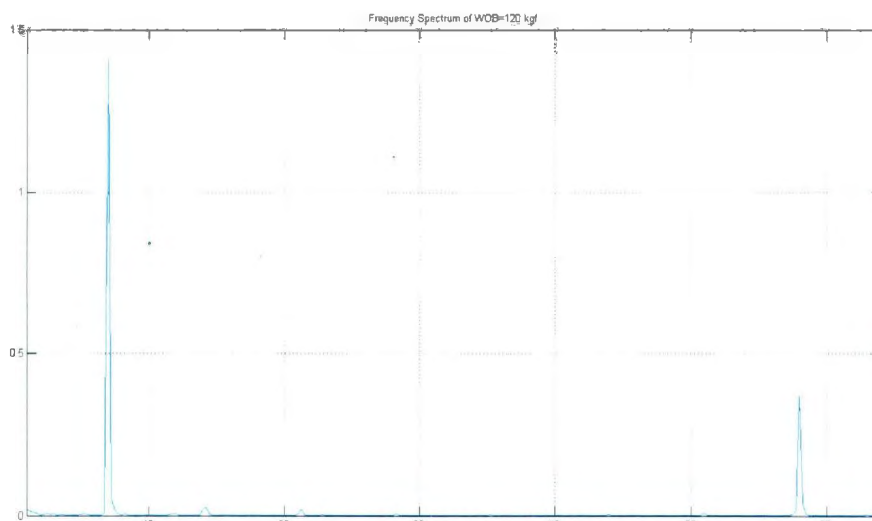


**Figure 4-9. Spectrum of rock displacement at WOB of 120 kgf, the frequency unit is Hz.**

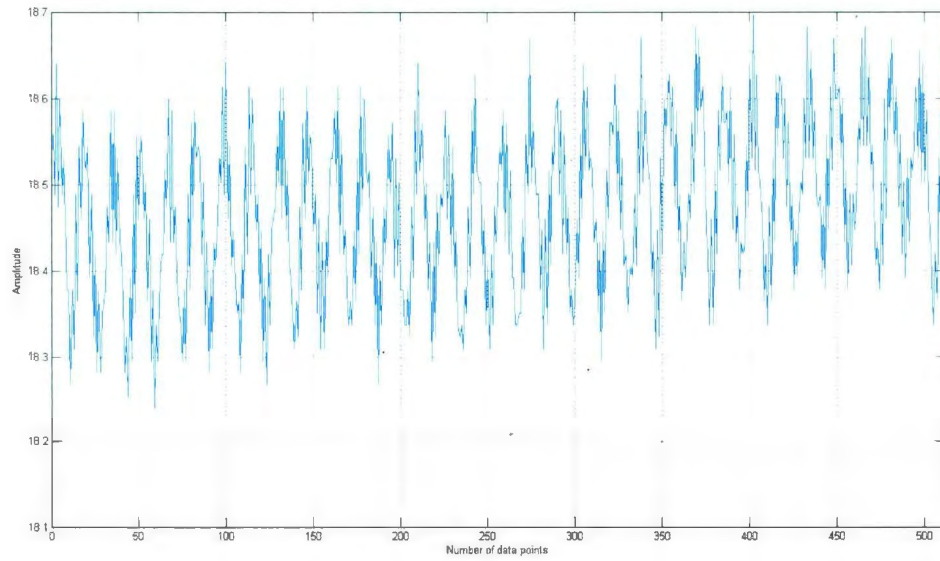


**Figure 4-10. Stationary part of the signal at WOB of 60 Kgf**

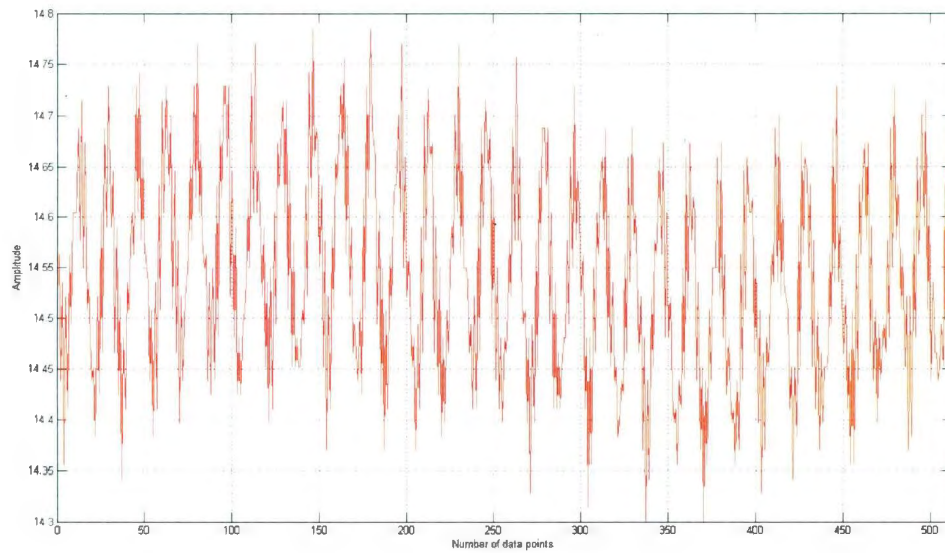


**Figure 4-11. Stationary part of the signal at WOB of 80 Kgf**

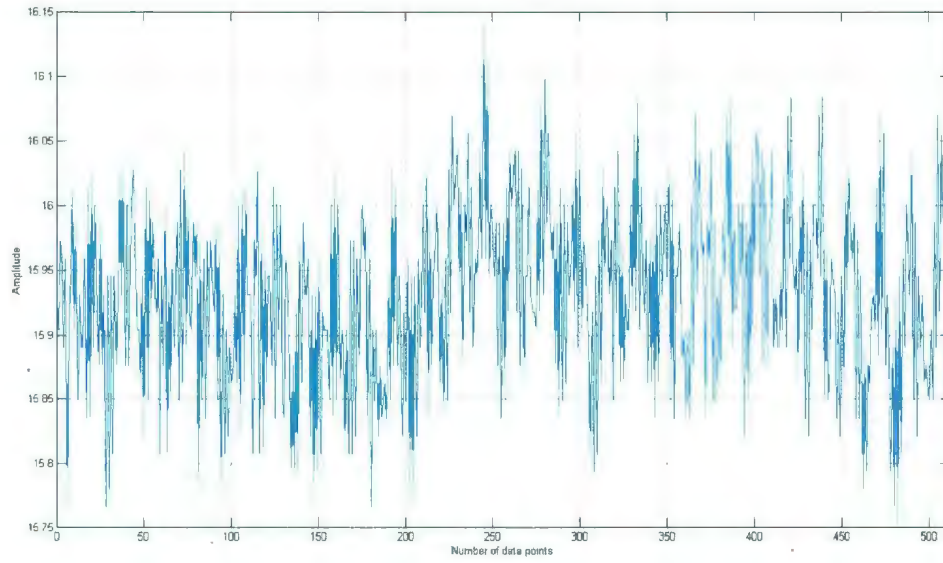


**Figure 4-12. Stationary part of the signal at WOB of 100 Kg**

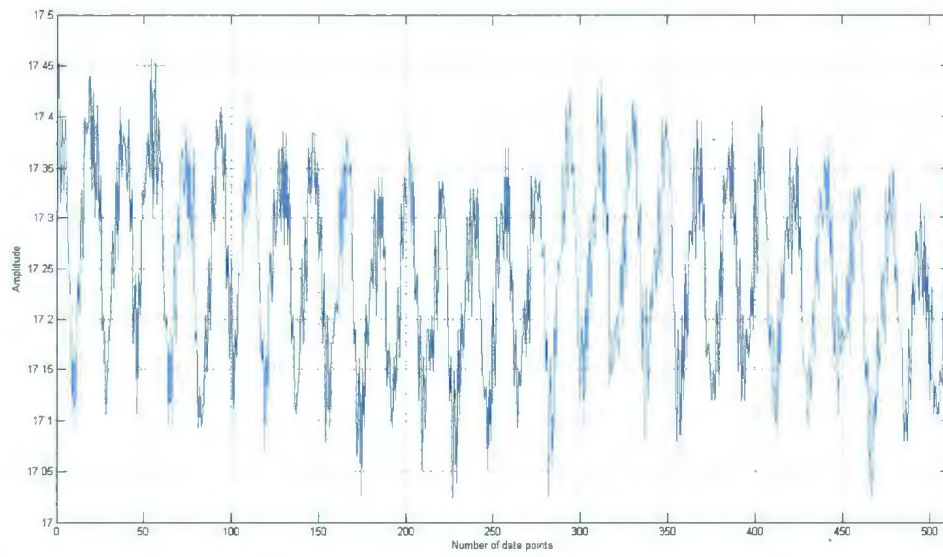


**Figure 4-13. Stationary part of the signal at WOB of 120 Kg**

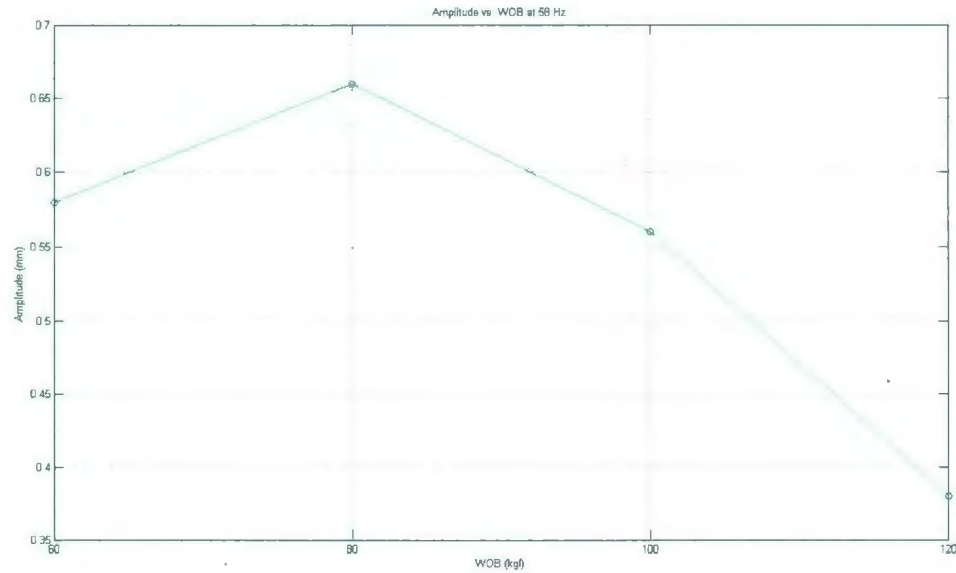


**Figure 4-14. The amplitude vs. WOB at 58 Hz**

The power to the vibration was supplied through a variable frequency drive (VFD) as in previous works; the frequency was set at 58 Hz. As shown in Figure 4-6 through 4-9, the applied vibratory force at 58 Hz is apparent in FFD analysis. There is a vibration at 8 Hz, then posttest experiments was conducted on the drill set up suggested the 8 Hz vibration is a resonance frequency of some part of drilling system. But the amplitude of 8 Hz vibration enhances by the location of LVDT and was not applied directly at the bit.

In the case of conventional drilling at high WOB and low flow rate an accumulation of cutting material around the bit was observed. This condition was also called founder point. This phenomenon appears to have occurred due to limitation in bottom hole cleaning. Since this phenomenon was observed in higher weights of bit and lower flow

rates, one can reason that the poor cleaning efficiency and high axial loads compact the cuttings and cause them to stick to the bit. Accumulation of the sticky material on the shank of the bit is shown in figure 4-15.

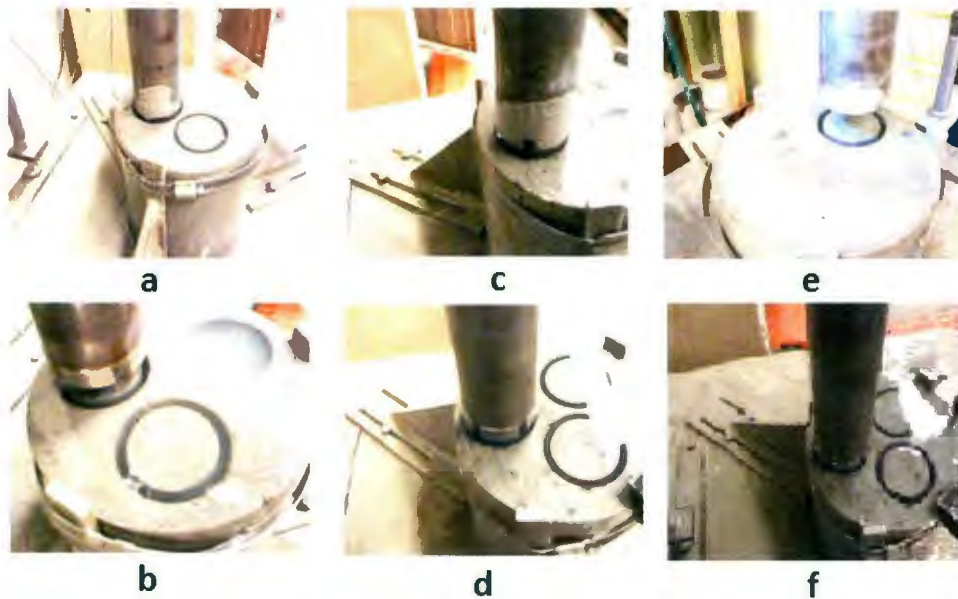


**Figure 4-15. Bit state after drilling. (a): WOB:100 kgf - GPM:1 (CONV), (b): WOB:100 kgf - GPM:1 (VIB), (c): WOB: 100 kgf - GPM:1 (CONV), (d): WOB: 100 kgf - GPM:1 (VIB), (e): WOB: 120 kgf - GPM:2 (CONV) (f): WOB:120 kgf - GPM:2 (VIB).**

Looking at Figure 4-15, case (a) shows the most severe state of this phenomenon. This case represents highest weight on the bit and lowest flow rate and conventional drilling. The next severe case pertains to the same operating conditions with lower weight on the bit. The next two, were the same sequence of weights on bit and the next higher flow rate, no notable instance of this phenomenon was observed in the vibration assisted drilling.

The conclusion is that conventional drilling low flow rates make this phenomenon very likely, especially, in high weights on bits.

Another conclusion is that, applying vibration (Vibration Assisted Drilling) prevents this phenomenon from happening to a very high degree. The reason is that the vibration provides excessive space and energy that helps the hydraulic system to clean up the cuttings in front of the cutting face of the bit. In other words, the vibration assists in bottom hole cleaning and lower flow rates are required for vibration assisted drilling to have the same performance as the conventional drilling.

Let us do a more in depth study of how this phenomenon affects the rate of penetration.

Looking at Figure 4-2, we can see that for the flow rates of 1 and 3 gpm the ROP-WOB curve with no imposed vibration exhibits a maximum at a WOB value close to 100 kgf. Interestingly, at the same two flow rates, the phenomenon occurs and even more interestingly, the phenomenon is observed at the weights on bit which are close to the maximum or after the maximum point.

#### **4.4 Wear Rate Data Acquisition and Analysis**

##### **4.4.1 Acquisition of Data**

For the wear study different methods were used to examine the rate of wear. Some techniques were used for better understanding and measuring of bit wear as follow:

- Surface cleaning
- Weight measurements with digital balance (Figure 4-17)
- Taking photos of bits
- Replication (Figure 4-18)
- Taking photos of replicas (Figure 4-16)

A Wild Makroskop M420 microscope (Figure 4-16) was used to study both matrix and diamond wear. For recording the data, taking photos after each experiment was performed and also replication was done to make a permanent record of bit teeth information.

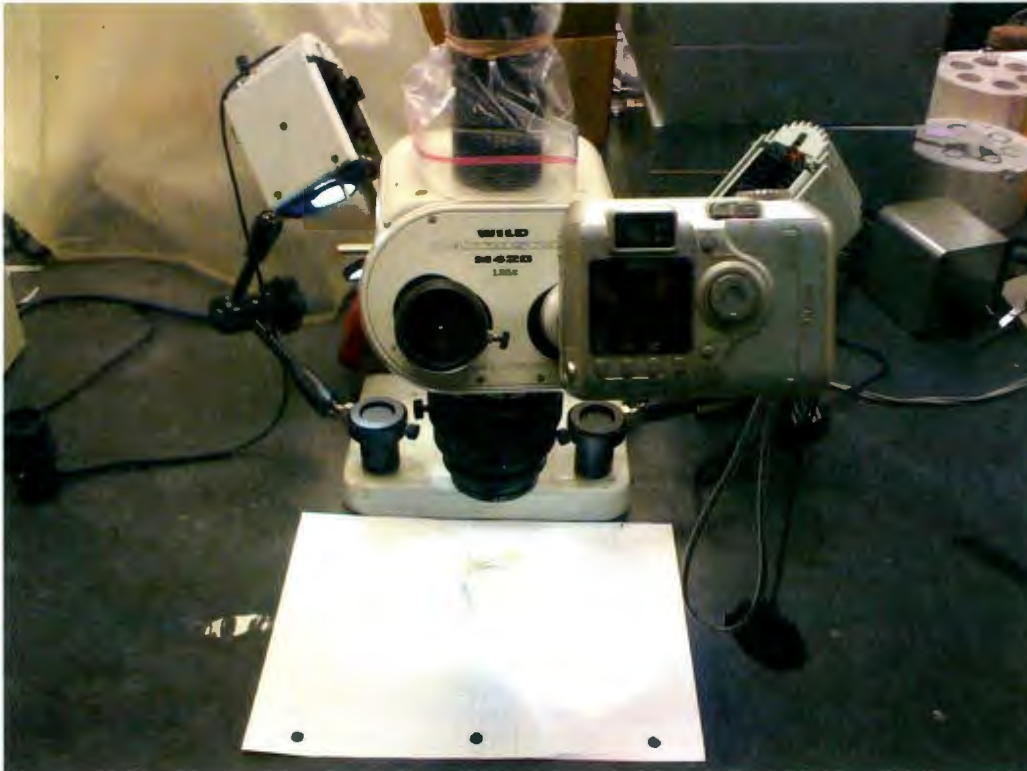


**Figure 4-16. Optical Microscope**



Figure 4-17. Weight measurement with digital balance



Figure 4-18. Replicas

#### 4.4.2 A Summary of the Analysis of the Wear Data

An extensive study on photos taken using the microscope and also weight measurement is presented in the Appendix. Detailed analysis is also given there. Please refer to the appendix for more information.

As seen in Figure 4-18 the cutting end of a bit has five segments, separated by water ways. In general one segment was chosen and examined and photographed with the optical microscope, looking and of the bit face, the end of the segment seen in the water ways and the outer gage surfaces referred to as side views. The locations examined on the bit face, were the leading and trailing edges. The side view and the water way views of these locations were compared. Bit profile before and after tests were compared. Not much wear was observed apart from some rounding at the edges. The prevailing trend in all these analyses is more rounding of the outer edges in the case of vibration assisted drilling. For the side views, in both cases, Gauge wear, i.e. wear of the cylindrical side surfaces of the segments is unlikely, especially for short length runs such as those conducted in these series of experiments. Furthermore, the vibration, as long as it is in axial mode, does not seem to contribute to any wear caused along the sides of the coring bit, which is confirmed by the experimental results. Those types of wear are the results of lateral forces and possible causes are lateral vibrations and/or bit whirl motion, which was not the case here.

In another detailed study on the diamonds, described in the Section 9.3 of the appendix four types of wear on diamonds are identified: 'Unworn', meaning no wear at all; 'wear flat', meaning a flat surface formed on the diamond; 'Microfracture', meaning that a small fracture is formed inside the diamond and finally 'pullout' meaning that the diamond is detached from the matrix.

Before doing the analysis, it was obvious that for this case the wear of the type 'wear flat' is very unlikely to happen because the hardness of the diamonds is much higher than the hardness of the matrix. The ratio of pull-out to fracture wear in conventional drilling is 2.9 and in vibration assisted drilling is 7.1. This means that the "vibration" contributes to the pull-out of the cutters while the "drag", which is the main mechanism of conventional drilling, contributes to fracturing and thereby the weakening of the diamonds. Another justification is that the drag mechanism in conventional drilling produces higher temperature that can cause damage to the structure of the diamonds, this higher temperature comes from the continuous contact and friction caused by the drag mechanism. On the other hand, the vibration mechanism is associated with very high compressive and shear forces that are capable of breaking the bonds between the diamond and matrix and can pull the diamonds out.

The same study shows that 27% of the diamonds in the vibration assisted drilling remained unworn and that number for conventional drilling was 49%. This means that the

wear rate of the conventional drilling is lower than the vibration assisted and this is in no contrast with the previous paragraph where we looked into the mechanism of wear.

Results of the weight loss studies also confirm this fact; the weight loss per unit depth drilled Figure 4-19 is significantly higher for vibration assisted drilling than conventional drilling.

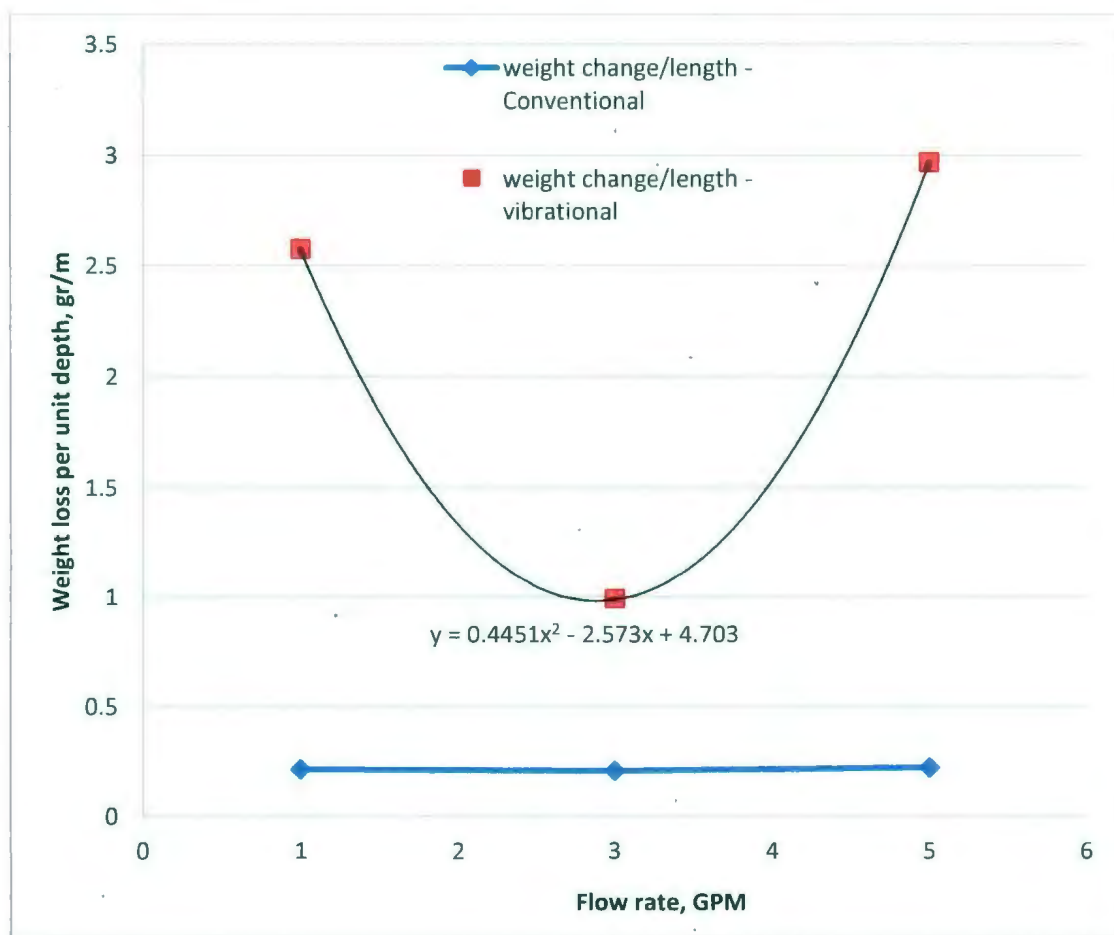


Figure 4-19. Weight change per unit depth drilling versus flow rate for different drilling modes

Another important trend is the sensitivity of the wear rate to the flow rate for vibration assisted drilling. There seems to be an optimum flow rate at which the wear rate attains a minimum value in vibration assisted drilling, in this case by taking the derivative of the trend line, that value is computed to be 2.81 gpm, for all practical purposes we can assume it to be 3 gpm.

In summary, the mechanism of wear is different for vibration and drag and drag seems to be more efficient when it comes to wear. Vibration assisted drilling is a combination of vibration and drag and depending on the relative dominance of each parameter, different rates of wear will be observed.

## **5 CERCHAR Test Summary and Results**

This chapter is a report on the work that was done to make the CERCHAR testing set-up ready and running. This chapter is divided in two parts, in the first part the work made to make a steel styli compatible to what is needed according to CERCHAR standard (please refer to Section 2.1) using heat treatment as the modification means, and hardness testing as a tool to evaluate the hardness of the product. The second part is about two series of CERCHAR tests made to make an assessment of the sensitivity of the CERCHAR test results with respect to the hardness of the styli. It shows that sensitivity is not a concern in the small range of hardness of a batch of steel styli heat treated together, following the determined standard heat treatment to be appropriate.

### **5.1 Heat Treatment and Preparation of Styli Required for a Standard CERCHAR Test**

The styli supplied to us had a hardness of over 62 HRC (Rockwell hardness, “C” scale) very much harder than the 55HRC hardness specified in the standard [28, 31, 33-36]. With many kinds of steels the hardness is commonly adjusted by heat treatment. The heat treatment depends on the type of the steel; it is usually a hardening treatment producing the highest hardness possible. This process is followed by a tempering treatment to reduce the excess hardness and increase toughness. This same procedure was performed for the steel used in the styli of this work’s tests.

The work described here had the following objectives:

1. Determine best tempering treatment of the styli supplied
2. To be sure tip hardness is the same as the rest of stylus
3. Determine a routine way to measure hardness, as check on styli before they are used

It is evident that the hardness at the tip of a stylus is, in fact, the key parameter to be sure of. The hardness of the tip could be different from that of the rest of a stylus for several reasons, including differing rates of heating and cooling and loss of carbon (decarburization) by reaction with oxygen during heat treatment. In the CECHAR test less than 0.5 mm axial length of stylus tip is abraded away (that would be the length change in a test resulting in a CAI of 10). This issue is not addressed in the standard, but it could be an issue after heat treatments that have not been conducted in a careful way.

The Rockwell Hardness test is a hardness measurement based on the net increase in depth of impression as a load is applied. Rockwell hardness numbers have no units. The higher the number in each of the several possible scales means the harder the material.

In testing harder materials, hard cast iron and many steel alloys, a 120 degrees diamond cone is used with up to a 150 kilogram load and the hardness is read on the "C" scale. The Rockwell test uses two loads, one applied directly after the other. The first load, known as the "minor", load of 10 kilograms is applied to the specimen to help seat the indenter and remove the effects, in the test, of any surface irregularities. In essence, the minor load

creates a uniformly shaped surface for the major load to be applied. The difference in the depth of the indentation between the minor and major loads provides the Rockwell hardness number. Fig (5-1) shows the apparatus that we use for our Rockwell tests.



**Figure 5-1. Rockwell hardness test apparatus**

A Rockwell hardness test is not possible on or near the tip of a stylus. Therefore it was decided to do micro hardness tests on tip, as we have a microhardnes tester with which both Vickers and Knoop microhardness tests can be performed. Both these tests are performed with a diamond indenter with a square based four-sided pyramid shape.

The Knoop hardness test is a microhardness test - a test for mechanical hardness often used for very brittle materials or thin sheets, where only a small indentation may be made for testing purposes. This test has been used on curved surfaces with very small radii of curvature in one direction, but linear in the direction perpendicular to the plane of the curvature as at the tip of CECHAR test styli. A pyramidal diamond point is pressed into the polished surface of the test material with a known force, for a specified dwell time, and the resulting indentation is measured using a microscope. The geometry of this indenter is an extended pyramid with the length to width ratio being 7:1 and respective face angles are 172 degrees for the long edge and 130 degrees for the short edge. Fig (5-2) shows the indentation that Knoop test machine perform on our sample and Fig (5-3) show the Knoop test apparatus that we used in this experiment. In our application of the test the indenter is aligned so that the longer dimension of the indentation is in the linear direction of the surface tested.

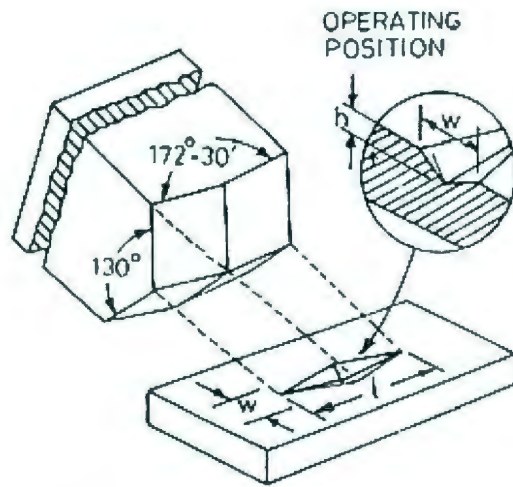


Figure 5-2. Indentation by the Knoop testing machine on the sample (ASTM E384)



Figure 5-3. Knoop test apparatus used for the tests

The reason for using the Knoop test is that this test makes testing on the very tip of the stylus possible. The very tip of the stylus is the most important part when it comes to characterizing the hardness of the metal since this is the part directly in contact with rock specimen during a scratch test.

In some of our tests on the hardness of styli, the effect of the various heat treatments tried out. Then the correlations between different hardness tests we tested directly on the cylindrical side of stylus and on cross-sections prepared perpendicular to the stylus axis were developed. It should be noted that the hardness of the cross sections perpendicular to stylus axis can be tested with both the Rockwell tester and the micro-hardness tester if a short portion of the stylus is mounted in plastic and the surface is prepared as described here. On the other hand, the hardness of the cylindrical side can only be tested using the Rockwell tester.

In our initial microhardness tests styli, a portion, about 10 mm long was cut from a stylus which was mounted in plastic, with the stylus axis perpendicular to the two more or less flat surfaces of the mount so that cross sections of the stylus could be tested. One of these cross sections could be close to the stylus tip, the other a complete cross-section of the stylus.

These surfaces were prepared for metallography by abrading them in a slurry in turn with increasing finer abrasive paper, followed by abrasion with diamond paste. Abrasion of a metal surface results in mechanical deformation of a layer at the surface which can work-

harden the surface. The coarser the abrasive used, the thicker this deformed layer. Each step in the surface preparation described removes the deformed layer from the previous step replacing it with a thinner deformed layer. After the final step using 1 micron diamond paste the thickness of the remaining deformed surface layer should be not much thicker than 1 micron and should not affect a hardness measurement.

As the stylus hardness is specified in Rockwell C units in the CECHAR test standard, it is appropriate to convert hardness values determined in other scales to Rockwell hardness. The ASTM has published conversion tables which are appropriate for many varieties of steel. Most hardness tests involve plastic deformation (i.e. permanent deformation) in indentation of the tested materials, but the pattern of stress and strain distribution around the indentation depends on the shape of the indentation and the stress-strain relationships, including work-hardening, of the material. Therefore the correlation between two different hardness scales does depend on the material and the loads used in the tests.

We have used the conversion table published by Wilson, the makers of our Rockwell hardness tester for conversions from Vickers and Knoop to Rockwell C, with some work, as described below, to test this conversion.

We mounted the stylus after we cut it to do the micro Vickers hardness (HV) tests on the polished full cross-section. The test was performed with 500 g test force. (A force of 150 kg is used in Rockwell C tests) The mean of the 10 tests was 851 HV that is equivalent to 65.5 HRC. This confirmed that the stylus hardness was too high for the CERCHAR test,

as the desired hardness value for the CERCHAR test is 55 HRC. Also we did 500 g test force Knoop test on cross-section at the mounted tip, prepared close to the point of the stylus. The average of 6 Knoop hardness (HK) readings was 775 HK that is equivalent to 62 HRC, which is still too high.

If we are to use the Knoop test routinely to test styli before or after using them in the CECHAR test it would be better to test directly on the side of tip without cutting the stylus or mounting in plastic, therefore; we developed a fixture to do that. Figure 5-4 shows the fixture. The fixture has the shape of a short cylinder, similar in size to a typical metallurgical specimen mounted in plastic. A stylus is held in the fixture at 45 degrees to the fixture axis, with the pointed tip of the stylus emerging at one end surface of the fixture, where Knoop hardness indentations can be placed on the curved surface close to the point of the tip, with the long diagonal of the indentation aligned with the stylus axis. In this orientation, the Knoop indentation is less affected by the curvature of the pin tip surface, than a Vickers indentation would be.



**Figure 5-4. Fixture developed to conduct the hardness tests on the tip of the styli**

The details of the test results using the Knoop hardness and also the effects of different heat treating methods on the corresponding hardness values are brought in the second Appendix. (Appendix 10)

#### **5.1.1 Conclusions of the Work**

The main results of the work described in this Section (and also the second Appendix data), is summarized here. First, it is shown that heat treatment of the steel styli according to ASM guidelines gives reasonable results, more specifically, tempering at 225 to 232 C

for 45 minutes is appropriate. Second, the micro hardness test can actually be applied to the very tip of the styli (which is the location of particular interest in this research) provided that the stylus surface is polished carefully.

Finally, it is important to see how sensitive the values of CERCHAR are with respect to the hardness values obtained (i.e. tip hardness in the range of  $\pm 2$  HRC unit's deviation from the standard 55 HRC). This leads us to the second section of this chapter which are the two important series of tests that are conducted to investigate this issue.

## **5.2 CERCHAR Tests Sensitivity to Stylus Hardness**

Accompanying the efforts made to record and adjust the hardness of the steel styli to be used in the CERCHAR test experiments, a series of CERCHAR tests on a specific rock sample were done and the results of the wear on the styli (the diameter) with respect to the hardness of the styli were recorded. The aim of these experiments was to verify and establish the fact that for the range of steel styli hardness values used, there is no significant change in the results obtained for the CERCHAR test which could be used as a guide for future research on the CERCHAR test.

The heat treatment of the styli aiming at a hardness of 55 HRC produces styli with hardness somewhere in the 53 to 57 HRC intervals. Fortunately, according to the results, the sensitivity of the CERCHAR test results to HRC in the aforementioned interval is insignificant compared to the systematic and random experimental error [49].

### 5.2.1 Procedure of CERCHAR Tests Performed

A standard way of conducting CERCHAR experiments is also explained in the second chapter which is the literature review part. The same practice was also undertaken in our research work. Figure 5-5 shows a photo of the set-up at its final stage and after modifications that were made and also has some signs to show the procedure of the performance of each test.

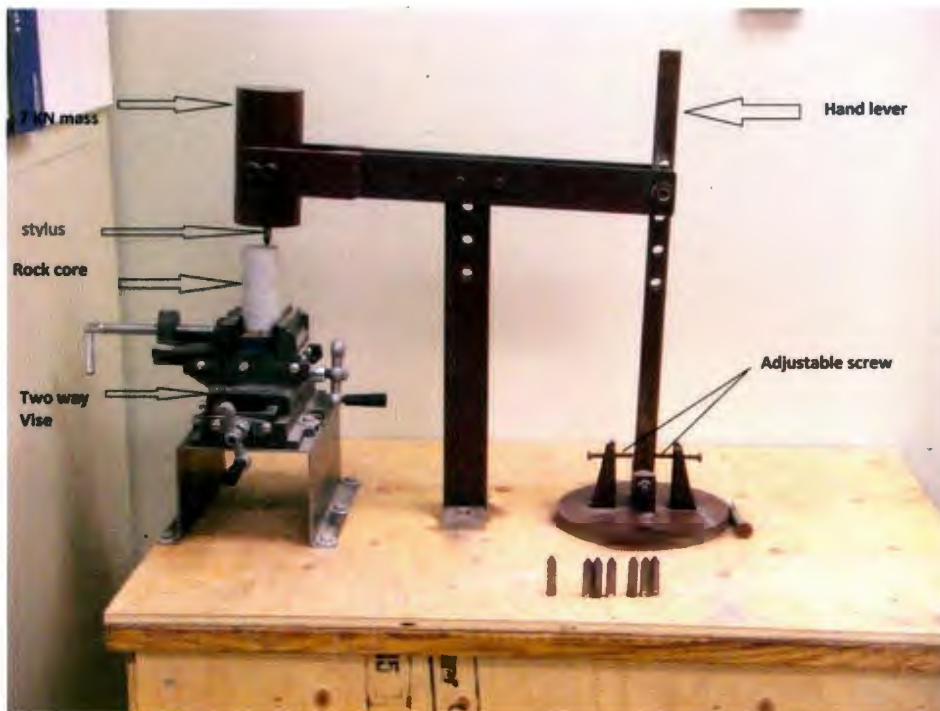


Figure 5-5. CERCHAR testing set-up in Memorial University of Newfoundland

In order to conduct the test, the rock specimen should be placed in the vice and fixed and there should be no movement possible in any direction for the sample. Then, place the styli on the proper spot on the rock surface. Care should be taken that the stylus is not damaged before the test starts. To conduct each repetition of the test, the lever, while a vertical load of 7 KN is on the stylus, should be moved with a certain velocity for a certain distance. This is repeated twice for each stylus and then the stylus's tip is studied using an optical microscope.

Figure 5-6 shows the styli and the core samples that were used in the experiments.



**Figure 5-6. Rock samples and styli used in the CERCHAR experiments**

### 5.2.2 The Results Obtained from the CERCHAR Tests

A series of experimental investigation has been conducted using Conception group siltstone with UCS value of 160.75 Mpa which was the reference for our study. Pins of the CERCHAR test, with HRC value ranging from 52 to 58, were used to observe the variation of CAI, i.e. diameter of the flat worn, vs. HRC. A number of 22 tests were conducted and the results are shown in Table.5-1. In addition Figure 5-7 shows variation of Diameter vs HRC value. The value of standard deviation in data calculated is 0.041. Regression line of these values is drawn on the scatter plot of data. The R-squared value of this line is 0.19 which is much less than 1.0 for a perfect correlation.

**Table 5-1. Diameter of the CERCHAR styluses' after standard CERCHAR test**

Diameter(mm)	HRC value	Diameter(mm)	HRC value	Diameter(mm)	HRC value
0.3	53.3	0.28	56	0.21	57.2
0.3	54	0.2	57	0.22	54.7
0.3	55.2	0.2	55.7	0.2	56.5
0.25	56	0.2	57	0.21	57.8
0.3	56.8	0.23	55.5		
0.21	52.7	0.2	56.8		
0.3	54	0.21	56		
0.24	55.7	0.2	57.2		
0.29	56.3	0.2	56		

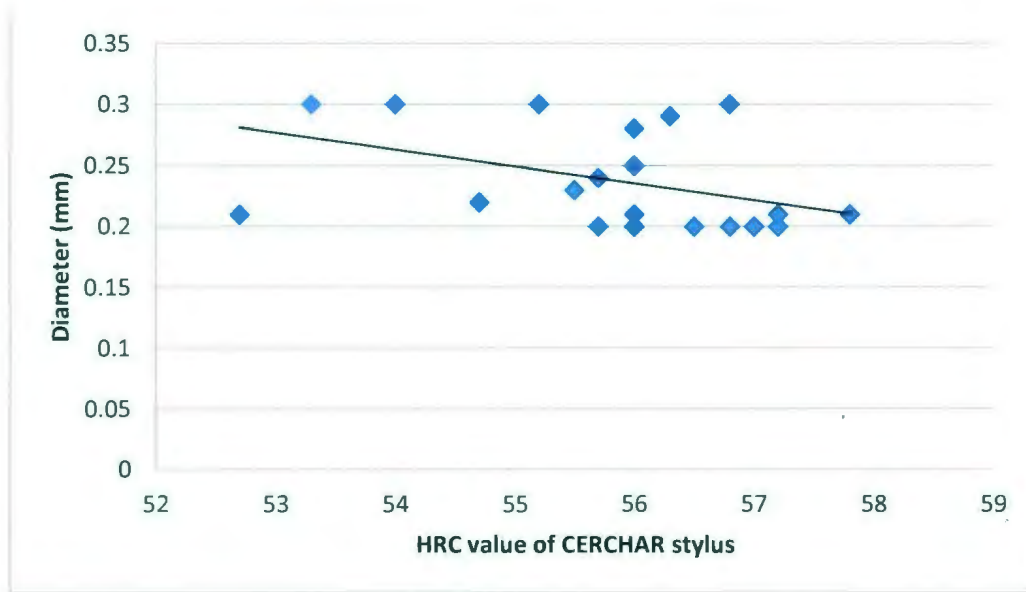


**Figure 5-7. Plot of Correlation between HRC value of the styluses and tip diameter after test**

Result of investigations of the CERCHAR tests, shows that there is no significant correlation between styli HRC value and diameter of the worn flat on the tip of the styli after standard wear test for the styli in the range of hardness used.

While no reliable correlation between stylus hardness and wear flat diameter was established for the relatively small range of hardness used (unlike the correlations reported elsewhere for wider hardness ranges [30]), the standard deviation for the present tests is useful.

The standard deviation was 0.041 for the diameter measurement on 22 styli (each value recorded is the average of two diameter of right angle on one stylus). Five styli are used for the determination of one CAI value. According to standard statistical theory the student t-value for 54 measurements is 2.8. Therefore the uncertainty of data (i.e. from

one stylus) is  $2.8 \times 0.041 = 0.115$ . The uncertainty of the mean from 5 pins is 0.05 i.e. 95% confidence limits for a mean is  $\pm 0.05$  mm. This is self-evident from the data as all the diameter data ranged between, and including 0.20 - 0.30 mm. Therefore the confidence limits for a CAI value on this rock are  $\pm 0.5$ , which appears to have a homogenous and fine grain structure. The same series of tests were done using concrete as the rock and the diameters after each test were recorded against the HRC hardness of the styli. Table 5-2 shows the tests results.

**Table 5-2. Pin HRC Hardness and pin diameter data**

Diameter, mm	HRC		Diameter, mm	HRC
0.4	54.5		0.2	54
0.29	55.2		0.2	57.5
0.18	56		0.22	57.3
0.2	52.2		0.3	56
0.29	56		0.28	53.3
0.2	54.5		0.23	54.7
0.3	56.8		0.3	56.3
0.2	56.7		0.3	54.5
0.21	57		0.22	54
0.2	54.7		0.2	54.5
0.24	56.8		0.3	55

The graph of the diameters obtained after each test versus the hardness values is shown in Figure 5-8.

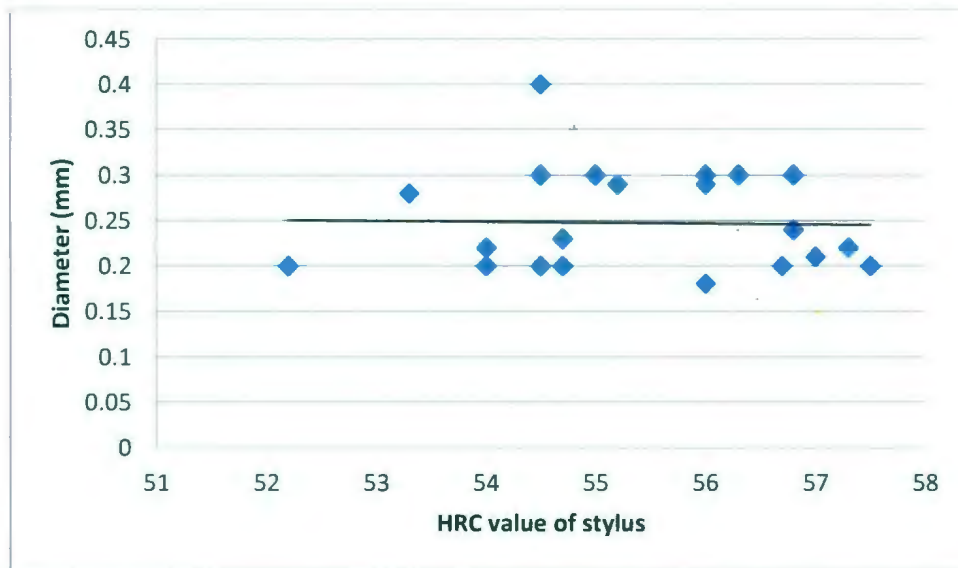


**Figure 5-8. Diameter in mm versus hardness**

The same conclusions as the previous set of tests can also be drawn here. The value of  $r$ -squared for the linear trend line fitted to data is 0.000 which means a complete randomness of the data and no obvious change in the behavior as long as the HRC values in the studied range are concerned. The results again confirm the previous conclusion for siltstone.

## 6 Conclusions

### 6.1 Coring Drilling Tests

The tests performed using the coring drilling bit to look into the effect of the flow rate on the drilling performance i.e. ROP and wear rate had interesting results. From an ROP point of view, the flow rate increased the rate of penetration. It was also observed that the vibration assisted drilling increases the rate of penetration not only by itself; but also, it interacts with the flow rate in which a better bottom hole cleaning can be achieved.

It appears that without vibration a large portion of the WOB is carried by the rock debris between the bit surface and rock. Most of the flushing action occurs at the water ways. With vibration some flushing can also occur between the segments and the rock. Enhancing the cutting action of imbedded diamonds and hence the ROP.

Furthermore, it was observed that the vibration, in total, causes more wear on the tool for unit interval drilled both from a weight loss and from a diamond loss point of view. Furthermore, with regards to the direct effect of the flow rate to the wear rate, the rate of wear was observed to be independent of the flow rate for conventional drilling. For the vibration assisted case, there seems to be an optimum value for the flow rate in which the rate of the wear of the tool is minimal.

## 6.2 CERCHAR Test Results and HRC

The CERCHAR facility was refurbished and several tests on two different types of rock (siltstone and concrete) were performed on it. The main purpose of the tests was to investigate the sensitivity of the test results to the HRC values of the hardness of the pins used. The test results show that this sensitivity is much less than the experimental random errors and conducting the experiments with the pins with a hardness in a range of 52 to 58 HRC will give results that are practically independent of the hardness value. In other words, the uncertainty inherent the experiment is larger than the effect of the hardness.

The main motivation for this study is to make sure that the CERCHAR tests to be conducted in future are not affected by the slight variations in the pin's hardness. This study assures that (at least for the rock types studied here, siltstone and concrete) the change in the measured diameter after the CERCHAR test is negligible if only the pin's hardness changes (as long as the change is in the range of 52 to 58 HRC). The available heat treatment methods are able to set the stylus's hardness in a range 3 HRC lower or higher than the target hardness value.

## **7 Recommendations for Future Work**

### **7.1 Flow Rate of Drilling Fluid and its Effect on the Drilling Performance**

The Range of flow rates tested was limited to 1 gpm to 5 gpm for the described drilling operational conditions. Close to linear trends of rate of penetration with the flow rate does not mean that for the entire range of practical flow rates this will be true. Expanding the range to higher flow rates will show this behavior and give more insight into the mechanisms by which the drilling hydraulics affects the performance.

The mechanism of wear for vibration and rotary drilling turned out to be different. A potential experiment to verify and also give more insight into this is to drill the same interval of a given rock once with pure rotation and once with pure vibration (no rotation) and the same WOB and then do the same diamond analysis that was also given in the wear study of this thesis. The theory posed in this thesis will be confirmed if the dominant mode of wear in the vibration case is the diamond-matrix bond failure (diamond pull-out) while that of the rotary case is the diamond-fracture. A vibration assisted case is a combination of both modes and the weight of each mode are determined by the vibration amplitude and the rotary speed. The theory can be developed to the point to predict the wear of a given vibration assisted drilling operation having the data of a pure-vibration and pure-rotation drilling case available.

Cost optimization study of the vibration assisted drilling can become more realistic by having the accurate data of the operational costs of the vibratory system as well as the set up itself and also the expenses that the wear rate imposes. The importance of this study is trivial since all the industrial interest in the drilling research at the end narrows down to one factor, which is cost of drilling.

## **7.2 CERCHAR Test and Hardness Effect**

The work presented in this thesis is in fact a starting point to look into the CERCHAR test more effectively. The refurbishment of this device will provide a great means to conduct more comprehensive abrasiveness studies and then relate those studies to the wear studies such as those presented in the previous chapter of this thesis.

The CERCHAR Abrasiveness Index (CAI) values are of very few practical interests in drilling engineering as long as there is no correlation to relate it to the tool wear. The literature review of this thesis went over some of the available works in this regard. For the specific purpose of vibration assisted drilling, a series of experiments can be designed to first measure the CAI value of a set of rocks and then conducting the drilling experiments using the impregnated diamond bit. A constant set of drilling operational parameters such as WOB, flow rate, rotary speed and etc. is to be applied throughout the tests while applying the vibrations with various amplitudes, a good correlation (if the effect is significant) will be obtained relating the wear rate to CAI and the vibrations amplitude.

## 8 References

[1] H. Li, "Experimental investigation of the rate of penetration of vibration assisted rotary drilling," M. Eng. Thesis, Memorial University of Newfoundland, St. John's, 2010.

[2] W. Zhang, Development of new techniques for impregnated diamond coring bit wear measurement in conventional rotary drilling and vibration assisted rotary drilling, M. Eng. Thesis, Memorial University of Newfoundland, St. John's, 2010.

[3] A. Abtahi, "Bit wear analysis and optimization for vibration assisted rotary drilling (vard) using impregnated diamond bits," M. Eng. Thesis, Memorial University of Newfoundland, St. John's, 2011.

[4] Y. Babatunde, "The effects of varying vibration frequency and power on efficiency in vibration assisted rotary drilling," M. Eng. Thesis, Memorial University of Newfoundland, St. John's, 2011.

- [5] H. Khorshidian, "Phenomena Affecting Penetration Mechanism of Polycrystalline Diamond Compact Bit" M. Eng. Thesis, Memorial University of Newfoundland, St. John's, 2010.
- [6] Johnson Jr, et.al. "Cavitating and Structured Jets for Mechanical Bits to Increase drilling Rate" in Energy Technology Conference, New Orleans, 1982.
- [7] W. MAURER, "The Perfect - Cleaning" Theory of Rotary Drilling," Journal of Petroleum Technology, vol.14, pp. 1270-1274, 1962.
- [8] A.T. Bourgoyne Jr, K.K. Millheim, M.E. Chenevert & F.S. Young Jr., "Applied Drilling Engineering," SPE, 1986.
- [9] G. A. Tibbitts. Effects of Bit Hydraulics on Full-Scale Laboratory Drilled Shale," SPE Journal of Petroleum Technology, 33(7), 1981.
- [10] Kien Ming Lim and G. A. Chukwu. "Bit Hydraulics Analysis for Efficient Hole Cleaning," in SPE, Anchorage, Alaska, 1996.

[11] M. N. Belavadi and G. A Chukwu. "Experimental Study of the Parameters Affecting Cutting Transportation in a Vertical Wellbore Annulus" SPE Western Regional Meeting, 23-25 March 1994, Long Beach, California.

[12] John R. Eckel and J. P. Nolley. "An Analysis of Hydraulic Factors Affecting the Rate of Penetration of Drag-type Rotary Bits," in API, Galveston, Texas, 1949.

[13] H.A. Kendall and W.C. Goins. "Design and Operation of Jet-Bit Programs for Maximum Hydraulic Horsepower, Impact Force or Jet Velocity," AIME, vol. 219, pp. 238-250, 1960.

[14] W. J. Bielstein and Gexirge E. Cannon "Factors Affecting the Rate of Penetration of Bits," in API, Dallas, Texas, 1950.

[15] John R. Eckel and W. J. Bielstein. "Nozzle Design and its Effect on Drilling Rate and Pump Operation, " in API, Beaumon, Texas, 1951.

[16] Earle C. Hellums, "The Effect of Pump Horsepower on the Rate of Penetration," in API, Shreveport, Louisiana, 1952.

[17] M. S. Bizanti and E. F. Blick, "Fluid Dynamics of Wellbore Bottomhole Cleaning," in SPE, Midland, Texas, 1986.

[18] Ledgerwood, L.W., Salisbury, D.P. (1991). Bit Balling and Wellbore Instability of Downhole Shales. SPE Annual Technical Conference and Exhibition. Dallas, Texas: 1991 Copyright 1991, Society of Petroleum Engineers Inc.

[19] E. Kuru; et.al. "Hydraulic Optimization of Foam Drilling For Maximum Drilling Rate," in SPE/IADC Underbalanced Technology Conference and Exhibition, Houston, Texas, 2004.

[20] Abdullah M. Qahtani and Md. Amanullah, "Prediction of Hole Cleaning Efficiency Using a Simple, User Friendly and Better Performing Simulation Model," in SPE/DGS Saudi Arabia Section Technical Symposium and Exhibition, Al-Khobar, Saudi Arabia, 2010.

[21] M. Malekzadeh and M. Mohammadsalehi, "Hole Cleaning Optimization in Horizontal Wells: A New Method To Compensate Negative Hole Inclination Effects," in SPE, Macaé, Brazil, 2011.

[22] A. Ersoy, "Performance analysis of polycrystalline diamond compact (PDC) core bits in rocks," PhD Thesis, The University of Nottingham, Nottingham, England, 1996.

[23] R. J. Plinninger, "Hardrock abrasivity investigation using the Rock Abrasivity Index (RAI)," Taylor and Francis, pp. 3445-3452, 2010.

[24] K.Thuro and R. J. Plinninger, "Hard Rock Tunnel Boring, Cutting, Drilling And Blasting: Rock Parameters For Excavatability," in ISRM, Sandton, South Africa, 2003.

[25] ] International Journal of Rock Mechanics and Mining Sciences, Commission on Standardization of Laboratory and Field Tests, "Suggested methods for determining hardness and abrasiveness of Rocks," Abstracts vol. 15, pp. 89-97, 1978.

[26] N. Innaurato and R. Mancini. "Forecasting the Rock Abrasivity in the Civil and Mining Technological Fields," in EUROCK 96 ISRM International Symposium, Turin, Italy, 1996.

[27] B. Nilsen; et. al. "Abrasivity testing for rock and soils," *Tunnels & Tunneling International*, pp. 47-49, 2006.

[28] G. West, "A Review of Rock Abrasiveness Testing For Tunnelling," in ISRM International Symposium, Tokyo, Japan, 1981.

[29] M. I. Smorodinov, "Express-method of the Rock Abrasiveness Estimation," in 1st ISRM Congress, Lisbon, Portugal, 1966.

[30] M. Alber, "Stress dependency of the CERCHAR abrasivity index (CAI) and its effects on wear of selected rock cutting tools," *Tunnelling and Underground Space Technology*, vol. 23, no. 4, p. 351–359, 2008.

[31] R. Plinninger. et. al., "Wear prediction in hardrock excavation using the CERCHAR Abrasiveness Index (CAI)," in Eurock & 53rd Geomechanics Colloquium, W. Schubert,(ed.), Salzburg, Austria, 2004.

[32] A. E. Gharebagh. et. al. " Review of Rock Abrasion Testing," in American Rock Mechanics Association, San Francisco, California, 2011.

[33] ASTM D-7625-10 "Standard Test Method for Laboratory Determination of Abrasiveness of Rock Using the CERCHAR Method, 2010.

[34] H. E. Kasling, "Abrasive investigations with the Cerchar scratch test an evaluation of the testing condition," in German Geotechnical society, Bochum, Germany, 2007.

[35] T. Michalakopoulos. et. al. "The influence of steel styli hardness on the CERCHAR abrasiveness index value," International Journal of Rock Mechanics and Mining Sciences, vol. 43, no. 2, pp. 321-327, 2006.

[36] Si. Al-ameen. M. D. Waller. " The influence of rock strength and abrasive mineral content on the Cerchar Abrasive Index," Engineering Geology, vol. 36, no. 3-4, pp. 293-301, 1993.

[37] R.H. Hatkinson and J.A. Hudson, " Hardness tests for rock characterization," Comprehensive Rock Engineering, vol. 5, pp. 105-117, 1993.

[38] A. Valantin. " Test CERCHAR pour la mesure de la dureté et de l'abrasivité des roches," Techniques de creusement, Luxembourg 1973 p. 137-140.

[39] M. Suana and T. J. Peters, "The CERCHAR Abrasivity Index and its relation to rock mineralogy and petrography," Rock Mechanics and Rock Engineering, vol. 15, no. 1, pp. 1-8, 1982.

[40] R. Plinninger. et. al. "Testing conditions and geomechanical properties influencing the CERCHAR abrasiveness index (CAI) value," Rock Mechanics and Mining science , vol. 40, pp. 259-263, 2003.

[41] T. Atkinson and VB. Cassapi "Assessment of abrasive wear resistance potential in rock excavation machinery," *Geotechnical and Geological Engineering*, vol. 4, no. 2, pp. 151-163, 1986.

[42] T. Atkinson. " The prediction and reduction of abrasive wear in mining excavation machinery," *Mechanical engineers*, pp. 165-174, 1984.

[43] J. Rostami. et.al. "Review of issues related to CERCHAR abrasivity testing and their implications on geotechnical investigations and cutter cost estimates," *RETC*, pp. 738-751, 2005.

[44] S. Ruehl and M. Alber "Initial stress conditions influencing the CERCHAR abrasiveness index," in *IAEG*, Nottingham, England, 2006.

[45] K. Thuro, "Drillability prediction - geological influences in hard rock drill and," Amsterdam, 1996.

[46] R. Selmer-Olsen and Ot. Blindheim , "Drillability of rock by percussive drilling," in ISRM, Belgrade, Serbia, 1970.

[47] G. Mensa-Wilmot and M. J. Fear, "The effects of formation hardness, abrasivness, heterogeneity and hole size on PDC bit performance," in SPE, Amsterdam, 2001.

[48] A. Besson. et.al. "How to Design Rock Bits To Drill Ultra abrasive Quartzitic Sandstone in Horizontal Wells, Algeria.," in SPE/IADC, Amsterdam, Netherland, 1999.

[49] J. Taylor, Statistical Analysis of Random Uncertainties, John Wiley & Sons, 1998.

[50] Design Expert 8.0.1, Stat-Ease Inc., Minneapolis, Minnesota, 2010

[51] D. Miller and A. Ball. "The wear of diamonds in impregnated diamond bit drilling," Wear, vol. 141, no. 2, p. 311–320, 1991.

## **Appendices**

### **9 Appendix 1. Wear Study Data and Details**

In the following section, pictures were taken from real bit surface at first step with lower magnification and then in the next section pictures were taken with higher magnification using replica.

It should be noted that the wear analysis data for each particular 'flow rate' is presented here. This means that the wear on the bit after performing all the three different weight on bit experiments is reported here. This is due to the size of the wear created on the bit, for just one flowrate-WOB experiment this amount is very small and is the results are analyzed that way, they will be subject to significant round-off errors. Using this method in the measurement and analysis of wear reduces the severity of this problem and makes the analysis of the data more reliable. Furthermore, the purpose of this study is to investigate the effect of flow rate after all.

## 9.1 Study on Leading Edge

### 9.1.1 One gpm experiment

Conventional

vibratory

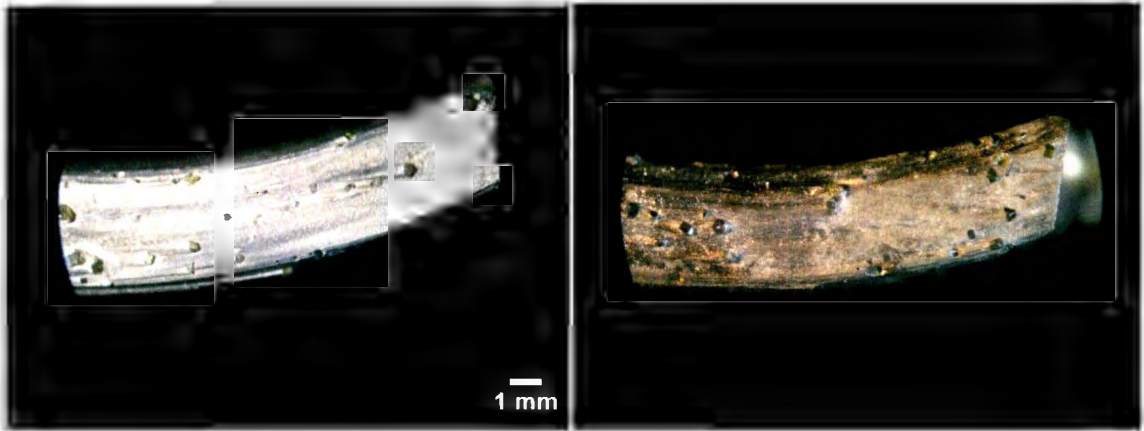


Figure 9-1 Before test

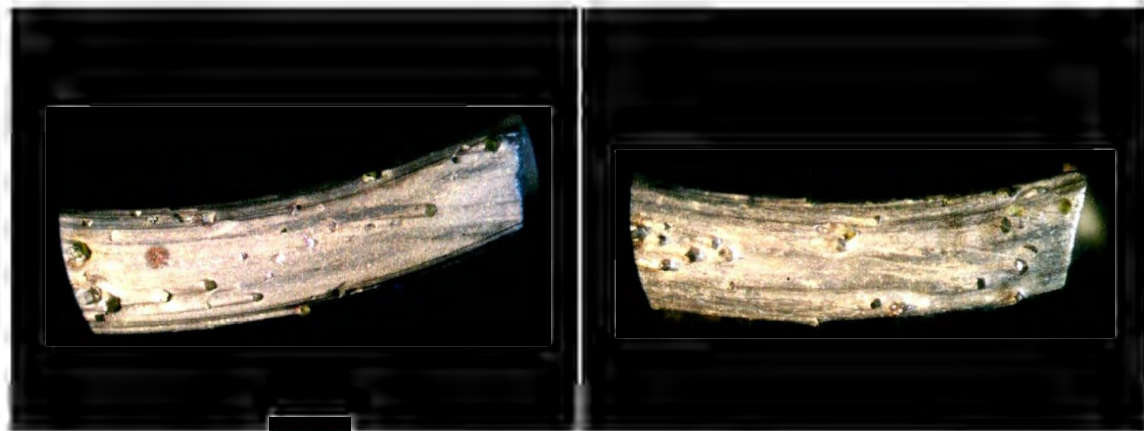


Figure 9-2 After test

### 9.1.2 Three gpm experiment

Conventional

Vibratory

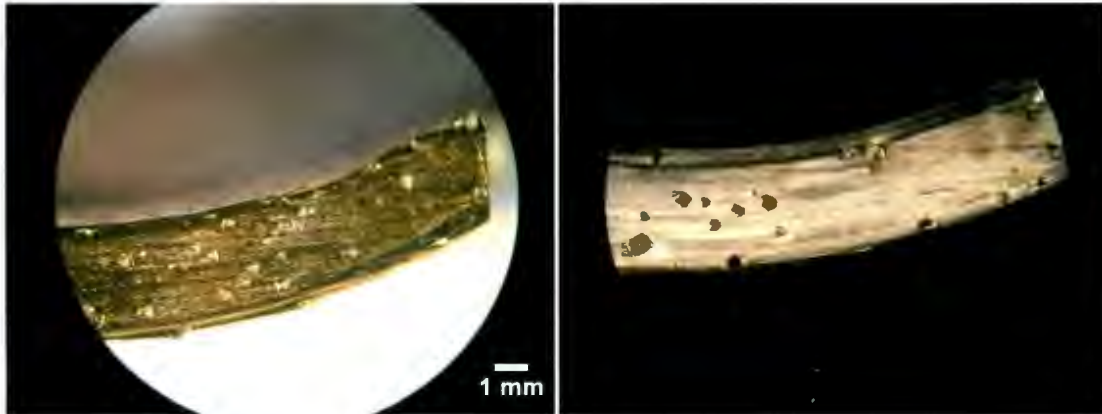


Figure 9-3. Before test

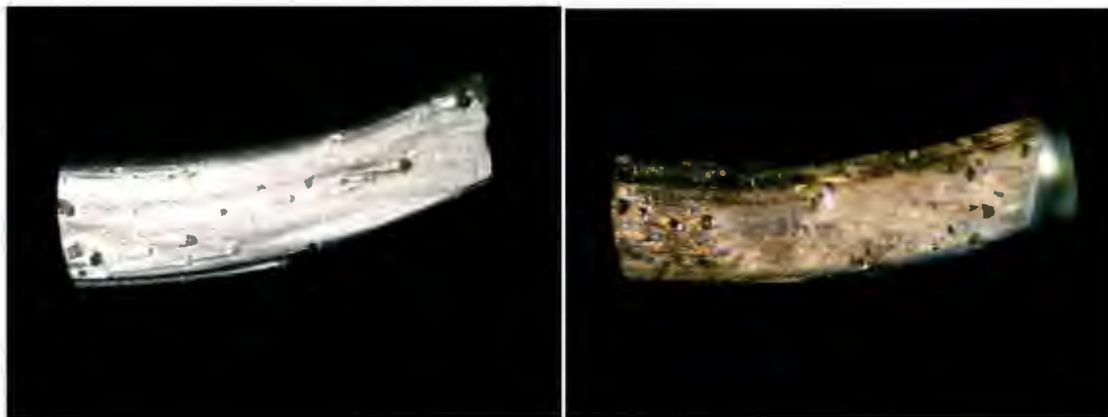


Figure 9-4. After test

### 9.1.3 Five gpm experiment

Conventional

Vibratory

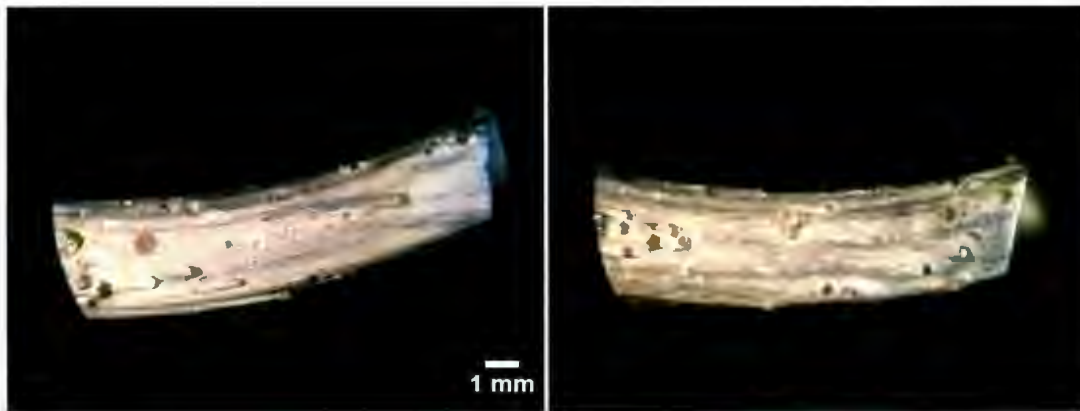


Figure 9-5. Before test



Figure 9-6. After test

Diamonds protruding from the matrix, mostly showing “tails,” i.e. ridges formed behind each diamond as the matrix is worn/eroded ahead and beside the diamond, but less so behind it. Evidently, there is evidence of “conditioning” of the bit segments before they are welded on to the bit through an initial wearing/grinding process producing tails that are parallel and do not follow the segment circumference, while drilling produce tails that are circumferential. The extent to which this change has occurred in the short runs is also an indication of the amount of wear. Also, it appears that with vibration the new tails are in some cases less distinct than those produced in conventional drilling.

## 9.2 Study on Trailing Edge

### 9.2.1 One gpm experiment

Conventional

Vibratory

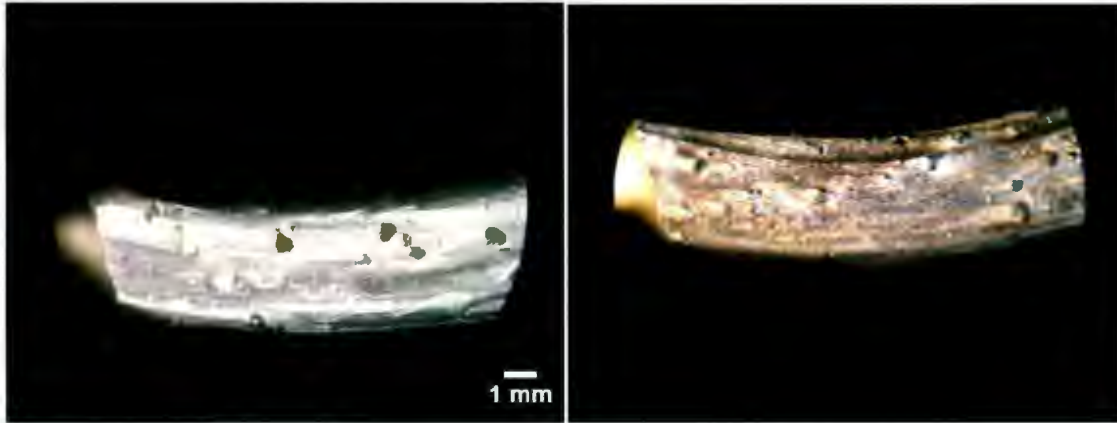


Figure 9-7. Before test

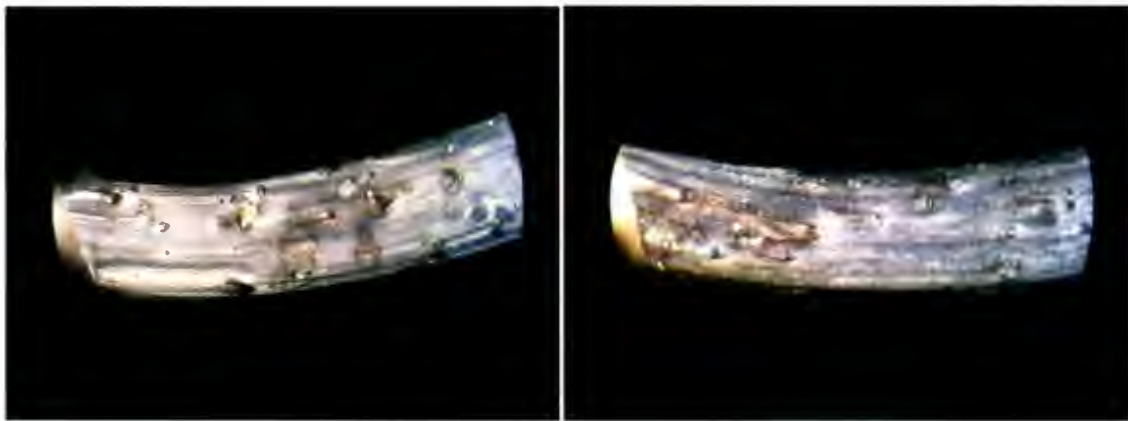


Figure 9-8. After

### 9.2.2 Three gpm experiment

Conventional

Vibratory

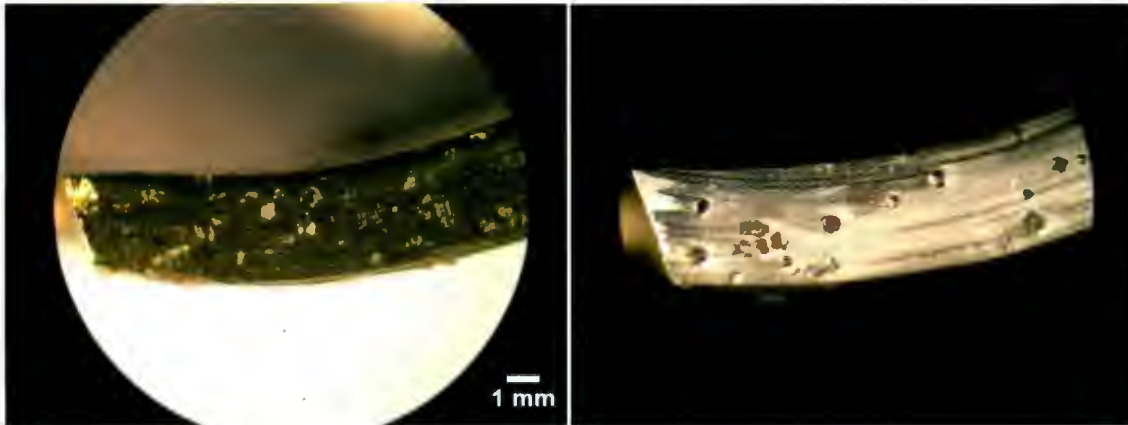


Figure 9-9. Before test

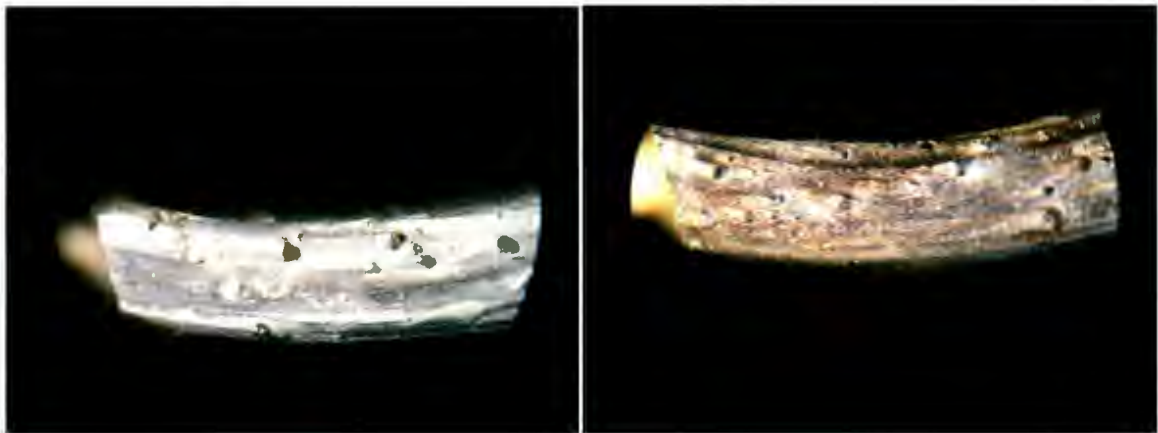


Figure 9-10. After test

### 9.2.3 Five gpm experiment

Conventional

Vibratory

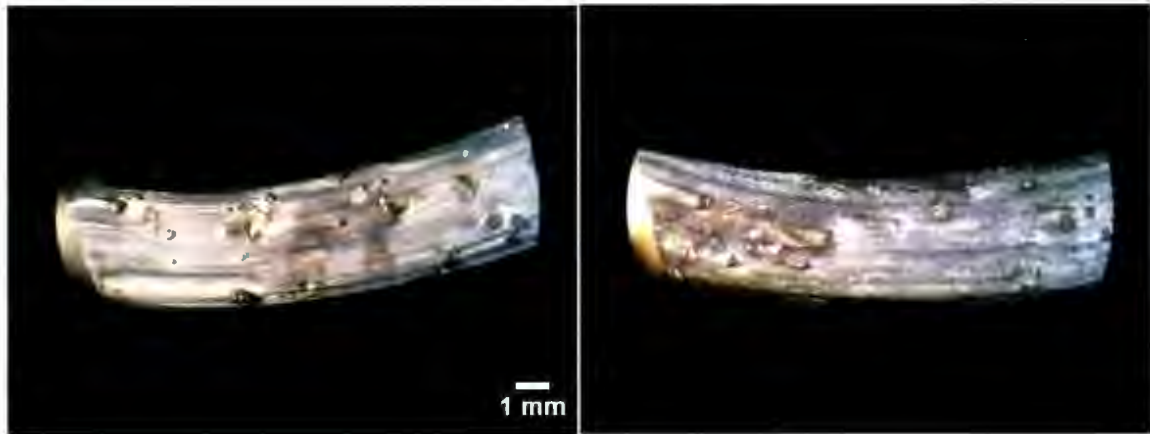


Figure 9-11. Before test



Figure 9-12. After test

### 9.3 Study on Diamonds

#### 9.3.1 One gpm experiment

Conventional

Vibratory

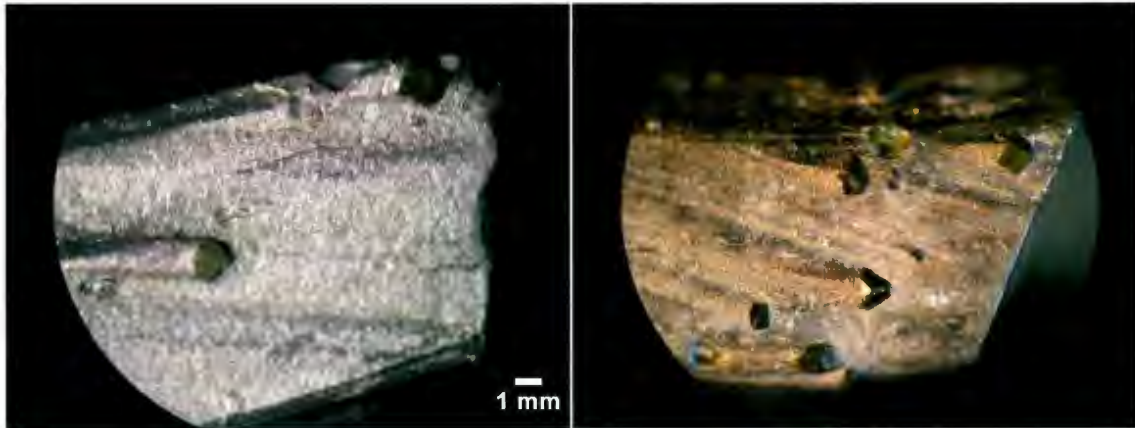


Figure 9-13. Before test

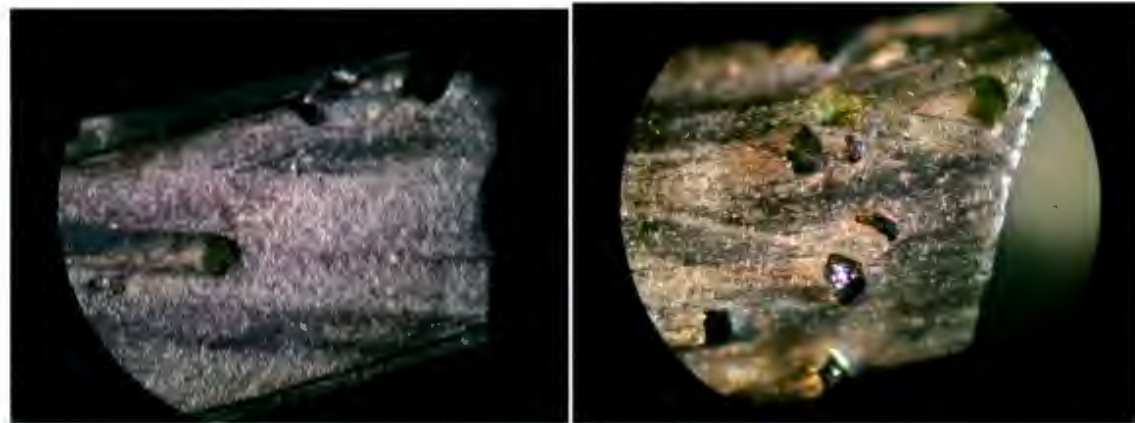


Figure 9-14. After test

Comparing these two pictures shows more rounding on outer edge in vibration assisted drilling, as more of the edge is out of focus when the center is in focus. A little wear on edge of conventional drilling is obvious.

### 9.3.2 Three gpm experiment

Conventional

Vibratory

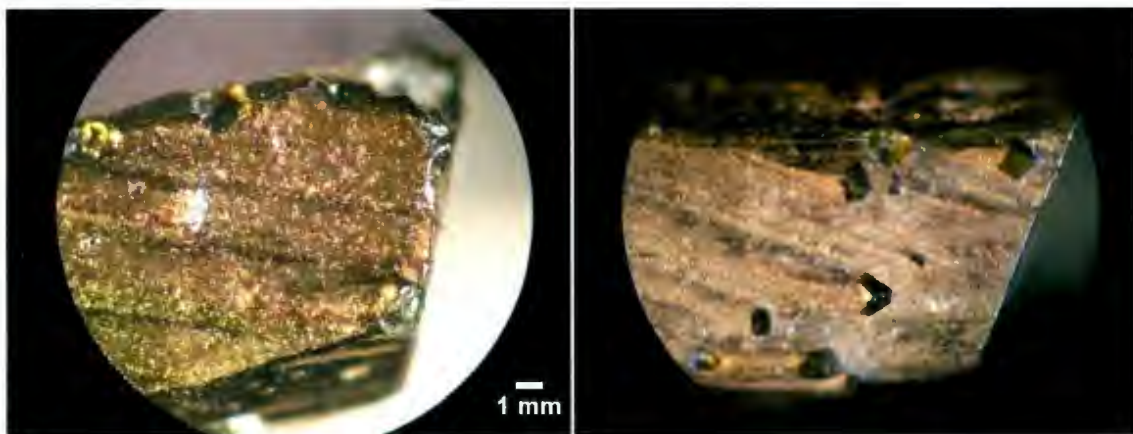


Figure 9-15. Before test

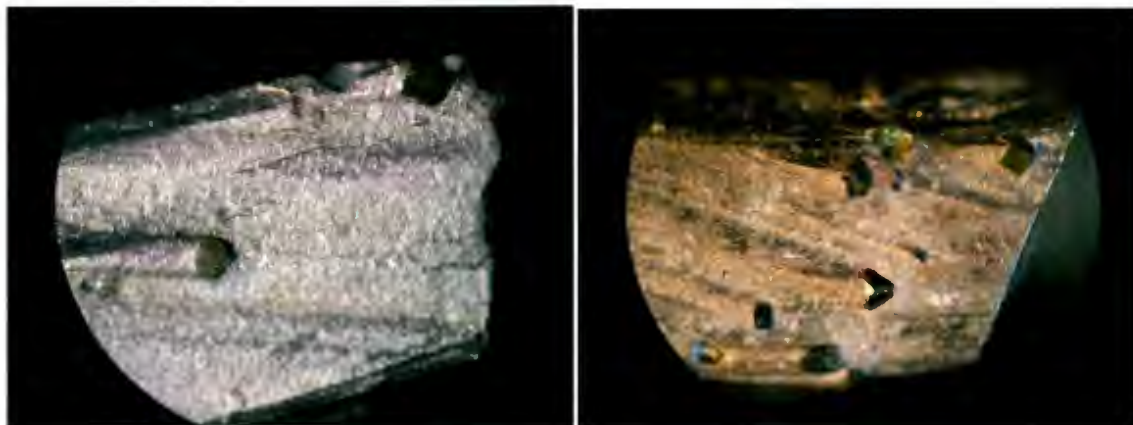


Figure 9-16. After test

Lower rate of wear is visible in 3 GPM.

### 9.3.3 Five gpm experiment

Conventional

Vibratory

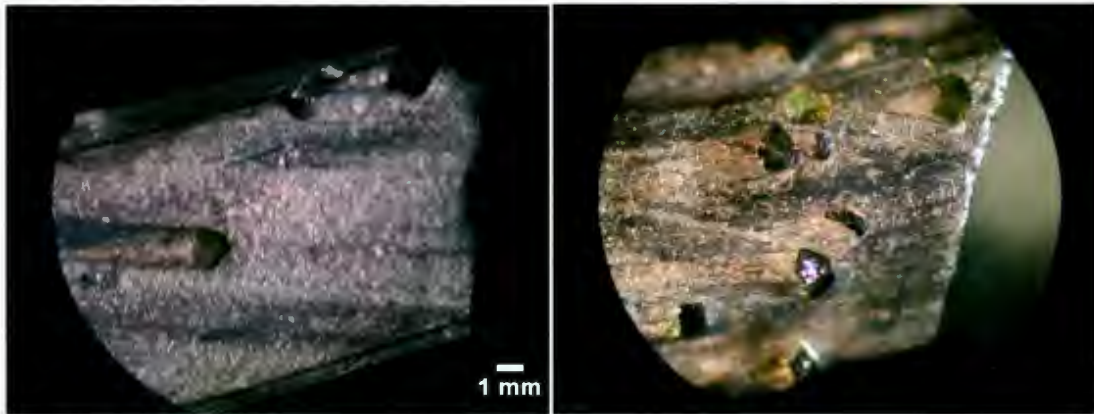


Figure 9-17. Before test

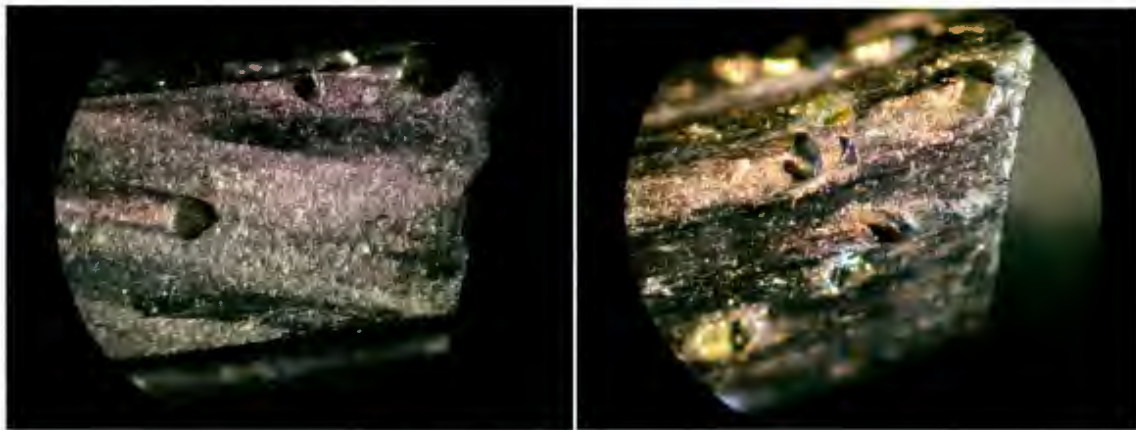


Figure 9-18. After test

More wear in vibration drilling is visible, But not very much in conventional drilling. All of different flow rates shows a little wear on diamonds.

## 9.4 Study on side view

### 9.4.1 One gpm experiment

Not much wear is visible on the following pictures on next pages of side views of bit.

Conventional

Vibratory

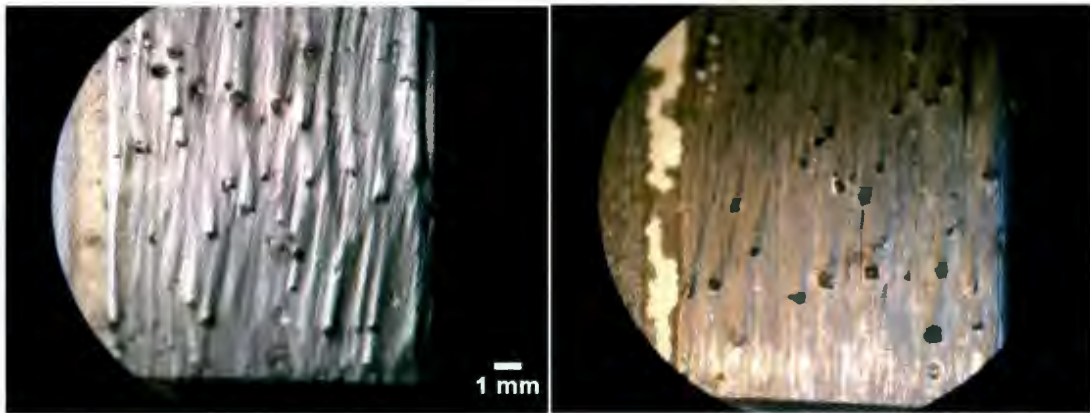


Figure 9-19. Before test



Figure 9-20. After test

### 9.4.2 Three gpm experiment

Conventional

Vibratory

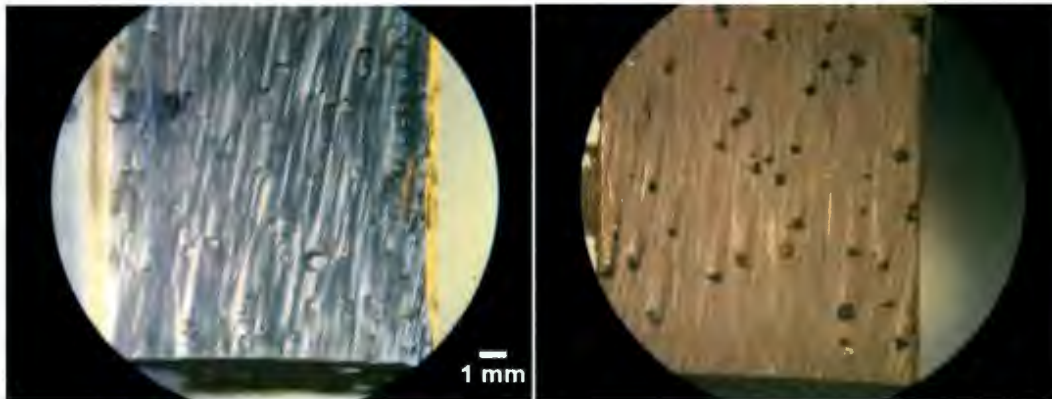


Figure 9-21. Before test

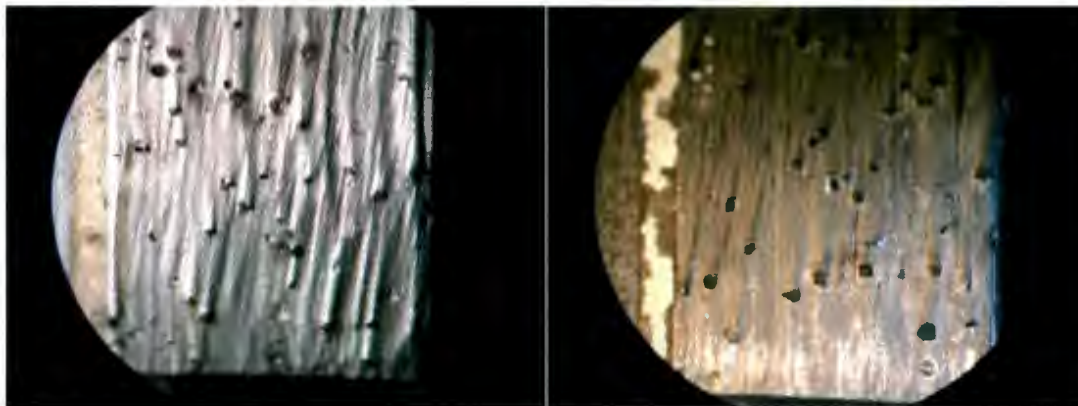


Figure 9-22. After test

### 9.4.3 Five gpm experiment

Conventional

Vibratory

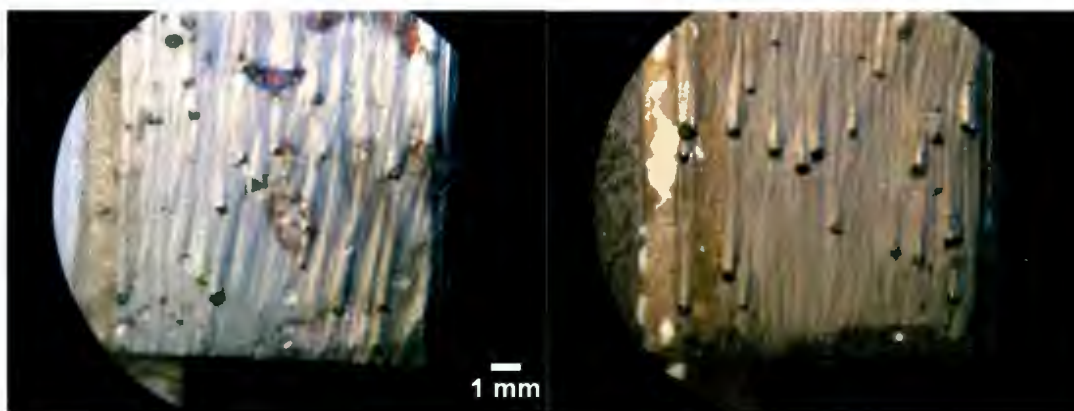


Figure 9-23. Before test

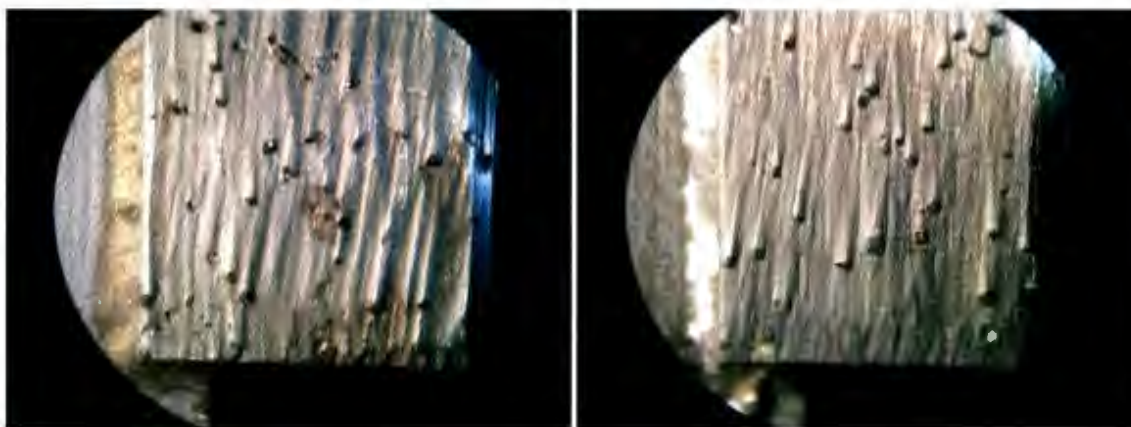


Figure 9-24. After test

## 9.5 Study on water ways

### 9.5.1 One gpm experiment

Conventional

Vibratory

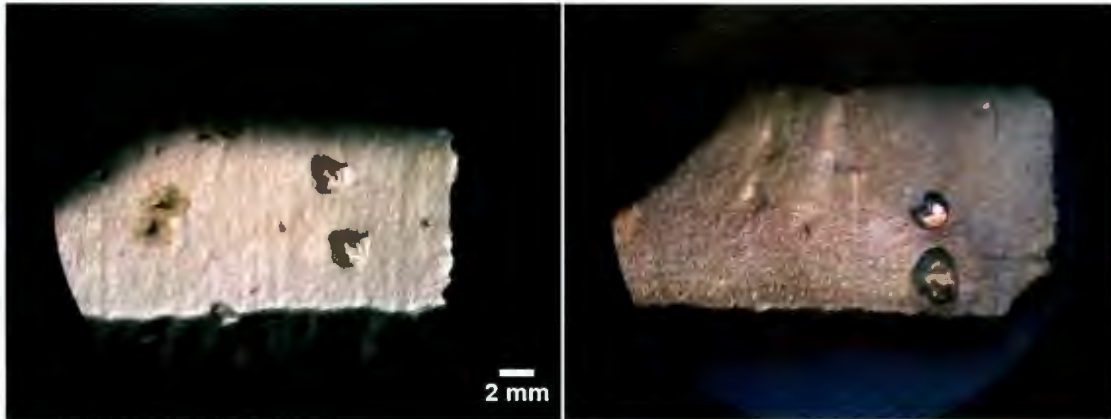


Figure 9-25. Before test



Figure 9-26. After test

Rounding of outer edges is also more visible at waterways. Also evidences are given in next pages.

### 9.5.2 Three gpm experiment

Conventional

Vibratory

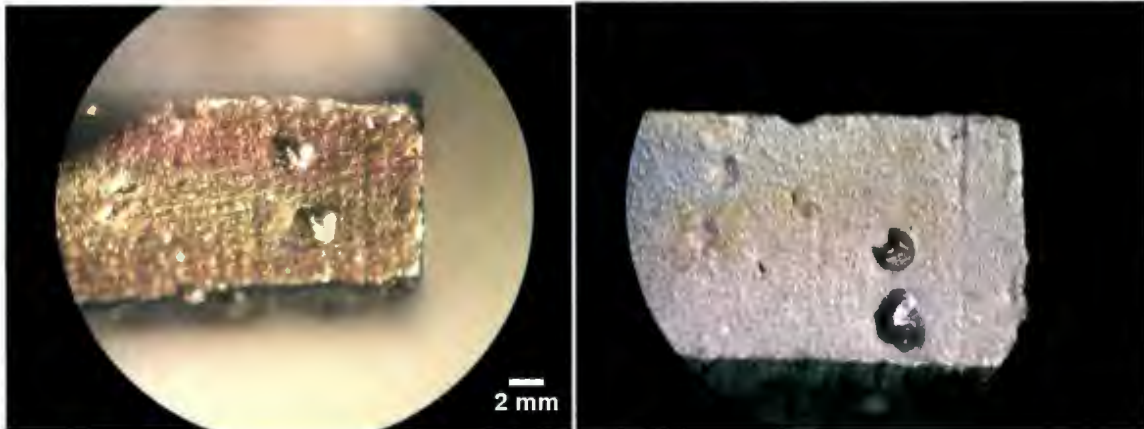


Figure 9-27. Before test



Figure 9-28. After test

### 9.5.3 Five gpm experiment

Conventional

Vibratory

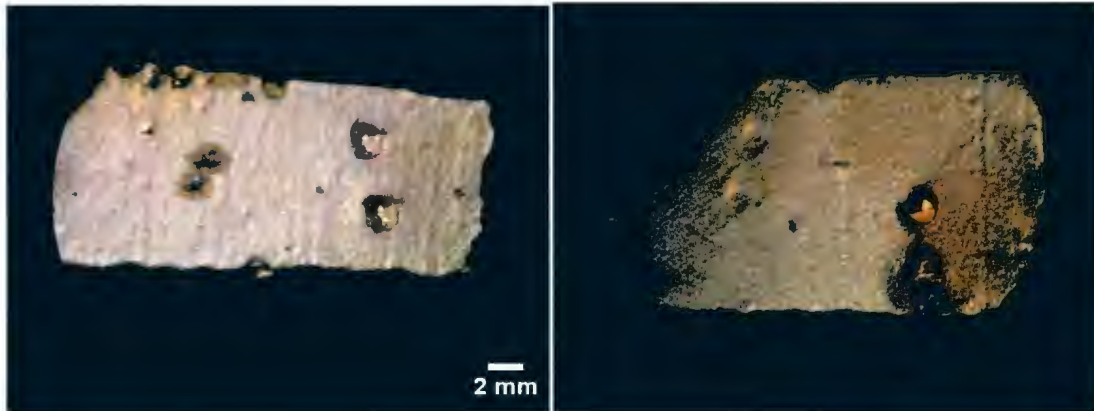


Figure 9-29. Before test



Figure 9-30. After test

### 9.6 Comparing bit profile before and after tests

Please note that the following pictures are composites – before and after pictures superimposed.

### 9.6.1 One GPM Experiment

Conventional

Vibratory

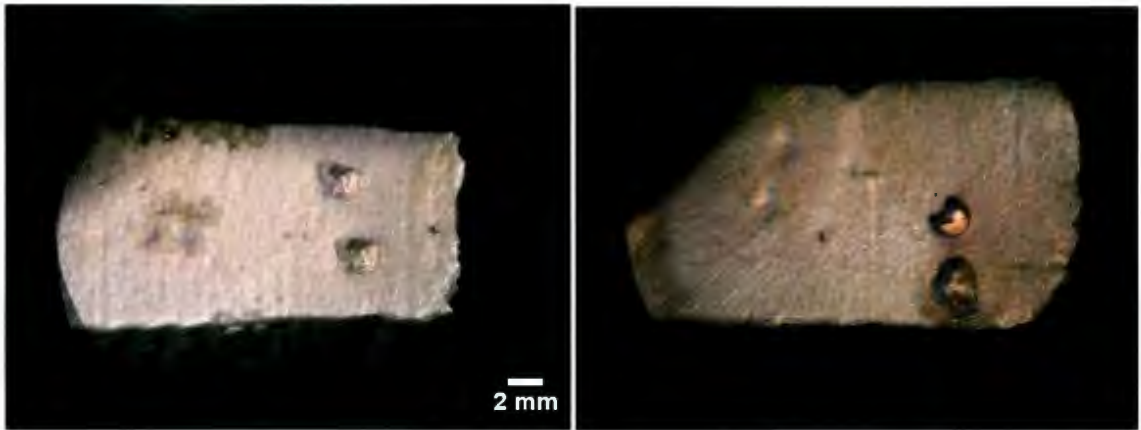


Figure9-31. Superimposed photos of before and after test for conventional and vibratory drilling

### 9.6.2 Three GPM Experiment

Conventional

Vibratory

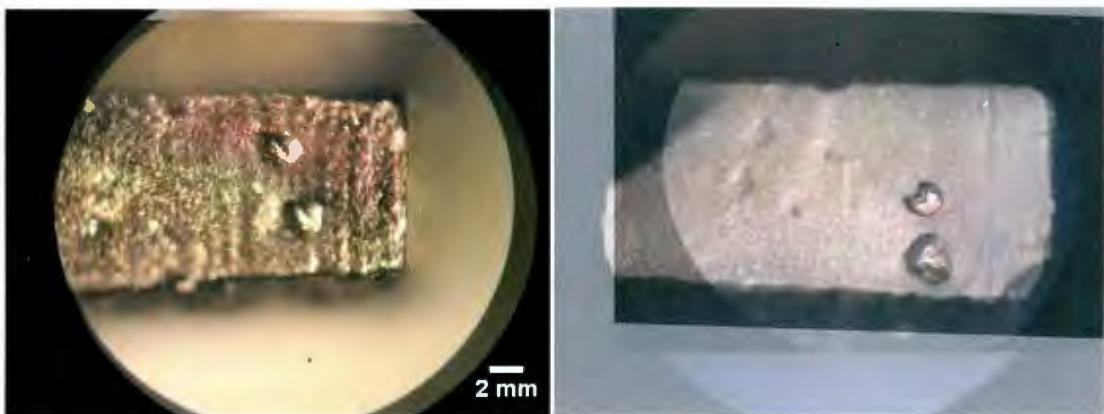
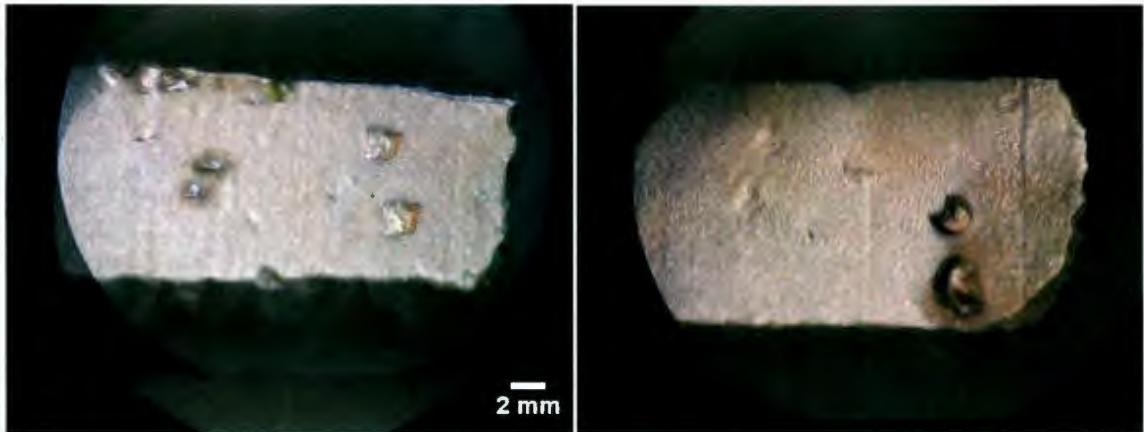


Figure9-32. Superimposed photos of before and after test for conventional and vibratory drilling

### 9.6.3 Five GPM Experiment

Conventional

Vibratory



**Figure 9-33 Superimposed photos of before and after test for conventional and vibratory drilling**

In general, more wear appeared on 5 gpm than 3 gpm and also 1 gpm. Little amount of wear appeared in conventional drilling and it's difficult to compare them together.

## 9.7 Comparing conventional and vibration drilling

Conventional

Vibratory

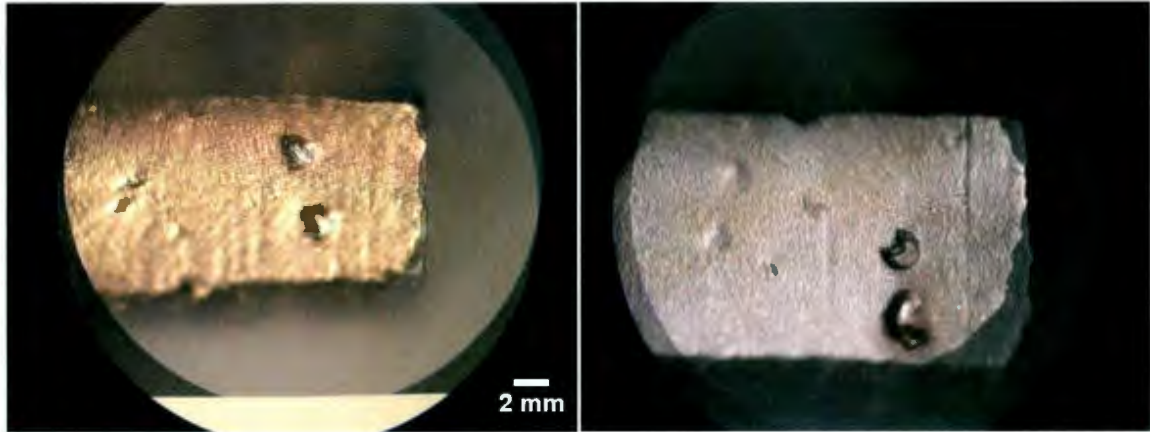


Figure 9-34. Comparing vibrational and conventional drilling wear rates, superimposed photos

Comparing vibration drilling and conventional shows more amount of wear in vibration drilling than a conventional one. Just a little wear almost on all of the conventional happened, but lots of rounding appeared in vibration drilling.

## 9.8 Study on diamonds before starting the runs and after finishing all the runs

This section is a more in-depth analysis of wear on the diamonds. Four modes of wear are identified and are shown in the pictures. Some diamonds after the test appear to be not changed at all and no damage is visible on them those are labeled as 'unworn'. Some diamonds seem to be fractured after the experiments, they are labeled with 'Microfracture'

[51] and finally some diamonds are completely lost which is a result of detachment from the body of the bit and they are labeled as 'pull out'. Another label that is not shown in the pictures is 'wear flat' which pertains to those diamonds that their surface is worn out and become flat. This type of wear is very unlikely to happen because the diamonds have a much higher hardness compared to the matrix.

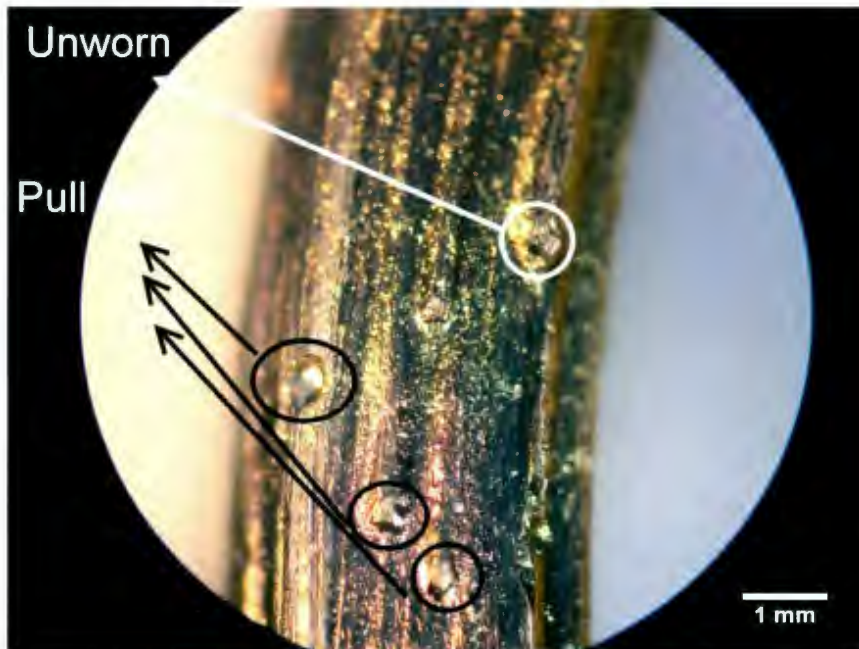
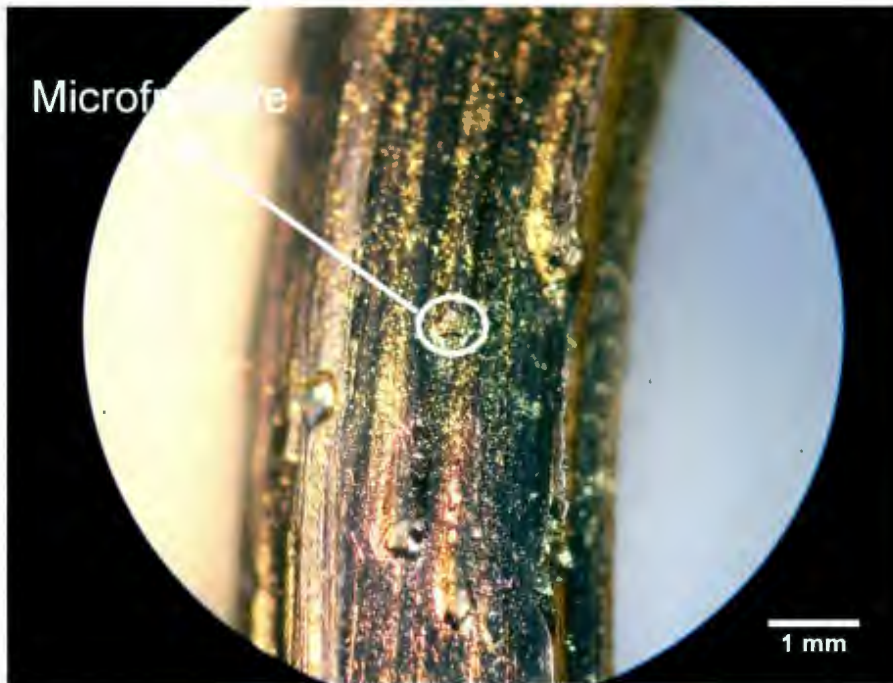


Figure9-35. 'pull out' and 'unworn' diamonds identified



**Figure9-36. Microfractured diamonds**

In the above pictures, the vibration drilling tests before and after of 3 gpm experiments are shown. The reason that we didn't choose the total before and after of all of experiments is because of lots of wear in vibration drilling, and it was not possible to compare the diamonds. In this, 2 experiments at 3 gpm, one with and without vibration were checked and the result for the 3 different segments is given below:

**Table9-1. Summary of wear types in vibratory and conventional drilling tests**

Diamond	Pull out	Unworn	Macro/micro fracture	Wear flat
Vibratory	64%	27%	9%	NEGLIGIBLE
Conventional	38%	49%	13%	NEGLIGIBLE

The number of diamonds with a wear flat was negligible in the amount. Pictures show just a portion of one segment as an example in vibration drilling. As you see, 3 different kinds of diamond wear were obvious. 3 pull out, one microfracture, and one unworn were observed.

In average, there are about 25 diamonds in each segment, and 2 of 5 segments were used for this calculation.

### 9.9 Study on weight loss

The following graph depicts the summary of the data acquired using the weight loss method. The digital high-precision scale was used to measure the weight of the core

barrel before and after drilling. It should be noted that the data reported in this graph are the weight change per unit length drilled.

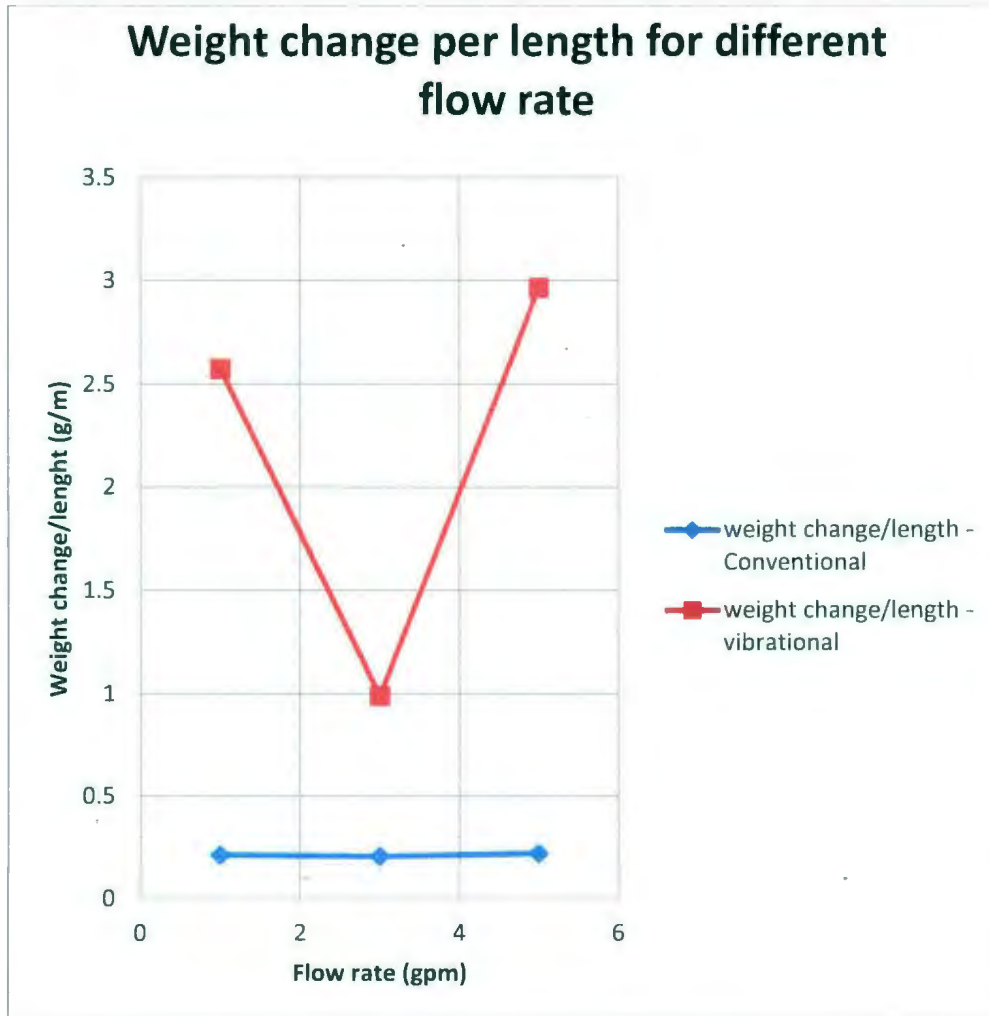


Figure9-37. Weight loss of the bit for two drilling modes versus flow rate

The main conclusion out of this graph is that the wear rate for vibration assisted drilling is significantly higher than that of conventional drilling and this finding is also supported by the microscopic analysis presented in the previous sections.

It appears that for the case of conventional drilling, the effect of flow rate on the wear rate is insignificant. For the case of vibration assisted drilling, there seems to be an optimum flow rate in which the wear rate is minimum (this optimum flow rate in this case turns out to be somewhere close to 3 gpm).

#### 9.10 Study on water ways

In the following pictures, water way views were used to show the bit wear in the case of matrix wear. In order to compare the bit wear, two pictures which the first is taken before drilling test at flow rate of 3 gpm and the second is taken after conducting the test at flow rate of 5 gpm, were combined, the final profile superimposed on the initial one. The outline of the final cross-section is outlined in red. In each case the test with a flow rate of 3 gpm was the first test and the 5 gpm test was the last.

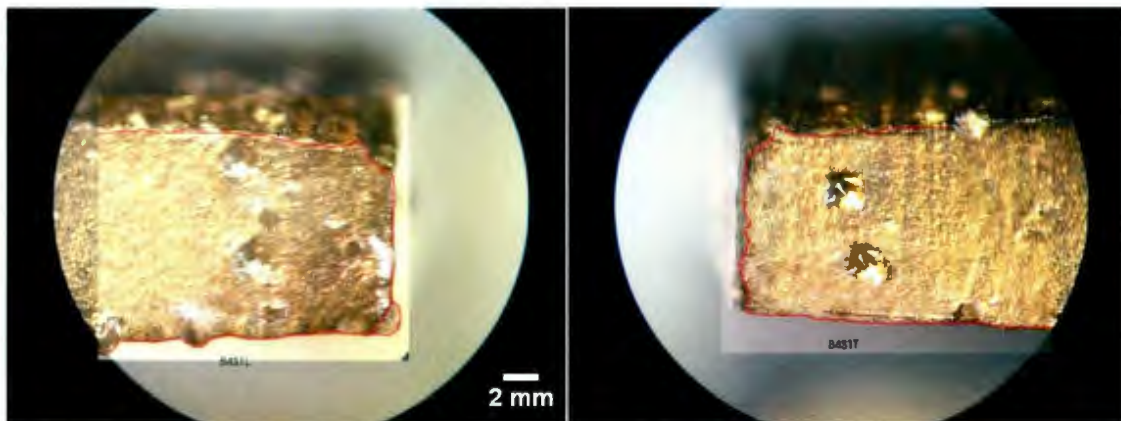


Figure 9-38. Bit 4 segment 1; left: leading, right: trailing (Conventional)

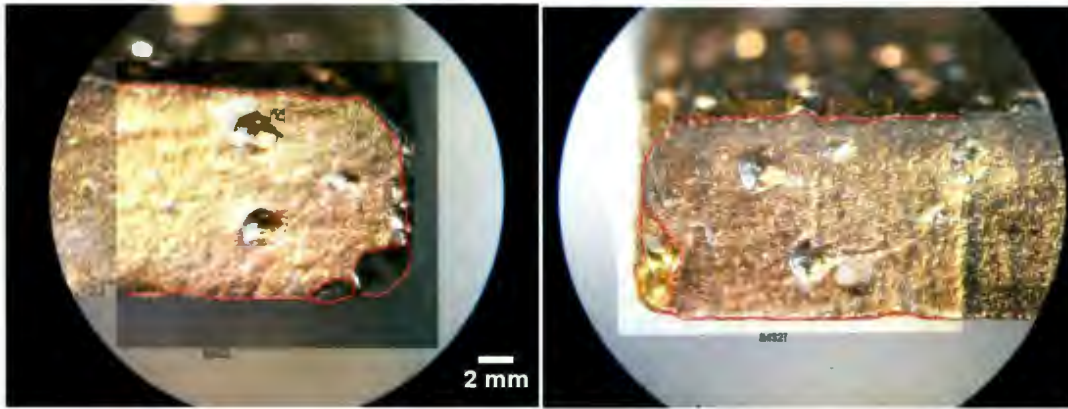


Figure 9-39. Bit 4 segment 2; left: leading, right: trailing (Conventional)

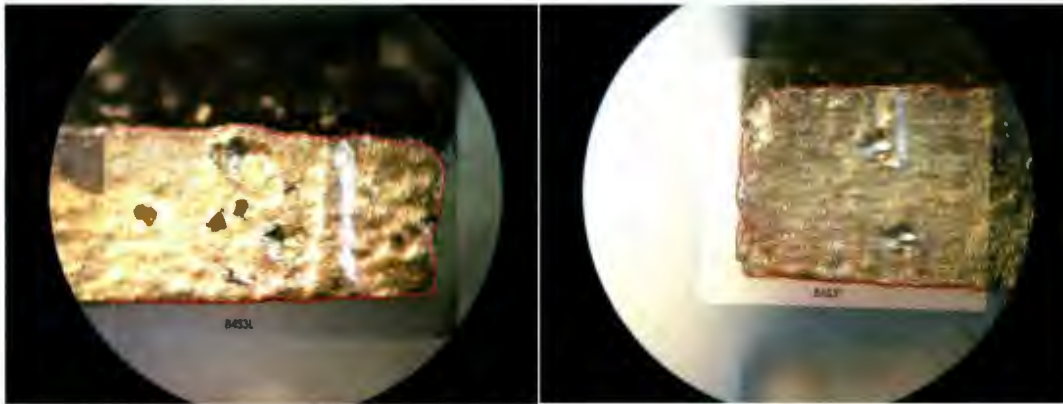
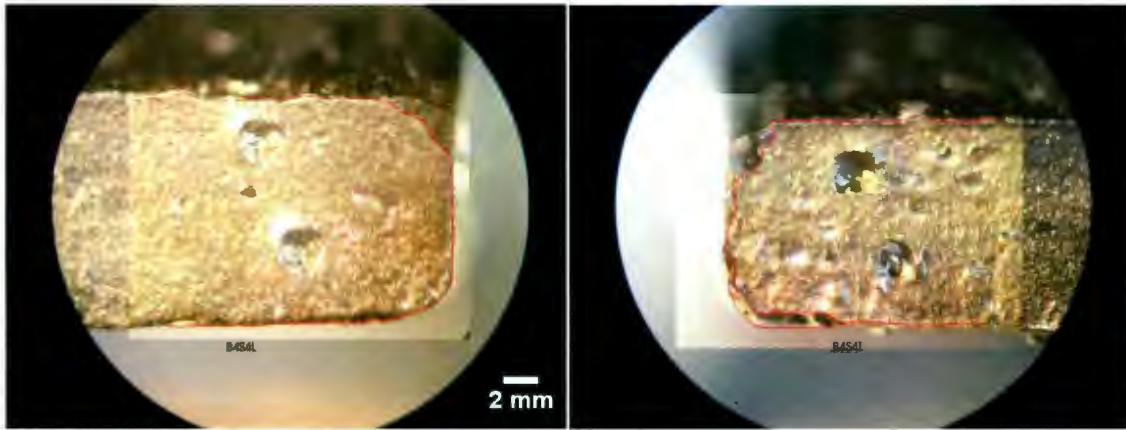
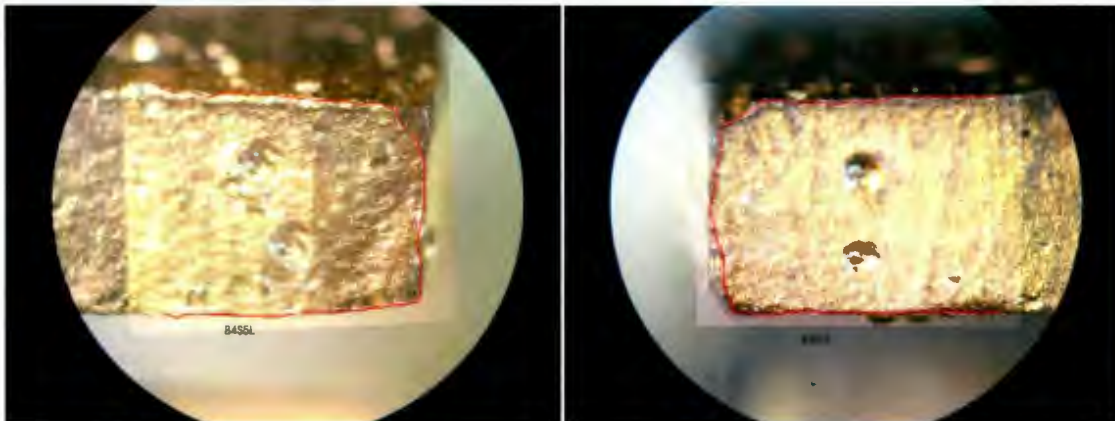


Figure 9-40. Bit 4 segment 3; left: leading, right: trailing (conventional)



**Figure 9-41. Bit 4 segment 4; left: leading, right: trailing (Conventional)**



**Figure 9-42. Bit 4 segment 5; left: leading, right: trailing (Conventional)**

On segment one in Figure 9-41, no wear at leading edge was observed but a little wear at trailing edge occurred.

For segment two in Figure 9-42, some wear observed at outer edge, both on leading and trailing edges.

On segment three in Figure 9-43 there is no wear at leading edge, a little at outer edge of trailing end.

For segment four in Figure 9-44 there is no wear, except at outer edges both on leading and trailing ends.

On segment five in Figure 9-45 no wear occurred, except at outer edges both on leading and trailing ends.

In the following pictures, different segments were chosen to show the effect of vibration on water ways for comparison to conventional.

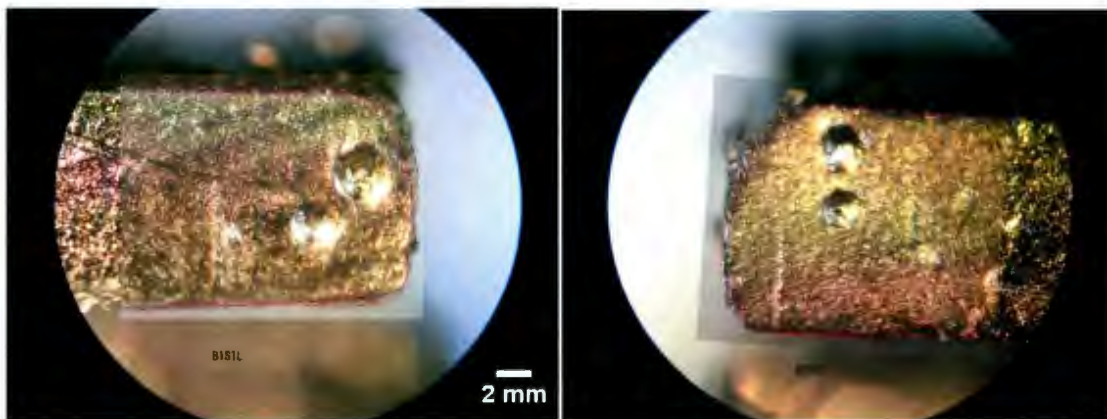


**Figure 9-43. Bit 1 segment 1; left: leading, right: trailing (Vibrational)**

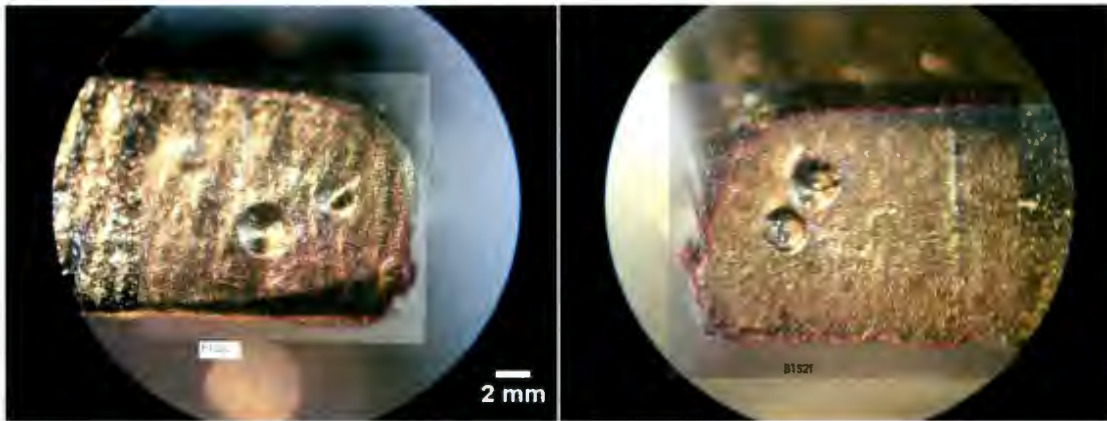


Figure 9-44. Bit 1 segment 2; left: leading, right: trailing (Vibrational)

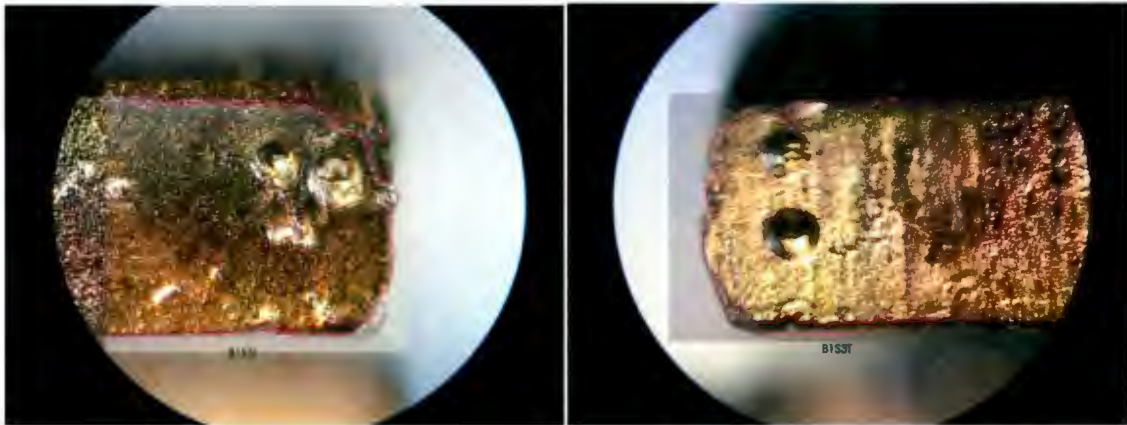
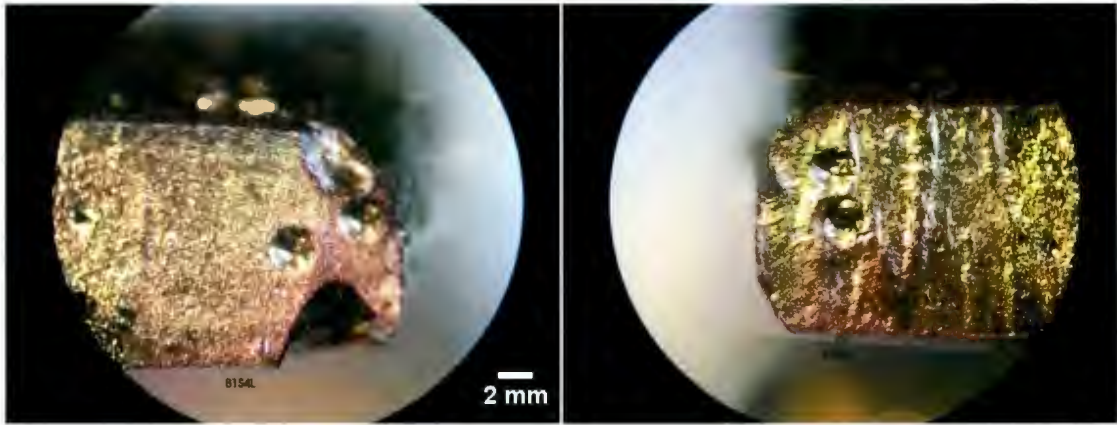
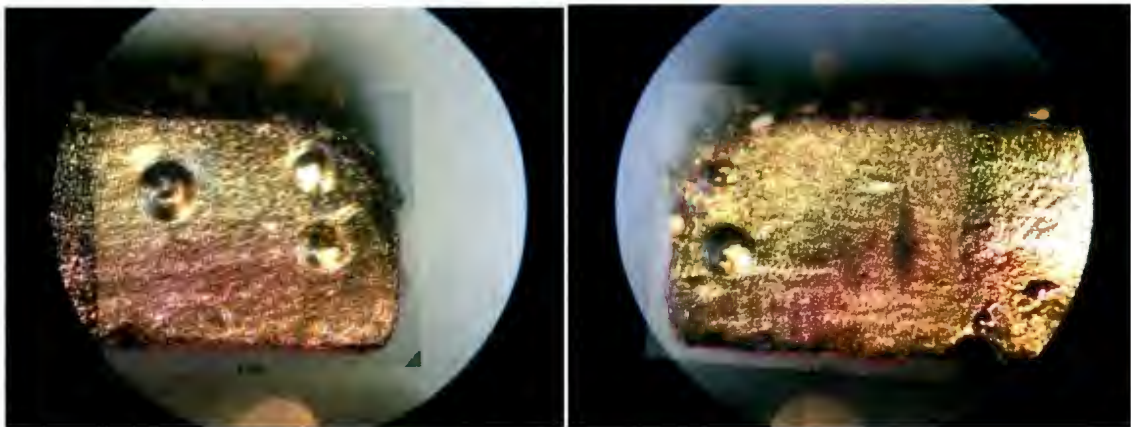


Figure 9-45. Bit 1 segment 3; left: leading, right: trailing (Vibrational)



**Figure 9-46. Bit 1 segment 4; left: leading, right: trailing (Vibrational)**



**Figure 9-47. Bit 1 segment 5; left: leading, right: trailing (Vibrational)**

Some wear at both inside and outside edges was observed, most wear occurred at outer edge.

There is zero wear at 1/4 and 1/3 width in from inner edge.

This bit had already been worn to some extent prior to test, showing rounding on inner edge.

## 10 Appendix 2. Styli Heat Treating and Hardness Testing Details

We used Knoop test because with Knoop test we can reach to very tip of stylus and measure the hardness that is the most important part of stylus to use in CERCHAR test.

The following describes Knoop tests on two samples, one of our samples is as received from technical services and the other one is one that Steve Steele tempered. We called them sample (1) and sample (2) in this report.

### 10.1 Sample (1):

First we started with sample (1) the mounted portion of an untempered stylus, including the tip, in plastic mounting material, in the manner usual in metallography, with the pointed tip perpendicular to a flat surface of the mount. We polished in the usual way for metallography, with emery papers of decreasing particle size, in turn, followed by polishing with 6 micron and 1 micron diamond paste. This removed all scratches on the surfaces tested. Then started the Rockwell test on sample (1) on both the tip and base of sample. After the Rockwell test we did a couple of Knoop tests on the same surfaces to compare Rockwell C value with Knoop to check the correlation provided on the Wilson chart (hardness conversion chart). In following tables (10.1-10.2) the values for the tip and base side of sample(1) are listed.

**Table 10-1. Tip Hardness Test Results for Sample(1)**

Test	Date	Description	HRC (Rockwell test)	Knoop test	Equivalent HRC (from Knoop)	Difference HRC and Equival. HRC
1	31-Jan-11	Tip side	65.2	703	58.6	6.6
2	31-Jan-11	Tip side	65.2	789	62.3	2.9
3	31-Jan-11	Tip side	66.1	799	63	3.1
Mean			65.5	763	61.3	4.2

**Table 10-2. Base Hardness Test Results for Sample(1)**

Test	Date	Description	HRC (Rockwell test)	Knoop test	Equivalent HRC	Difference of HRC
------	------	-------------	---------------------	------------	----------------	-------------------

		n	test)	(kg/mm <sup>2</sup> )	nt HRC	and Equiv HRC
1	31-Jan-11	Base side	62	595	53	9
2	31-Jan-11	Base side	64.1	622	54.6	9.5
3	31-Jan-11	Base side	64.2	826	64.1	0.1
Mean			63.4	681	57.2	6.2

The previous Knoop tests on the base were at random locations, and the test locations for Rockwell and Knoop tests with the same test number are not necessarily adjacent. There is the possibility of variation of hardness at different locations of the steel due to the fact that the steel, or its heat treatment, is not perfectly homogenous. While the locations selected for the Knoop tests were close to the indentations produced by Rockwell test; however, a certain distance from each indentation was chosen so that the plastic deformation produced by Rockwell hardness test does not affect the Knoop test results.

The approximate locations of the indentations and Knoop test location points are shown in Figure(10-1) .

Considering the averages the Knoop test would appear to convert to an equivalent HRC about 4-6 units higher than a direct measurement of HRC.

After we finished these tests on sample (1) we decided to do another set of four Knoop tests somewhere between five Rockwell test points on the base side of sample (1) along a line near the center from one edge to another. We choose a center line (diameter) of circle and also a line 3 mm above that . The data are in Tables (10-3)and (10-4).

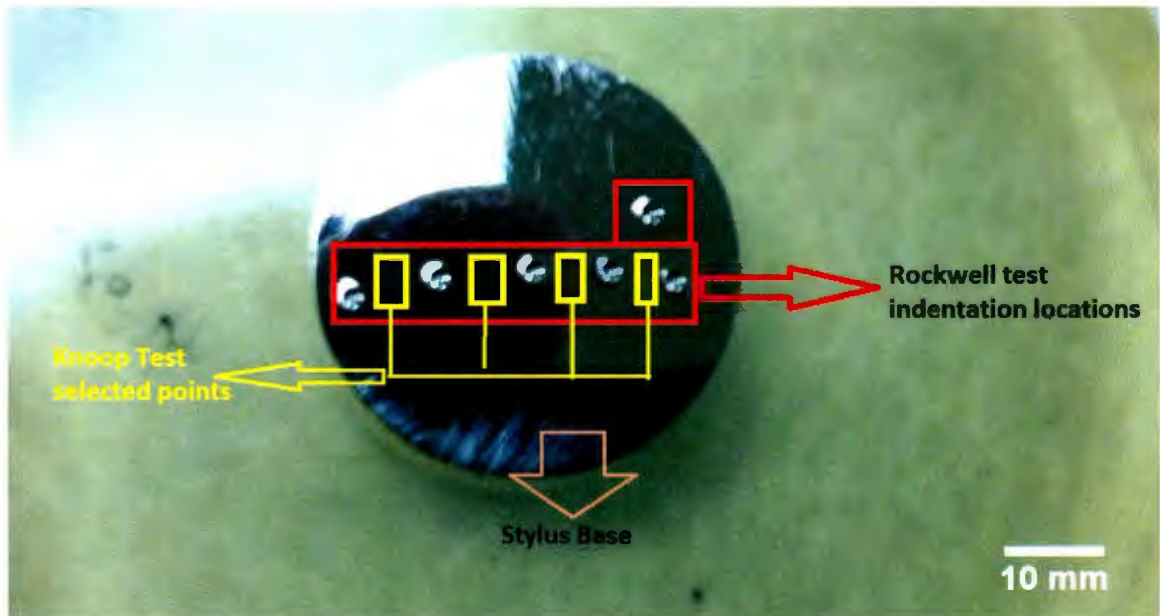


**Figure 10-1.** five tests done on a stylus base and the proposed locations for conducting the Knoop test

**Table 10-3.knoop Tests on the base side of sample (1)**

Test (center line)	Date	Description	Knoop No.	HRC equivalent
	2/28/2011	Base side	626	54.9

## 10 Appendix 2. Styli Heat Treating and Hardness Testing Details

We used Knoop test because with Knoop test we can reach to very tip of stylus and measure the hardness that is the most important part of stylus to use in CERCHAR test.

The following describes Knoop tests on two samples, one of our samples is as received from technical services and the other one is one that Steve Steele tempered. We called them sample (1) and sample (2) in this report.

### 10.1 Sample (1):

First we started with sample (1) the mounted portion of an untempered stylus, including the tip, in plastic mounting material, in the manner usual in metallography, with the pointed tip perpendicular to a flat surface of the mount. We polished in the usual way for metallography, with emery papers of decreasing particle size, in turn, followed by polishing with 6 micron and 1 micron diamond paste. This removed all scratches on the surfaces tested. Then started the Rockwell test on sample (1) on both the tip and base of sample. After the Rockwell test we did a couple of Knoop tests on the same surfaces to compare Rockwell C value with Knoop to check the correlation provided on the Wilson chart (hardness conversion chart). In following tables (10.1-10.2) the values for the tip and base side of sample(1) are listed.

These results appear to confirm that the previous Knoop tests and the difference between the equivalent values in HRC and the actual HRC.

### 10.2 Sample(2) :

First we did grinding with abrasive paper and then did polishing with 6 and 1 micron diamond paste on a mounted portion of an annealed stylus. Several Knoop tests were conducted on both the base and the tip of the sample We did six Rockwell tests on the base of our sample, but just one test for the tip side, as such tests must be some distance from the edge of a sample. All the Rockwell tests for the base side were along the center line of our sample and the one for the tip was in the middle. In tables (10-5) and (10-6) are the data for both Rockwell and Knoop tests.

**Table 10-5. . Knoop Tests on the tip side of sample (2)**

Test	Date	Description	Knoop test	Equivalent HRC
1	7/Feb/2011	Tip side	617	54.1
2	7/Feb/2011	Tip side	636	55.4
3	7/Feb/2011	Tip side	702	58.7
4	7/Feb/2011	Tip side	712	59.1
5	7/Feb/2011	Tip side	767	61.5
Mean			727(Mean of test 3-5)	59.8(Mean of test 3-5)

Tests 1 and 2 were not included in the average. Their lower values could be due to being close to the edge of the pin. We obtained 59 HRC from our Rockwell test that is fairly close to the average of HRC equivalent of the Knoop tests, for instance; test numbers 3, 4 and 5 are 59.8 in average.

**Table 10-6. Knoop Tests on the base side of sample (2)**

Test	Date	Description	HRC(Rockwell test)	Knoop test	Equivalent to HRC	Difference of HRC and Knoop
1	7-Feb-11	Base side	37.8	596	53.1	15.3
2	7-Feb-11	Base side	54.2	594	53	1.2
3	7-Feb-11	Base side	57.8	657	56.3	1.5
4	7-Feb-11	Base side	58	648	55.5	2.5
5	7-Feb-	Base	58	680	57.5	0.5

	11	side				
6	7-Feb-11	Base side	60.1	679	57.5	2.6
7	7-Feb-11	Base side		685	57.5	
8	7-Feb-11	Base side		661	56.5	
9	7-Feb-11	Base side		641	55.5	
10	7-Feb-11	Base side		587	52.6	
11	7-Feb-11	Base side		683	57.7	
Mean			58.5(Mean of 3-6)	668(Mean of 3-8)	56.8(Mean of 3-8)	

Scrutinizing Table 10-6, it can be noted that for test number 1 the difference between Rockwell test and Knoop test is high and there is almost 40% difference between the two values. While one of the measurements may simply be due to an error, this difference is due to the fact that this test was done on a location on the base which is very close to the edge of the base

In table (10-6) we can see the average of Rockwell tests 3,4,5,6 is 58.5 and the HRC equivalent of the average of Knoop tests 3,4,5,6,7,8 converted to HRC using the table provided by Wilson is 56.9. All these tests were done near the center of base side sample. In this case there is good agreement between Rockwell C tests and the Knoop test values converted to HRC.

**Correlation Test:** (Calibration of knoop test apparatus)

To further check the equivalence of Knoop and direct Rockwell C tests we performed four tests on two different certified standards supplied for the Rockwell tests. These pieces of metal are produced so that any part of its surface has the specified hardness and can be used to check the calibration of a hardness tester. These have polished flat surfaces and have dimensions such that they could be mounted in the microhardness tester, and tests performed on some portions of the surface. The Rockwell C hardness is marked on them by the supplier of the standards, with certificates supplied.

Table (10-7) and (10-8) shows the results.

**Table 10-7. Knoop test for calibration**

<b>Test No.</b>	<b>Knoop test</b>	<b>HRC equivalent</b>
<b>1</b>	<b>490</b>	<b>46.7</b>
<b>2</b>	<b>482</b>	<b>46.1</b>

**Table 10-8. Standard with 60.91+- 0.5HRC**

<b>Test No.</b>	<b>Knoop test</b>	<b>HRC equivalent</b>
<b>1</b>	<b>653</b>	<b>56.1</b>
<b>2</b>	<b>671</b>	<b>57.0</b>

With the 44.6 HRC standard the Knoop test gave an equivalent HRC about 2 units higher than the actual HRC, while the 60.9 HRC standard the HRC equivalent to the Knoop HV was 4 to 5 units lower than actual HRC.

The hardness of one of these standards is higher and that of the other is lower than the hardness expected for a CECHAR test stylus. For a stylus correctly tempered to the 54 HRC, it would appear that there may be little difference between a Knoop test converted to HRC and the actual HRC.

With the portions of styli that we have been using for testing the conversion between Knoop hardness and Rockwell C hardness there may be some non-uniformity in the hardness in these pieces of metal, due to variations in composition or heat treatment. This could be the reason for the range of hardness values on each sample that we measured with both testers. The closeness of the two hardness values that we measured on each commercially supplied standard indicates that these test pieces are indeed uniform, as they should be. We did not want to conduct more tests on these particular standards, which were purchased for general use in the Metallurgy Laboratory to confirm the calibration of the equipment.

#### Conclusion:

From the tests conducted so far there is some uncertainty in the correlation between Knoop and Rockwell C tests, using a standard conversion table. Before any further work is done to check this conversion it would be appropriate to check how important this could be in relation to the uncertainty of CAI values and the uncertainty in the correlation of CAI with stylus hardness, which will be studied when our tester is ready for use and repeat determinations of CAI can be made using repeatable abrasive test surfaces.

New series of tests :

The hardness achieved in tempering the styli according the ASM Metals Handbook guide data for tempering O1 tool steel did not produce the expected hardness. The hardness values were closer to the handbook correlation for hardness versus tempering temperature for S1 tool steel, shown here in Figure 10-2. Both these tool steels are produced with compositions covering a range of values for similar elements. An SEM EDAX analysis of the metal used in our styli is close to the composition of steel O1 in the ASM standard, except that the detected presence of vanadium in it is more typical of S1 steel. Therefore we decided to use the tempering guidelines for S1 for our tempering experiments.

Fig (10-2) is the diagram in the Metals Handbook for the tempering behavior for several S1 steels, each with a slightly different composition. Rockwell hardness values achieved as a function of temperature are plotted. The trend line for S1 steel type 5, which had the closest composition to our steel, is shown in the graph. As it can be seen from the figure, to achieve a hardness of 55 for the steel; we need a tempering temperature in the range of 225-275 °c.

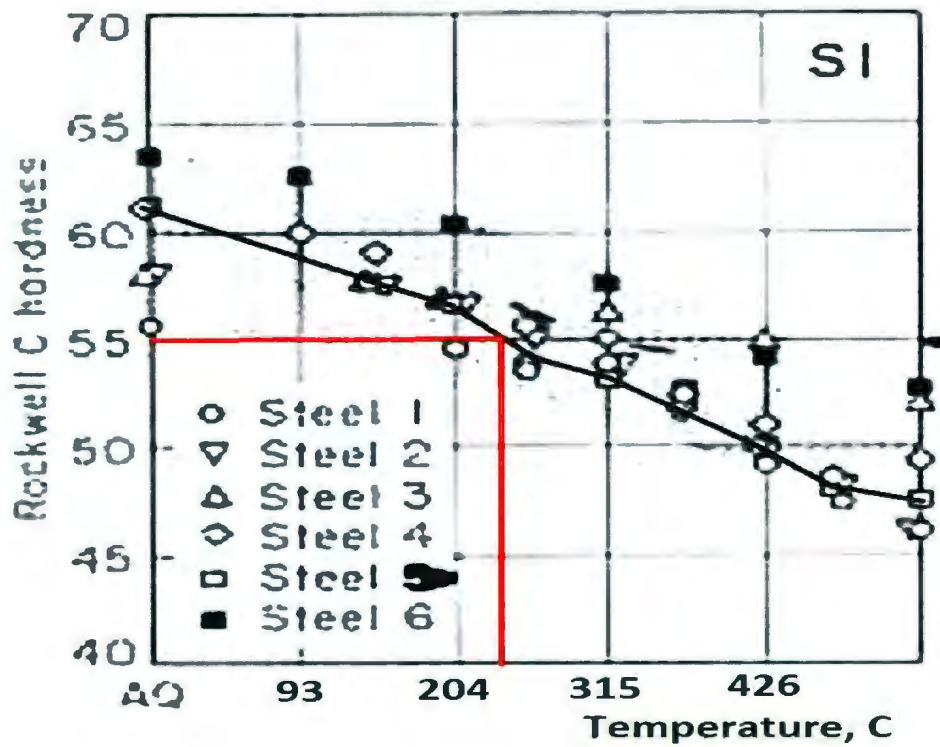


Figure 10-2. Rockwell Hardness vs. temperature of heat treatment

So according to metal handbook ASM and our last experience we asked Steve Steele to temper 3 sets of styli at 3 different temperatures to establish the best tempering, as follows. (Table 10-9 to 10-12).

Table 10-9. Heat treatment of samples

Number of stylus	Temperature	Time
10	275 c	45 min
10	250 c	45 min

14	225 c	45 min
----	-------	--------

After doing tempering operation we started to do Rockwell hardness test on them and we gained the following results as it can be seen in next three tables, for the three temperatures used. Tempering tests also used to test consistency of pin hardness and reproducibility of hardness test. We are particularly interested in the tests near the styli tips. Mean near tip is 52.4

**Table 10-10. Tempered at 275°C for 45 min**

Stylus:	A <sub>1</sub>	A <sub>2</sub>	A <sub>3</sub>	A <sub>4</sub>	A <sub>5</sub>	A <sub>6</sub>	A <sub>7</sub>	A <sub>8</sub>	A <sub>9</sub>	A <sub>10</sub>
Near base	53	50	51	50	49	49	54	55	55	51
Middle	51	49	48	53	51	51	55	59	50	52
A little above middle	52	53	50	55	52	53	55	52	46	52
Near Tip	54	50	53	52	52	52	53	51	52	55

**Table 10-11 Tempered stylus at 250°c for 45 min**

<b>Stylus:</b>	<b>C1</b>	<b>C 2</b>	<b>C 3</b>	<b>C 4</b>	<b>C 5</b>	<b>C 6</b>	<b>C 7</b>	<b>C 8</b>	<b>C 9</b>	<b>C 10</b>	<b>C 11</b>	<b>C 12</b>	<b>C13</b>
<b>Near base</b>	53	55	53	50	54	53.2	50.9	46	52	52	50	55	52
<b>Middle</b>	53	53	54	55	56.1	53.4	53	50	54.8	52.3	50.2	54	54
<b>little above middle</b>	50	54	55	50.3	53.2	51	53.4	49	51.8	52	52	54.8	53
<b>Near Tip</b>	54.1	52.3	53.3	55	52	52	53.3	50.1	53	51.3	50	52	52

**Table 10-12 Tempered Stylus at 225°c for 45 min**

<b>Stylus:</b>	<b>B1</b>	<b>B 2</b>	<b>B 3</b>	<b>B 4</b>	<b>B 5</b>	<b>B 6</b>	<b>B 7</b>	<b>B 8</b>	<b>B 9</b>	<b>B10</b>
<b>Near base</b>	55	57.1	55	57.1	57.2	57	56	56.3	55.1	56.9
<b>Middle</b>	56.1	58	56.8	54.2	54	58.8	55	54	55.2	57
<b>Little above middle</b>	56.4	56.3	55.1	55.2	55.2	56.8	56.3	56	55.2	55.8
<b>Near Tip</b>	55.1	56.9	55	55.2	56	56.8	55.1	55.9	55	55.1

Mean near tip is 55.6.

While the mean hardness value near the tip of 55 HRC for the styli tempered at 225 °C indicates that this is the appropriate tempering treatment for our styli, there is a variation within and between styli. This could be due to similar variations between and within styli as received hardened by Technical Services.

Therefore, we decided to do the Rockwell test on styli that were received from Technical Services. Hardness values before tempering were the objective of these experiments to observe whether there were differences between and within styli. We can see the result of these hardness tests in the following table(10-13).

**Table 10-13 Styli as received from Technical Services**

<b>Stylus:</b>	<b>1</b>	<b>2</b>	<b>3</b>	<b>4</b>	<b>5</b>	<b>6</b>	<b>7</b>	<b>8</b>	<b>9</b>	<b>10</b>
<b>Near base</b>	62.3	62	63.3	61.3	63.1	63	63	61	62.2	62.1
<b>middle</b>	59.1	63.2	61	63.9	64	62.8	63.1	63.8	62.1	63.3
<b>little above middle</b>	62.1	64	63	63	62.8	63	63	62.1	62	62.2
<b>Near Tip</b>	59	63.1	61.4	62	62.9	60.8	60.8	62	62.4	61

Mean near tip: 61.5

Then we picked two different styli randomly and did the Rockwell test on them 3 times again. The results are in next table (10-14).

**Table 10-14 randomly Rockwell test on stylus**

<b>Stylus(1)</b>	<b>Stylus(2)</b>
<b>60.6</b>	<b>63</b>
<b>61.9</b>	<b>61.2</b>
<b>62.7</b>	<b>62.2</b>
<b>Mean: 61.7</b>	<b>Mean: 62.1</b>

From this it would appear that an individual test can be within  $\pm 1.8$  of the average of 3 tests.

We repeated this process with two of the styli that we had tempered at 225 °C for 45 min.

We cut a short portion from each stylus close to its tip and mounted them in plastic so as to be able to grind and polish a flat circular cross section close to the stylus point to be able to perform a Knoop test on that section.

Then we did these tests, because the best results are related to the stylus that we tempered them at 225°C for 45 min so we pick two of these styli to redo hardness test on them, this time with Knoop test to achieve closer to the tip of stylus.

To make sure the tip has the right hardness for our CERCHAR test we couldn't do it with Rockwell hardness test so we decided to cut the samples and mount them with plastic material to do another set of Knoop test very close to the tip. Following tables (10-15 to 10-16) show us the results.

**Table 10-15 Stylus tempered at 225°C for 45 min**

<b>Test</b>	<b>Knoop value</b>	<b>Equivalent HRC</b>
<b>1</b>	<b>683</b>	<b>58</b>
<b>2</b>	<b>680</b>	<b>57.5</b>
<b>3</b>	<b>692</b>	<b>58.1</b>
<b>Mean</b>	<b>685</b>	<b>57.8</b>

**Table 10-16 Stylus tempered at 225°C for 45 min**

<b>Test</b>	<b>Knoop value</b>	<b>Equivalent HRC</b>
<b>1</b>	<b>673</b>	<b>57.1</b>
<b>2</b>	<b>658</b>	<b>56.4</b>
<b>3</b>	<b>691</b>	<b>58</b>

<b>Mean</b>	<b>674</b>	<b>57.1</b>
-------------	------------	-------------

These Knoop tests for both stylus tempered at 225°C for 45 min show that hardness near the tip are acceptable.







